

**AN INTERACTION MATRIX OF BTB DOMAIN-CONTAINING  
TRANSCRIPTION FACTORS**

by  
LİYNE NOĞAY


Submitted to the Graduate School of Engineering and Natural Sciences  
in partial fulfilment of  
the requirements for the degree of Master of Science

Sabancı University  
December 2019

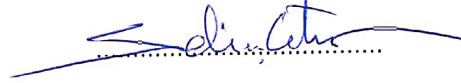
**AN INTERACTION MATRIX OF BTB DOMAIN-CONTAINING TRANSCRIPTION  
FACTORS**

Approved by:

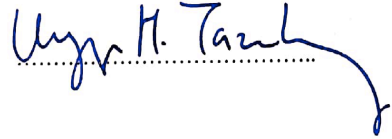
Prof. Dr. Batu Erman  
(Thesis Supervisor)



Prof. Dr. Selim Çetiner



Prof. Dr. Uygur Halis Tazebay



Approval Date: December 5, 2019

LİYNE NOĞAY 2019 ©

All Rights Reserved

## ABSTRACT

### AN INTERACTION MATRIX OF BTB DOMAIN-CONTAINING TRANSCRIPTION FACTORS

LIYNE NOĀAY

Molecular Biology, Genetics and Bioengineering, MSc Thesis, December 2019

Thesis Supervisor: Prof. Batu Erman

Keywords: BTB domain, transcription factors, NCOR/SMRT corepressors, surface plasmon resonance, fluorescent two-hybrid assay

The Bric-a-brac, Tramtrack, and Broad (BTB) domain is a protein-protein interaction unit found in eukaryotes. It forms a distinct multimeric structure with a large interaction surface. The exposed residues of each monomer are highly variable and can allow dimerization, oligomerization, and interactions with several other proteins such as the corepressors nuclear receptor corepressor (NCOR) and silencing mediator of retinoic acid and thyroid hormone receptor (SMRT). BTB-containing transcription factors are diverse and control various physiological processes ranging from immune system development to cell cycle regulation. To understand the structural basis of these functions, we assessed the interaction networks of these proteins. In this study, we developed specific and systematic assays to screen the interactions between various BTB domain-containing transcription factors and their interaction partners in vitro and in vivo, using surface plasmon resonance (SPR) and fluorescent two-hybrid (F2H) assays. We constructed a homo- and hetero-dimerization matrix of several BTB domains of interest.



## ÖZET

### BTB DOMAIN İÇEREN TRANSKRİPSİYON FAKTÖRLERİNİN ETKİLEŞİM MATRİKSİ

LİYNE NOĞAY

Moleküler Biyoloji, Genetik ve Biyomühendislik, Yüksek Lisans Tezi, Aralık 2019

Tez Danışmanı: Prof. Batu Erman

Anahtar Kelimeler: BTB bölgesi, transkripsiyon faktörleri, NCOR/SMRT  
eşbaskılayıcıları, yüzey plasmon rezonans, flörosan ikili hibrit tekniği

BTB protein bölgesi, ökaryotlarda bulunan bir protein-protein etkileşim birimidir. Geniş bir etkileşim alanına sahip, ayırt edici bir üç boyutlu yapıdadır. Dıştaki amino asitleri çok çeşitlilik göstermekle birlikte; dimerizasyon, oligomerleşme ve NCOR SMRT gibi eşbaskılayıcılarla etkileşim işlevlerine sahip olabilir. BTB sahibi transkripsiyon faktörleri çok çeşitlidir ve bağışıklık sistemi gelişiminden hücre döngüsü kontrolüne kadar bir çok süreçte rol alırlar. Bu işlevleri tam olarak anlamak için, söz konusu proteinlerin etkileşim ağlarının gösterilmesi gerekmektedir. Bu çalışmada, çeşitli BTB bölgesi içeren transkripsiyon faktörleri ve onların etkileşim ağlarını, in vivo ve in vitro ortamlarda yüzey plazmon rezonansı (SPR) ve flörosan ikili-hibriti (F2H) yöntemlerini içeren, özel ve sistematik deneyler geliştirmek amaçlanmıştır. Bu doğrultuda BTB protein bölgelerinin kendi içlerinde ve diğer farklı BTB bölgeleriyle gerçekleştirdikleri dimerizasyon matrisini oluşturduk.

## ACKNOWLEDGEMENTS

I would like to express my deep and sincere gratitude to my thesis advisor Prof. Dr. Batu Erman for his continuous support of my M.Sc study; his patience and immense knowledge. His dynamism, vision and motivation have inspired me during my studies. It was a great privilege and honor to work and study under his guidance. Being a member of this academic environment, which he provided, strengthened my scientific background and skeptical thinking ability. I am also thankful to my jury members Prof. Dr. Selim Çetiner and Prof Dr. Uygur Tazebay for their interests and feedbacks about my thesis.

I would like to thank all the past and present members of our lab: Melike Gezen, Sarah Barakat, Sofia Piepoli, Gülin Baran, Sanem Sarıyar, Nazife Tolay, Hakan Taşkiran, and Sinem Usluer. Among these great people, I would like to express my great appreciation to Melike for her endless help, support and unique friendship. I am very thankful to Sanem, Sarah and Sofia for their honest friendship, support and guidance. Without them, it would not be possible to complete this thesis study. This long journey would be harder without friends. I would like to thank to my fellows; to Işık Kantarcıoğlu for her hearty friendship and sisterhood; to Françesko Hela for his sincere fellowship and support; and to Tandaç Fırkan Güçlü for his close friendship. I would not skip my roommate Gizem Acar, we have been roommate for 2 years and our long chats during our breaks are unforgettable memories for me.

I am grateful to my beloved family. They always supported me and never lose their belief in me. I learned how to cope with difficulties from my parents and brother who is a unique ally of mine for whole life. Without their endless help and unconditional love, I would not be able to fulfill my studies and make it this far.

Lastly, I would like to acknowledge the Technological Research Council of Turkey (2210- National Scholarship Program for MSc Students) for financial support. This study was supported by TUBITAK grant ‘Protein- Protein Bağlantısını Kontrol Eden Nanobodilerin Keşfi’ Grant Number: 118Z015

*To my family...*  
*Canım aileme...*

## TABLE OF CONTENTS

LIST OF TABLES.....	x
LIST OF FIGURES .....	xi
LIST OF ABBREVIATIONS .....	xiii
1. INTRODUCTION .....	1
1.1. Overview of BTB Domains and Zinc Finger Motifs .....	1
1.2. Architecture and Functions of BTB Domains .....	2
1.3. Evolution of BTB-Containing Proteins .....	3
1.4. BTB-Zinc Finger Protein Family .....	5
1.4.1. The Modes of Action of BTB-ZF Proteins in Transcriptional Regulation	8
1.4.2. The Biological Functions of Selected BTB-ZF Proteins in Transcriptional Regulation .....	9
1.5. BACH1 and BACH2 Proteins.....	22
1.6. Fluorescent Two Hybrid (F2H) Assay .....	23
2. AIM OF THE STUDY .....	25
3. MATERIALS & METHODS.....	27
3.1. Materials .....	27
3.1.1. Chemicals.....	27
3.1.2. Equipment .....	27
3.1.3. Solutions and Buffers.....	27
3.1.4. Growth Media.....	29
3.1.5. Molecular Biology Kits.....	30
3.1.6. Enzymes .....	30
3.1.7. Bacterial Strains.....	30

3.1.8.	Mammalian Cell Lines.....	30
3.1.9.	Plasmid and Oligonucleotides.....	30
3.1.10.	DNA and Protein Molecular Weight Markers .....	38
3.1.11.	DNA Sequencing.....	38
3.1.12.	Software, Computer-based Programs, and Websites.....	38
3.2.	Methods .....	40
3.2.1.	Bacterial Cell Culture .....	40
3.2.2.	Mammalian Cell Culture.....	42
3.2.3.	Vector Construction.....	43
3.2.4.	Protein Purification.....	44
3.2.5.	Surface Plasmon Resonance.....	50
3.2.6.	Fluorescent Two- Hybrid (F2H) Assay .....	52
4.	RESULTS.....	57
4.1.	Protein Purification of FAZF-BTB, MIZ1-BTB, PATZ1-BTB and PATZ2-BTB domains.....	57
4.2.	Screening the interactions of MIZ1-BTB, PATZ1-BTB and PATZ2-BTB domains <i>in vitro</i> by surface plasmon resonance (SPR).....	65
4.3.	Fluorescent two-hybrid assay for assessing the rules of dimerization of BTB domains with each other and with NCOR/SMRT corepressors.....	69
5.	DISCUSSION.....	87
6.	BIBLIOGRAPHY .....	93
	APPENDIX A .....	103
	APPENDIX B.....	105
	APPENDIX C.....	107
	APPENDIX D .....	107
	APPENDIX E.....	108

## LIST OF TABLES

Table 1. 1 List of human BTB-ZF proteins and the numbers of ZF motifs in these proteins (21) .....	6
Table 3. 1 List of plasmids.....	31
Table 3. 2 List of oligonucleotides .....	36
Table 3. 3 List of software and computer-based programs and websites .....	39
Table 3. 4. List of PEI transfection ingredients and conditions .....	43
Table 3. 5 Combination of plasmids and their amounts .....	55
Table 4. 1 Estimated molecular weights of selected BTB domains in this part of the study.....	57
Table 4. 2 Overall information and immobilization results related to selected BTB domains .....	66
Table 4. 3 The obtained results for MIZ1-BTB ligand; MIZ1-BTB, PATZ1-BTB and PATZ2-BTB analytes .....	67
Table 4. 4 The obtained results for PATZ1-BTB ligand; MIZ1-BTB, PATZ1-BTB and PATZ2-BTB analytes .....	67
Table 4. 5 The obtained results for PATZ2-BTB ligand; MIZ1-BTB, PATZ1-BTB and PATZ2-BTB analytes .....	68
Table 4. 6 The quantification table for all positive interactions.....	86

## LIST OF FIGURES

Figure 1. 1 The BTB protein families and their mode of interactions.....	4
Figure 1. 2 Structure of BCL6 protein and its physiological functions.....	10
Figure 1. 3 Structure of FAZF protein and its physiological functions.....	12
Figure 1. 4 Structure of KAISO protein and its physiological functions.....	13
Figure 1. 5 Structure of LRF protein and its physiological functions .....	15
Figure 1. 6 Structure of MIZ1 protein and its physiological functions .....	16
Figure 1. 7 Structure of PATZ1 protein and its physiological functions.....	18
Figure 1. 8 Structure of PLZF protein and its physiological functions .....	21
Figure 1. 9 Fluorescent Two Hybrid (F2H) assay .....	24
Figure 3. 1 Bacterial induction and expression of His-tagged proteins.....	47
Figure 3. 2 Steps of immobilized metal affinity chromatography (IMAC).....	48
Figure 4. 1 Construction of bacterial expression plasmids for selected BTB domains..	58
Figure 4. 2 Colony screening for FAZF-BTB, PATZ2-BTB and MIZ1 BTB domains.	60
Figure 4. 3 Affinity purification of His-tagged FAZF-BTB, MIZ1 BTB, PATZ1-BTB and PATZ2-BTB domains .....	61
Figure 4. 4 Size exclusion chromatography result of FAZF-BTB, MIZ1-BTB, PATZ2- BTB and PATZ1-BTB domains.....	63
Figure 4. 5 Standard curve for low molecular weight proteins.....	64
Figure 4. 6 pH scouting experiment for MIZ1-BTB, PATZ1-BTB and PATZ2-BTB ..	66
Figure 4. 7 Binding assay for MIZ1-BTB, PATZ1-BTB and PATZ2-BTB.....	69
Figure 4. 8 Constructed plasmids for F2H assay and their transfection method.....	71
Figure 4. 9 Experimental approach of fluorescent two-hybrid (F2H) assay for this study and positive controls .....	72
Figure 4. 10 F2H assay verification.....	73

Figure 4. 11 Homodimerization patterns for selected BTB domains .....	74
Figure 4. 12 The pie charts for the colocalization of green and red foci in the homodimerizations of selected BTB domains.....	76
Figure 4. 13 Heterodimerization experiment for PATZ1-BTB and PATZ2-BTB domains .....	76
Figure 4. 14 The pie charts for the colocalization of green and red foci in the heterodimerizations of PATZ1 and PATZ2 BTB domains.....	77
Figure 4. 15 Heterodimerization experiment for selected BTB domains .....	79
Figure 4. 16 An interaction matrix for the selected BTB-domains .....	79
Figure 4. 17 The interaction table for BCL-BTB dimers and BFP-NCOR/BFP-SMRT and BFP-Only proteins .....	82
Figure 4. 18 The pie charts for the colocalization of green, blue and red foci for interactions between TagGFP-BCL6-TagRFP-BCL6 dimers and NCOR/SMRT corepressors; and the colocalization of green and blue foci for interactions between TagGFP-BCL6 dimers and NCOR/SMRT corepressors .....	83
Figure 4. 19 F2H assay to check the availability of interaction between PATZ1-BTB dimers and NCOR/SMRT corepressor .....	84
Figure 4. 20 The pie charts for the colocalization of green and blue foci in interactions between PATZ1 homodimers and NCOR/SMRT corepressors.....	84
Figure 4. 21 F2H assay to check the necessity of NCOR/SMRT proteins for interaction. .....	85



## LIST OF ABBREVIATIONS

$\alpha$	Alpha
$\beta$	Beta
$\lambda$	Lambda
$\mu$	Micro
A	Ampere
APL	Acute promyelocytic leukemia
ARF	Alternative reading frame protein
ATR	Ataxia telangiectasia and Rad3 related
BACH1&2	BTB Domain and CNC Homolog 1&2
BAX	Bcl-2-associated X protein
BAZF	Bcl6-associated zinc finger protein
BCL6	B-cell lymphoma 6
BCOR	BCL6 corepressor
BHK	Baby Hamster kidney
Blimp-1	B lymphocyte-induced maturation protein 1
BTB	Broad-Complex, Tramtrack and Bric a brac
bZip	Basic leucine zipper domain
bp	Base pair
CDCA7	Cell Division Cycle-Associated 7
CHEK	Checkpoint kinase
Chl	Chloramphenicol
COMP	Cartilage oligomeric matrix protein
CSR	Class-switch recombination
Cul1&2	Cullin1&2
DMEM	Dulbecco's Modified Eagle Medium
DMSO	Dimethyl sulfoxide
DN	Double negative
DNA	Deoxyribonucleic acid

DNM3B	DNA-methyltransferase 3 beta
DP	Double positive
<i>E. coli</i>	<i>Escherichia coli</i>
EDTA	Ethylenediaminetetraacetic acid
FAZF	Fanconi anemia zinc finger protein
FBS	Fetal bovine serum
FNI-I	Factor Binding to IST1
GBP	GFP-binding protein
GC	Germinal center
GFP	Green Fluorescent Protein
GBP	GFP-binding protein
HDAC	Histone deacetyltransferase
IL	Interleukin
IMAC	Immobilized Metal Affinity Chromatography
IST	Inducer of short transcript
IRF	Interferon regulatory factor
Kan	Kanamycin
KBS	KAISO binding site
kDa	Kilo Dalton
LB	Luria broth
LRF	Leukemia/Lymphoma Related Factor
MAZ	Myc associated zinc finger
MDM2	Murine double minute 2
MIZ1	Myc-Interacting Zinc Finger Protein-1
mRNA	Messenger ribonucleic acid
MW	Molecular weight
NCBI	National Center for Biotechnology
NCOR	Nuclear receptor corepressor
NES	Nuclear export signal
NF- $\kappa$ B	Nuclear factor kappa-light-chain- enhancer of activated B cells
NLS	Nuclear localization signal

PATZ1&2	POZ/BTB And AT Hook Containing Zinc Finger 1&2
PBS	Phosphate-buffered saline
PCR	Polymerase chain reaction
PEI	Polyethyleneimine
PLZF	Promyelocytic Leukemia Zinc Finger
POZ	Pox virus and Zinc finger
RAR $\alpha$	Retinoic acid receptor, alpha
RHD	Rel homology domain
Rpm	Revolution per minute
SDS-PAGE	Sodium Dodecyl Sulfate-Polyacrylamide Gel Electrophoresis
SEC	Size exclusion chromatography
SMRT	Silencing-Mediator for Retinoid/Thyroid hormone receptors
SPR	Surface plasmon resonance
TCEP	Tris (2-carboxyethyl) phosphine hydrochloride
TF	Transcription factors
V	Volt
ZID	Zinc Finger Protein with Interaction Domain
ZF	Zinc finger

## 1. INTRODUCTION

### 1.1. Overview of BTB Domains and Zinc Finger Motifs

The BTB domain was firstly discovered in the genome of a DNA virus (poxvirus) as a conserved sequence motif (1). Its name is derived from the studies of Laski and his colleagues which found that the *Drosophila* transcription factors Bric-a-brac, Tramtrack, and Broad complex all possess an N terminal region whose sequence is similar to the viral sequence motif (2,3). Simultaneously, Bardwell and Treisman described a novel zinc finger protein, ZID (zinc finger protein with interaction domain) which has a 120 amino-acid conserved motif at its N terminus and is a large family of poxvirus proteins and zinc finger proteins such as GAGA, ZF5 and Ttk. They named this region as POZ (Pox virus and Zinc finger) domain (4). These two motifs refer to the same region and are known as BTB/POZ domain which is generally abbreviated as the 'BTB domain' in a simple way.

BTB domains are evolutionarily conserved protein-protein interaction domains. They have ability to establish stable and transient interactions at the same time. Moreover, they have evolved to gain new binding functions. Also, the combination of this domain with other domains can lead to several distinct functions. In some proteins, the BTB domain is coupled with a DNA binding domain to form a dimerizing transcription factors. In other proteins, this domain is coupled with ubiquitin ligase domains. Furthermore, it is coupled with transmembrane channels as a structural unit (5).

The zinc finger (ZF) motif was firstly discovered in a transcription factor IIIA protein of *Xenopus laevis* (6). The name is derived from the fact that its structure coordinates a zinc ion and grasped DNA. This motif has a conserved sequence that contains two cysteines

in close proximity to two histidines (C<sub>2</sub>H<sub>2</sub>). These four amino acids are necessary to coordinate the zinc ion. This consensus sequence is encoded by 3% of all human genes and thus it is one of the most common DNA-binding motifs (7). The zinc finger is a common evolutionarily conserved DNA binding motif that also has variants that do not have the C<sub>2</sub>H<sub>2</sub> structure. The focus of this thesis is the ZBTB transcription factor family that has an N-terminal BTB domain and a C-terminal zinc finger DNA binding domain.

## **1.2. Architecture and Functions of BTB Domains**

The length of BTB domains is about 120 amino acids (4) and these domains are generally found as a single copy which is in combination with a variety of other domains. Although there are more than 20 different domains that can be found with BTB in proteins, five of these are the most commonly observed. These are MATH, Kelch, NPH3, Ion transport and Zinc Finger domains (5). Also, some proteins are only composed of a BTB domain. For example, Skp1 (involved in the protein degradation) and ElonginC (involved in the regulation of transcriptional elongation) proteins are in this group (8).

To solve the structure of BTB domains, numerous studies used X-ray crystallography. Although their primary sequences are not well conserved, the secondary structure and tertiary structure and overall architectures of known BTB domain structures are very similar (8). This domain is composed of five  $\alpha$ -helix cluster which is capped from one end by a short three-stranded beta sheet. Its final shape is globular and compact (5).

The fundamental function of BTB domains is to govern protein-protein interactions. The functional result of these interactions changes according to the type of their associated domain partners (8). For instance, the MATH domain is a member of TRAF-like domain which is generally involved in cytoplasmic signal transduction when it is in company with BTB domain (9). For the Kelch domain, this partnership can lead to interactions with actin filaments through its  $\beta$ -propeller structure, responsible for providing stability and dynamics of actin filaments (10, 11, 12). The BTB-containing proteins associated with NPH3 domain are plant specific and involved in phototropism signaling function (13).


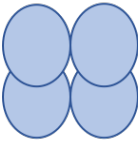

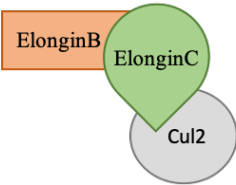
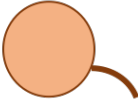
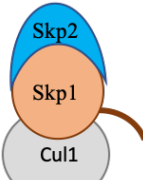

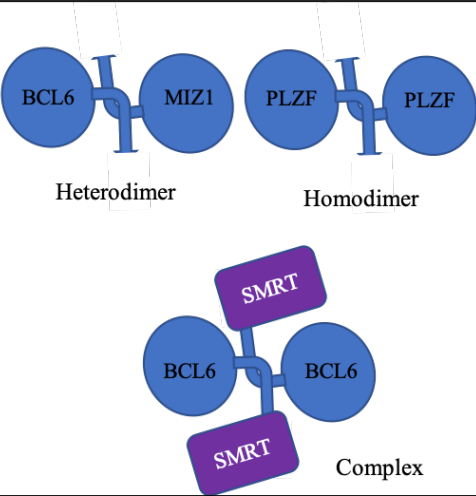
BTB domain can also be found in ion transport domain containing proteins that form voltage gated potassium channels (14). Lastly, BTB-ZF proteins generally function as transcription factors that regulate cell survival and differentiation. Although these proteins are functionally diverse, they all use their BTB domains for protein-protein interactions. However, each different BTB domain has its own behavior during the course of these interactions (Figure 1.1). For example, BTB domains of BTB-ZF transcription factors can homodimerize or heterodimerize and also lead to the recruitment of corepressor proteins (15, 16). On the other hand, BTB domains of ion channels, known as T1 domain, promote tetramerization (17).

The functional differences of BTB containing proteins originate from two structural variations. First, the core BTB domain has extensive sequence variability. The conserved part of the sequence is considerably small and most of invariant residues are buried into the scaffold of the domain due to their hydrophobic nature while exposed surfaces have highly variable residues. The types of residues are the major determinants of the oligomerization of this domain and its interaction with other proteins. Secondly, the presence of class-specific extensions from either the N or C terminus of the core domain are responsible for different interactions (8). BTB domains can be classified into the T1, Skp1, ElonginC and BTB-ZF families (Figure 1.1). The T1 domain containing proteins possess only the core BTB domain. ElonginC does not have the last  $\alpha$ -helix of this core domain. On the other hand, Skp1 contains two additional helices located at the C terminus and this creates a large surface for interactors. Finally, BTB-ZF proteins possess a 25 amino acid extension at the N terminus of the core domain. The tertiary structure of BTB-ZF proteins contain an extra beta-sheet and an  $\alpha$ -helix. These extra structures contribute to dimerization (5). In this study, we studied the dimerization properties of BTB-ZF proteins.

### **1.3. Evolution of BTB-Containing Proteins**

The BTB domain is encoded by the genomes of viruses and eukaryotes ranging from fungi to metazoans and plants. Therefore, it is likely that this domain evolved after the

origin of eukaryotes (5). Except for *Candidatus Protochlamydia amoebophila*, it is not seen in bacteria or archaeabacteria (18). There is a correlation between the complexity of organisms and the number of BTB domain proteins it encodes. The human genome encodes more than 350 different BTB-containing proteins.

Family	Structure	Mode of Binding
<b>T1</b>		 Tetramer
<b>ElonginC</b>		 Complex
<b>Skp1</b>		 Complex
<b>BTB-ZF</b>		 Heterodimer      Homodimer  Complex

**Figure 1. 1 The BTB protein families and their mode of interactions**

Four subtypes of BTB domains are available and they have distinct structures and mode of bindings. T1 domain is a BTB domain found in ion channels and it possesses a

fundamental core and tetramerizes in the cells. The ElonginC family proteins have a core BTB domain lacking the last  $\alpha$ -helix. The Skp1 family proteins contain a core domain which additionally has two C terminal  $\alpha$ -helices. ElonginC and Skp1 are accompanied by an adaptor protein, Cul2 and Cul1 respectively, in E3 ubiquitin ligase complexes. Lastly, BTB-ZF proteins have the core BTB domain with two additional  $\alpha$ -helices at the N terminus. Different proteins in this family have ability to dimerize or make complexes with other proteins.

However, there are some exceptions to this correlation. For instance, the worm *C. elegans* has a large number of BTB-containing proteins in spite of its complexity level (5). Some organisms have BTB domains which can only be coupled with certain other domains. For example, BTB-NPH3 proteins are only available in *Arabidopsis*. On the other hand, *Arabidopsis* does not contain BTB-ZF or BTB-Kelch proteins. Similarly, *C. elegans* has a large number of MATH-BTB proteins but no BTB-Kelch and BTB-ZF proteins. It is worth noting that MATH-BTB proteins are thought to participate in the defense against parasites and therefore under strong positive selection pressure (19). Among all the BTB domains, the MATH-BTB proteins are the most common (20).

#### **1.4. BTB-Zinc Finger Protein Family**

The human genome contains 156 genes that encode BTB-containing proteins. Of these, 49 have C<sub>2</sub>H<sub>2</sub> zinc fingers (Table 1.1) (21) and are named as BTB-ZF. Another name for this family is POZ/Krüppel like (POK), which originated from the definition of N-terminal POZ domain and C<sub>2</sub>H<sub>2</sub> zinc finger Krüppel proteins responsible for segmentation in *Drosophila* (22). Although they are found in the genomes of viruses, BTB-ZF genes are restricted to higher eukaryotic genomes, mostly the vertebrates' (21). Many of the genes encoding mammalian BTB-ZF proteins are found in leukemic translocations. ZF motifs are DNA binding motifs that provide the sequence specificity of the transcription factors. Their BTB domains are responsible for oligomerization and interactions with transcriptional regulators. BTB domains can recruit corepressor proteins such as NCOR (Nuclear Receptor Corepressor) and SMRT (Silencing Mediator for Retinoid and Th thyroid Hormone Receptor) (23) as well as activators such as p300 (24).



**Table 1. 1 List of human BTB-ZF proteins and the numbers of ZF motifs in these proteins (21)**

<b>Name (in humans)</b>	<b>Synonyms</b>	<b>Number of ZFs</b>
ZBTB1	ZNF909	8
ZBTB2	ZNF437	4
ZBTB3		2
ZBTB4	KAISO-L1, ZNF903	6
ZBTB5		2
ZBTB6	ZID, ZNF482	4
ZBTB7A	FBI-1, LRF, pokemon, ZBTB7, ZNF857A	4
ZBTB7B	c-Krox, Th-POK, ZBTB15, ZFP67, ZNF857B	4
ZBTB7C	ZBTB36, ZNF857C	4
ZBTB8A	BOZF1, ZBTB8, ZNF916A	2
ZBTB8B	ZNF916B	2
ZBTB9	ZNF919	2
ZBTB10	RINZF	2
ZBTB11	ZNF913	12
ZBTB12	G10, NG35, Bat9	4
ZFP161	ZBTB14, ZNF478, ZF5	5
ZBTB16	PLZF, ZNF145	9
ZBTB17	MIZ1, pHZ-67, ZNF151, ZNF60	13
ZNF238	C2H2-171, RP58, TAZ-1, ZBTB18	4
PATZ1	MAZR, PATZ, RIAZ, ZBTB19, ZNF278, ZSG	7
ZBTB20	DPZF, ODA-8S, ZNF288	5
ZNF295	ZBTB21	8

ZBTB22	BING1, fruitless, ZBTB22A, ZNF297, ZNF297A	3
GZF1	ZBTB23, ZNF336	10
ZBTB24	BIF1, PATZ2, ZNF450	8
ZBTB25	KUP, ZNF46	2
ZBTB26	ZNF481	4
BCL6	BCL5, BCL6A, LAZ3, ZBTB27, ZNF51 BAZF,	6
BCL6B	BAZF, ZBTB28, ZNF62	5
HIC1	ZBTB29, ZNF901	5
HIC2	HRG22, ZBTB30, ZNF907	5
MYNN	SBBIZ1, ZBTB31, ZNF902	8
ZBTB32	PLZP, FAXF, FAZF, Rog, TZFP, ZNF538	3
ZBTB33	KAISO, ZNF-kaiso, ZNF348	3
ZBTB34	ZNF918	3
ZBTB37	ZNF908	3
ZBTB38	CIBZ, ZNF921	10
ZBTB39	ZNF922	8
ZBTB40	ZNF923	12
ZBTB41	FRBZ1, ZNF924	14
ZBTB42	ZNF925	4
ZBTB43	ZBTB22B, ZNF-X, ZNF297B	3
ZBTB44	BTBD15, ZNF851	4
ZBTB45	ZNF499	4
ZBTB46	BTBD4, RINZF, ZNF340, zDC	2

ZBTB47	ZNF651	9
ZBTB48	HKR3, ZNF85	11
ZBTB49	ZNF509	7
ZNF131		6

#### **1.4.1. The Modes of Action of BTB-ZF Proteins in Transcriptional Regulation**

BTB-ZF proteins are essential transcription factors with roles in biological processes such as gastrulation, limb formation, DNA damage response, progression of cell cycle in both normal and oncogenic tissues, stem cell pool maintenance, and gamete formation (25). Recent studies also revealed the importance of these proteins in the development and function of the immune system (26). ZFs bind to DNA in a sequence-specific manner, specifically recognizing the regulatory regions of target genes. DNA binding is coupled with recruitment of cofactors that are members of chromatin remodeling complexes or transcriptional activation/silencing complexes (26).

Cofactor complexes are formed with the mediation of BTB domains. BTB domains directly contact with corepressors and histone modifying enzymes such as SMRT, NCOR and Histone deacetylase (HDAC)1, -2, -4, -5 and -7 (27). For example, B-lymphoma 6 (BCL6) is a member of this family and it is also known as a proto-oncoprotein due to its capability to help cancer progression when it becomes oncogenes. BCL6 is able to bind to its corresponding specific DNA sequence and leads to the repression of transcription via recruiting HDACs through corepressor proteins BCL6 corepressor (BCOR), NCOR and SMRT, which are all known as silencers. BCL6 is necessary for germinal center (GC) formation because it represses the expression of several genes necessary to sustain mutagenic activity without DNA damage response activation or apoptosis with the help of this cofactor complex formation. BCL6 proteins in GC does not allow maturation of B cells to memory cells or plasma cells to keep de-differentiated state stable by repressing the genes responsible for differentiation through corepressor complexes (28, 29, 30, 31).

Addition to recruitment of corepressors, BTB domains facilitate homodimerization or heterodimerization between the members of this protein family. For example, BCL6 has

ability to homodimerize but also it might heterodimerize with other BTB-ZF proteins such as LRF, MIZ1, PLZF and BAZF (32, 33, 34, 35). These homodimerizations or heterodimerizations have ability to direct whole transcription factors to the corresponding region of DNA and eventually end up with increased binding affinities and distinct functions (5). For instance, BCL6-MIZ1 heterodimerization leads to interaction of BCL6 and MIZ1 proteins which eventually causes repression of *CDKN1A* cell cycle arrest gene so that BCL6 is able to promote proliferative expansion of the germinal center in the course of normal immune response (33).

#### **1.4.2. The Biological Functions of Selected BTB-ZF Proteins in Transcriptional Regulation**

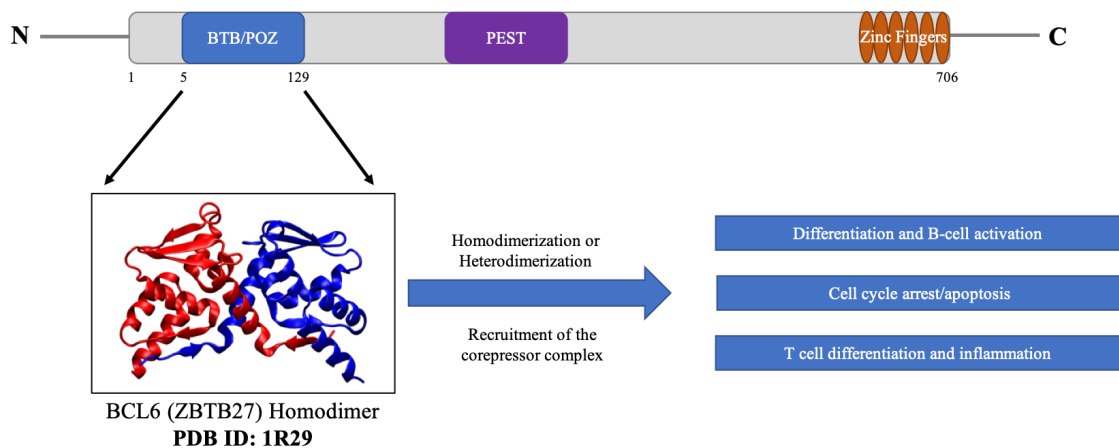
There are at least 49 known BTB-ZF proteins in human and they are responsible for silencing the expression of corresponding genes in a sequence-specific way. In this study, we focused on the most studied and biologically significant members. Their detailed physiological functions and structural descriptions are seen in the following subsections.

##### **1.4.2.1. B-Cell Lymphoma 6 (BCL6)**

The BCL6 protein is encoded by *ZBTB27* gene in humans. It is composed of 706 amino acids. It has an N-terminal BTB domain and six C terminal ZF domains (36). These domains are responsible for regulation of transcription of target genes in distinct ways which have been already mentioned in section 1.4.1. The structure and functions of the domains of BCL6 are shown in figure 1.2.

The BCL6 protein was firstly discovered as an oncoprotein in diffuse large B cell lymphoma, which is known as the most common non-Hodgkin's lymphoma type (37). This proto-oncoprotein nature of BCL6 originates from its ability to prevent expressions of tumor suppressor and cell cycle arrest genes such as p53, CHEK, CDKN1A/p21, and ATR (38). The expression of BCL6 protein is highly seen in germinal centers (GC) of B cells in which affinity maturation and class switch recombination (CSR) events take

place. Its expression is downregulated upon selection for differentiation into memory or plasma cells or apoptosis (36). Mice lacking BCL6 were not able to form GC after they immunized with the antigens in T-cell dependent way. Furthermore, antigen specific B cells of these mice could not undergo affinity maturation and CSR to form their IgG types. Finally, they experienced elevated level of inflammation in their certain organs such as lung and heart which resulted from Th2 dependent hyper-immune responses, which suggests that BCL6 controls the expression of Th2 cytokines, important for development of GC memory B cells and generation of antigen specific T cells (39, 40). Also, BCL6 promotes the repression of Blimp-1 protein expression, which is a transcription factor responsible for plasma cell differentiation (41). Apart from these functions, BCL6 is able to prevent cell cycle arrest and apoptosis in the B cells of GC, which provides DNA damage to take place under the conditions in which no activation of cell cycle checkpoints occurs. This is crucial because after affinity maturation and CSR, DNA damage is the result and by repressing p53, ATR, CHEK1 and p21, cell cycle checkpoint activation is prevented to sense this damage (42).



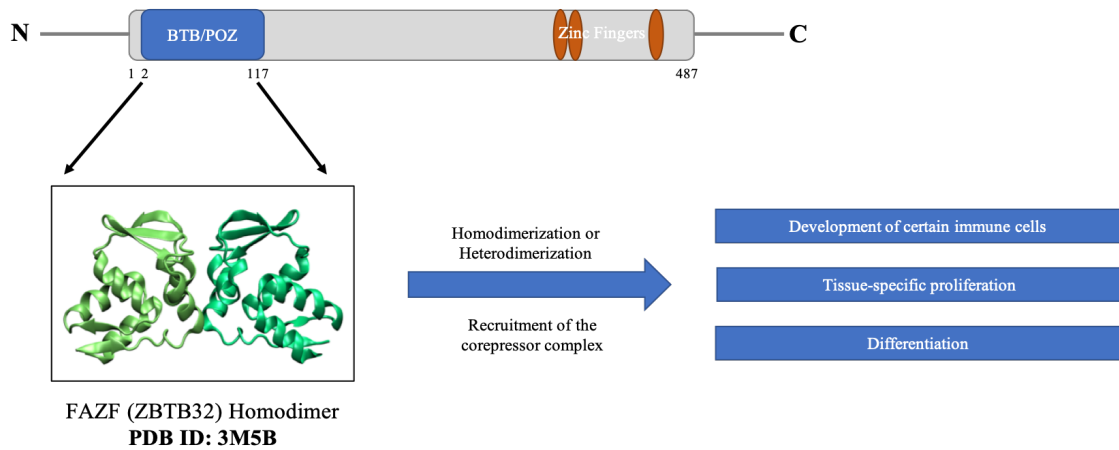
**Figure 1. 2 Structure of BCL6 protein and its physiological functions**

The diagram exhibits the overall architecture of BCL6 protein. BTB domain is responsible for protein protein interactions. PEST is a protein sequence composed of proline (P), glutamic acid (E), serine (S) and threonine (T) amino acids and known as signal peptide for degradation of the whole protein under suitable conditions. The ZF motifs are responsible for DNA binding in a sequence specific manner. When BCL6 homodimerization (or heterodimerization for some cases) occurs, the recruitment of corepressors takes place and large corepressor complex is formed. Eventually, certain physiological functions are carried out. The crystal structure of BCL6 homodimer is visualized by using VMD program.

#### **1.4.2.2. Fanconi Anemia Zinc Finger (FAZF)**

The FAZF protein is encoded by *ZBTB32* gene in humans. It is composed of 487 amino acids. It has an N-terminal BTB domain and three C-terminal ZF motifs. It was initially discovered as a binding partner of Fanconi Anemia (FA) group C protein (FANCC) (43). FA is a disease whose characterization is done by the presence of hypersensitivity to DNA crosslinking agents and it is known as either autosomal or X-linked recessive. FA patients frequently show bone marrow failure and defects in congenital development. FANCC has a region which is necessary for the interaction with FAZF; this interaction is not mediated with the BTB domain of FAZF and this region is mutated in the patients (44). FAZF is also known as testis zinc finger proteins (TZFP), repressor of GATA (RoG) or PLZF-like zinc finger proteins (PLZP). This protein is responsible for the recruitment of histone modifying enzymes to regulate the target gene expression. Generally, corepressors such as NCOR and HDACs are recruited to the corresponding chromatin region (45).

FAZF shares 68% identity with PLZF and thus it is able to bind to similar DNA sequences as PLZF does. Moreover, they have ability to heterodimerize but the physiological roles of this heterodimerization is still obscure (43). FAZF can also interact with other transcription factors essential in hemopoiesis. For example, FAZF can repress GATA3-induced cytokine expression that is necessary for T cell lineage development. The estimation about this repression is that FAZF can cause direct recruitment of HDAC to cytokine promoter and repress interleukin-4 (IL4) expression in CD8<sup>+</sup> T cells (46). This estimation is compatible with the results coming from knock-out mouse studies. FAZF-deficient mice showed elevated T lymphocyte proliferation and cytokine production in CD8<sup>+</sup> and CD4<sup>+</sup> T cells. Also, these mice had elevated number of HSCs in G1 phase of cell cycle which implies that FAZF possesses roles in cell proliferation event (47). The structure and functions of the domains of FAZF are shown in figure 1.3.



**Figure 1. 3 Structure of FAZF protein and its physiological functions**

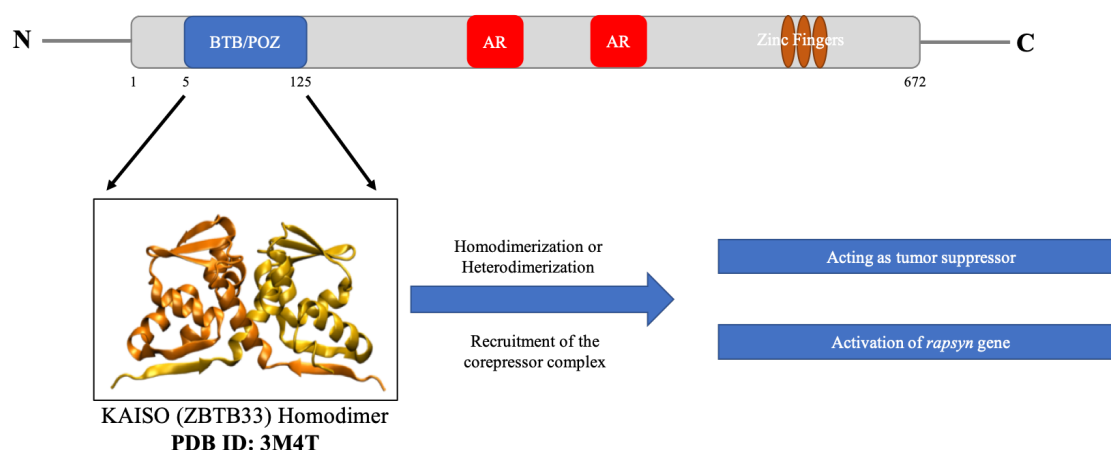
The diagram exhibits the overall architecture of FAZF protein. BTB domain is responsible for protein protein interactions and ZF motifs are able to bind to DNA in a sequence specific manner. When FAZF homodimerization (or heterodimerization for some cases) occurs, the recruitment of corepressors takes place and large corepressor complex is formed. Eventually, certain physiological functions are carried out. The crystal structure of FAZF homodimer is visualized by using VMD program.

#### 1.4.2.3. KAISO

The KAISO protein is encoded by *ZBTB33* in humans. It has an N-terminal BTB domain and three C-terminal ZF motifs; and in total 672 amino acids. It was firstly discovered with a yeast-two hybrid experimental setting in which armadillo repeat domain protein (, p120 catenin, was used as a bait. According to the interaction map of this system, p120 catenin bound to the C-terminal 200 amino acids of KAISO and this binding was completely independent from BTB domain (48).

The KAISO protein shows bimodal specificity for DNA binding: it is able to bind to the consensus sequence TCCTGCNA, known as KAISO binding site (KBS), specifically. Also, it can bind to DNA sequences with methylated CGCG (CpGs) (49). p120 catenin binding site is found within the KAISO ZF domain region, thus p120 catenin can inhibit DNA binding of KAISO protein when they interact and this leads to abrogation of transcription repression mediated by KAISO (50). KAISO generally acts as a transcriptional repressor in such a way that first it directly binds to DNA by two of its three ZF motifs, then it uses its BTB domain for homodimerization or heterodimerization depending on the context. After dimerization, the recruitment of corepressors such as

NCOR takes place and further HDAC components are added to this large complex (51). On the contrary, between its BTB domain and ZF motifs, there are two highly acidic regions available in KAISO protein. Those acidic regions are thought to activate transcription of target genes such as neuromuscular gene *rapsyn* and this reflects the presence of transcriptional activator nature of KAISO (50, 52). The structure and functions of the domains of KAISO are shown in figure 1.4.



**Figure 1. 4 Structure of KAISO protein and its physiological functions**

The diagram exhibits the overall architecture of KAISO protein. BTB domain is responsible for protein protein interactions and ZF motifs are able to bind to DNA in a bimodal fashion. AR regions are two acidic regions. When KAISO homodimerization (or heterodimerization for some cases) occurs, the recruitment of corepressors takes place and large corepressor complex is formed. Eventually, certain physiological functions are carried out. The crystal structure of KAISO homodimer is visualized by using VMD program.

According to previous studies, KAISO is implicated in tumorigenesis. For instance, several target genes of KAISO such as *MTA2*, *siamois*, *cylinD1* and *MMP7* are related to cell proliferation or tumor metastasis. The target genes of Wnt/ $\beta$ -catenin/TCF, *siamois*, *cylinD1* and *matrilysin*, were exposed to KAISO mediated repression in the luciferase-reporter assays, which might prove that they are target genes for KAISO (50). Furthermore, KAISO was found as one of the direct repressors of target genes in Wnt signaling which is an essential pathway for embryonic development and tissue regeneration (51). These findings can be interpreted as KAISO is a potential tumor suppressor in certain cancer types. Surprisingly, according to one study, the mice which were KAISO-deficient were still alive without any detectable developmental



abnormalities or tumors (53). This might be due to the fact that the presence of some other KAISO-related proteins such as ZBTB4 can compensate KAISO loss in these mice (50).

#### **1.4.2.4. Leukemia/Lymphoma Related Factor (LRF)**

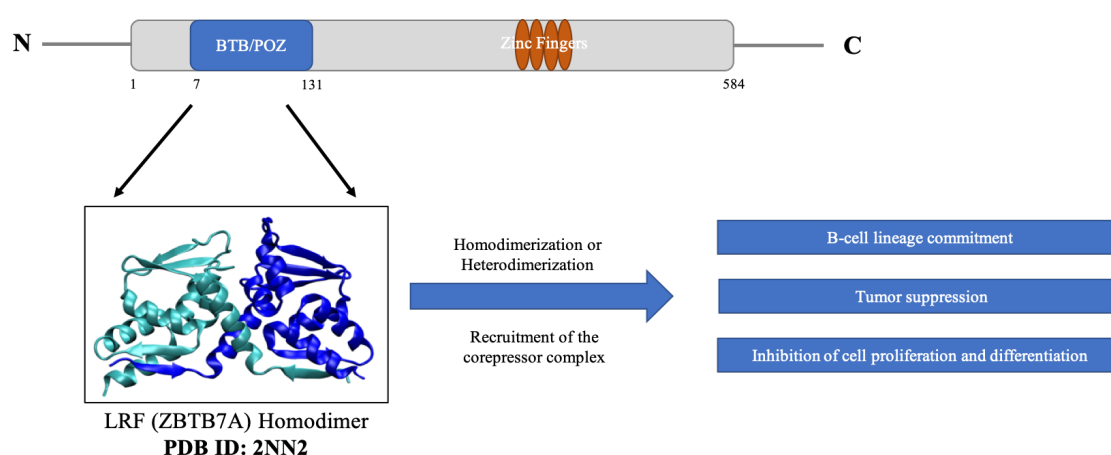
The LRF protein is encoded by *ZBTB7A* gene in humans. It is composed of 584 amino acids. It has an N-terminal BTB domain and four C-terminal ZF motifs. It is also known as Pokemon, FB-1 and OCZF in the literature. It acts as a transcriptional repressor and also an proto-oncoprotein which can be associated with malignancy in solid epithelial tumors and lymphomas (54). This protein was firstly named as FNI-1 or Factor Binding to IST1 because it has ability to bind to the regions located on HIV1 genome and called as the inducer of short transcripts (IST) (55). This FBI-1 protein is able to interact with itself and also with HIV-1 viral activator, Tat (56).

Later studies have shown that LRF can bind and control the expression of several other genes, which have consensus binding sequence for LRF. They can be exemplified as the genes coding extracellular matrix collagen type I, II, IX, X and XI; fibronectin, elastin, human cartilage oligomeric matrix protein (COMP), alcohol dehydrogenase ADH5, ARF tumor suppressor, c-fos and c-myc oncoproteins (57, 58, 54, 55). Furthermore, LRF is able to enhance the transcription of the response genes of NF-kB in such a way that it facilitates nuclear import and stabilization of this transcription factor and also it blocks nuclear export of it. To interact, LRF uses its BTB domain and NF-kB uses its Rel Homology Domain (RHD) of p65 subunit (58). Moreover, LRF is able to repress *ARF* tumor suppressor gene (*p14<sup>ARF</sup>* in human, *p19<sup>Arf</sup>* in mouse) and thus is kind of a central regulator in oncogenesis. When LRF is overexpressed, ARF level is reduced and this leads to degradation of nuclear p53 and eventually transformation into oncogenicity. On the contrary, the reduction in LRF level results in senescence and apoptosis (59).

LRF is known as master regulator in the fate decision of B lymphoid versus T lymphoid. According to the literature, when conditional deletions of LRF in HSCs were performed to the mice, the numbers of peripheral B cells reduced dramatically, which proves that these cells require LRF to progress to the B cell commitment and development. In the

same cells, these conditional deletions resulted in extrathymic T cell development in the bone marrow. Additional experiments supported that LRF is responsible for suppression of Notch-dependent T cell lineage commitment in the lymphoid progenitor cells localized in bone marrow. When LRF was absent, genes found in Notch signaling were abnormally upregulated in progenitors and this prevented B cell development and triggered the T cell development outside of the thymus (60).

Although LRF is highly similar to PLZF, it cannot heterodimerize with PLZF. On the other hand, LRF is able to interact with BCL6 when both proteins simultaneously have their BTB domains and ZF motifs. However, it has not been properly known that what physiological functions appear after this heterodimerization process (32). The structure and functions of the domains of LRF are shown in figure 1.5.



**Figure 1. 5 Structure of LRF protein and its physiological functions**

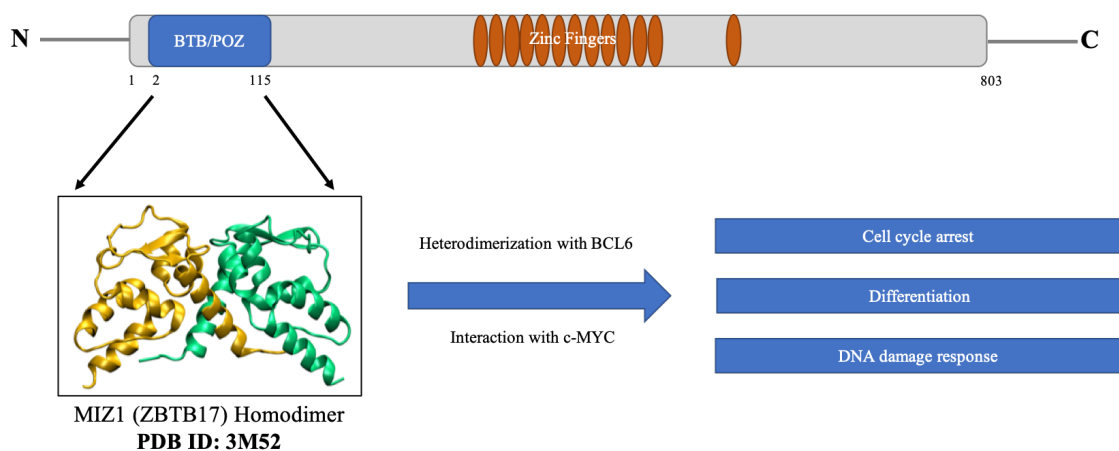
The diagram exhibits the overall architecture of LRF protein. BTB domain is responsible for protein protein interactions and ZF motifs are able to bind to DNA specifically. When LRF homodimerization (or heterodimerization for some cases) occurs, the recruitment of corepressors takes place and large corepressor complex is formed. Eventually, certain physiological functions are carried out. The crystal structure of LRF homodimer is visualized by using VMD program.

#### 1.4.2.5. Myc-Interacting Zinc Finger Protein-1 (MIZ1)

The MIZ1 protein is encoded by *ZBTB17* gene in humans. It is composed of 803 amino acids and has an N-terminal BTB domain and thirteen C-terminal ZF motifs. It was firstly discovered in a two-hybrid assay experiment as a protein which interacted with c-MYC.

The interaction of MIZ1 and MYC is mediated by the part of 50 amino acid stretch of MIZ1 that is localized between ZF 12 and 13 thus it is independent from BTB domain (61). MIZ1 BTB domain was crystallized as in the tetramer form (62).

MIZ1 is responsible for the regulation of DNA-damage induced cell cycle arrest, cell proliferation and development. Due to its interaction with BCL6 and c-MYC, it has certain roles in human cancers (62). The interaction of MIZ1 with BCL6 is mediated by BTB domains of these proteins. This interaction leads to suppression of *CDKN1A* gene which encodes p21Cip1 protein, responsible for cell cycle arrest. This suppression might facilitate the proliferation in germinal centers during normal immune response because during this response, extensive DNA damage takes place due to class switching reactions and affinity maturation of B cells and there should be an antagonizing response towards p53-dependent p21Cip1 protein upregulation. When this system is deregulated, the pathological expansion of B cell lymphomas might be seen (63). Furthermore, the interaction between MIZ1 and c-MYC targets promoters of several genes and together they act as a transcriptional repressor. The best studied promoters belong to the two cell cycle inhibitors, p15Ink4b and p21Cip1 and MIZ1-cMYC transcriptional repressor complex represses their expressions. Moreover, this complex acts on the tumor suppressor and DNA damage-dependent pathways in an interfering way. For all these transcriptional repression steps to take place, MIZ1 should bind to the core promoter of target gene, interact with c-MYC and have the integrity of its BTB domain (64). The structure and functions of the domains of MIZ1 are shown in figure 1.6.



**Figure 1. 6 Structure of MIZ1 protein and its physiological functions**

The diagram exhibits the overall architecture of MIZ1 protein. BTB domain is responsible for protein protein interactions and ZF motifs are able to bind to DNA specifically. When MIZ1 heterodimerization with BCL6 occurs or the interaction with c-MYC protein takes place, certain physiological functions are eventually carried out. The crystal structure of MIZ1 homodimer is visualized by using VMD program.

#### **1.4.2.6. POZ/BTB and AT Hook Containing Zinc Finger 1 (PATZ1)**

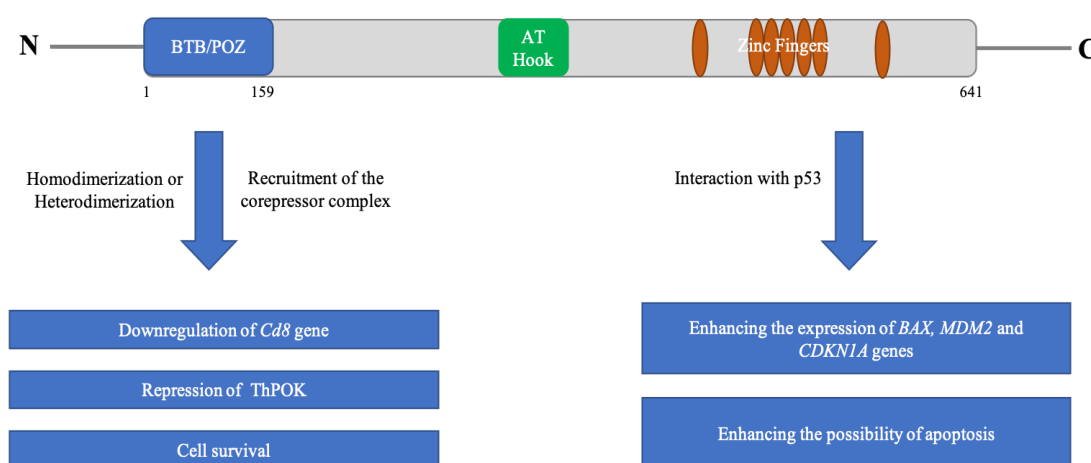
The PATZ1 protein is encoded by *ZBTB19* gene in humans. It has an N-terminal BTB domain, an A-T hook DNA binding motif responsible for binding to other DNA binding structures during its involvement in chromatin remodeling and transcription regulation, and seven C-terminal ZF motifs. It has four alternatively spliced versions which are composed of 687, 537, 641 and 537 amino acids. It was firstly discovered in a two-hybrid screen assay where BTB domain of BACH2 (BTB and CNC Homology) protein was used as a bait. This association of BACH2-PATZ1 was mediated by their BTB domains. PATZ1 is also named as MAZR, MYC-associated Zinc Finger Related, because of having ZF motifs similar to the ones in MYC-associated Zinc Finger (MAZ) proteins (65).

PATZ1 is highly expressed in double negative (DN) thymocytes (during early stages of T cell development) and then its expression is down-regulated in double positive (DP) and CD8<sup>+</sup> thymocytes (during later stages of T cell development) (66). In DN thymocytes, PATZ1 is recruited to the *Cd8* gene loci and bound to the *Cd8* enhancer via its ZF motifs. Here, it interacts with NCOR through its BTB domain. Eventually, this leads to the regulation of chromatin modification at these loci in a negative way so that transcription activation does not take place and CD8 expression is repressed at DN stage of T cell development. Almost no expression of PATZ1 is seen in the peripheral T cell population (67). During these processes, PATZ1 represses the expression of ThPOK (ZBTB7b; cKrox), another member of BTB-ZF transcription factor family (68). In addition to thymus, PATZ1 is also expressed in fetal liver and bone marrow as well (65).

The functions of PATZ1 are not limited to T lymphocyte development. For instance, this protein also acts as a crucial regulator of p53 in such a way that it is able to bind to p53 by using its negatively charged region localized between the sixth and seventh ZF motifs. Eventually the interaction prevents p53 from binding to DNA and the pattern of p53-

dependent transcription of target genes is altered. Furthermore, PATZ1 proteins have sensitivity towards DNA damage and during the early time points of DNA damage, the level of PATZ1 stays constant and p53 level rises rapidly. Therefore, they can exist together and interact to some extent. Later time of this damage, the level of PATZ1 and p53 becomes inversely proportional. The reduction in the PATZ1 level is due to its proliferative effects on cells and not controlled by the interaction of these two proteins. It has been estimated that ubiquitination-dependent degradation of proteasome system might be the mediator of this reduction (69). The interaction also facilitates the expression of certain genes, such as *BAX*, *MDM2* and *CDKN1A* which are controlled by p53, then further increases the possibility of apoptosis. This reflects the tumor suppressor nature of PATZ1. On the other hand, when p53 is absent, PATZ1 inhibits the same genes and triggers the cell survival, which reflects its oncogenic nature. These two conditions explain the dependency of PATZ1 function on the cellular context that it is involved (70).

PATZ1 is able to homodimerize and also heterodimerize with other BTB-ZF transcription factors such as BACH2 (65) and PATZ2 (71). The structure and functions of the domains of PATZ1 are shown in figure 1.7.



**Figure 1. 7 Structure of PATZ1 protein and its physiological functions**

The diagram exhibits the overall architecture of PATZ1 protein. BTB domain is responsible for protein protein interactions, AT Hook and ZF motifs are able to bind to DNA non-specific way. When PATZ1 homodimerization occurs or the interaction with p53 protein takes place, certain physiological functions are eventually carried out. The crystal structure of PATZ1 protein for human is not available.

#### **1.4.2.7. POZ/BTB and AT Hook Containing Zinc Finger 2 (PATZ2)**

The PATZ2 protein is encoded by *ZBTB24* gene. It has an N-terminal BTB domain, A-T hook DNA binding motif which is able to interact with minor groove of AT rich sequences, eight C-terminal ZF motifs and 697 amino acids in total. PATZ2 protein is not properly studied in terms of its function.

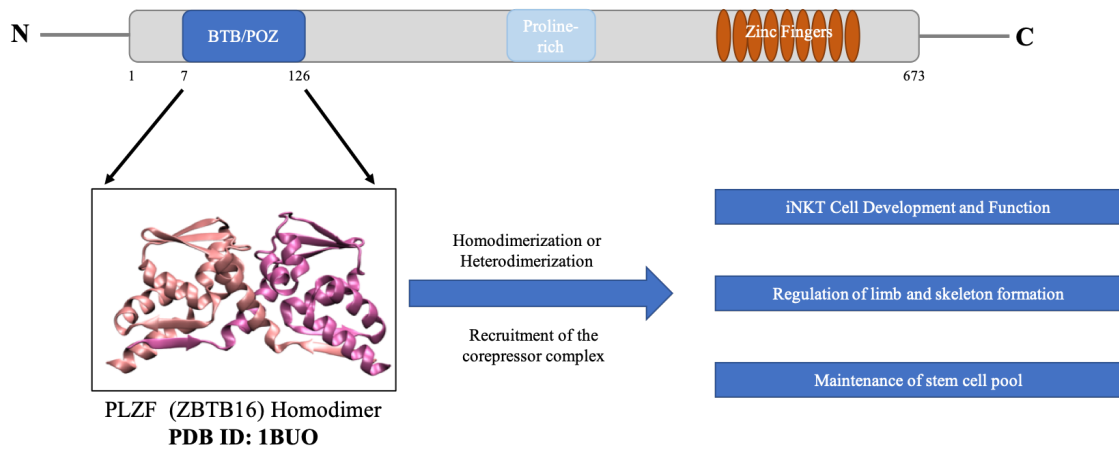
*ZBTB24* gene is one of the genes mutated in immunodeficiency, centromeric instability and facial anomalies (ICF) syndrome. When this gene is mutated in this disease, the disease is described as ICF type 2 or ICF2. In this type, serum antibody and circulating memory B cell numbers are greatly lower. The other genes which are involved are *DNMT3B* (DNA methyltransferase 3B, ICF1), *CDCA7* (cell division associated 7, ICF3) and *HELLS* (helicase, lymphoid-specific, ICF4) (72, 73). Apart from this, the knockdown studies of endogenous PATZ2 revealed that there was a decrease in proliferation of human B cell line (Raji cells) by blocking the G0/1 to S cell cycle phase progression and no apoptosis induction. Moreover, when PATZ2 was downregulated, the expression level of interferon regulatory factor 4 (IRF4) and B lymphocyte-induced maturation protein 1 (Blimp-1), two essential factors responsible for proliferation and differentiation of B cells, was increased. All these functions are performed by PATZ2 in an independent way from BCL6. These results show that PATZ2 might be considered as one of the transcriptional factor important in human B cell function (74). In addition to these, according to one study, the mice which were homozygous for a BTB deletion in PATZ2 are prone to be early embryonic lethal. This might suggest that PATZ2 may have an essential function in developmental processes (75).

#### **1.4.2.8. Promyelocytic Leukemia Zinc Finger (PLZF)**

The PLZF protein is encoded by *ZBTB16* gene. It is composed of 673 amino acids and has an N-terminal BTB domain and nine C-terminal ZF motifs. It was firstly discovered with a chromosomal translocation, t(11;17)(q23;q21), in acute promyelocytic leukemia (APL) in which *ZBTB16* fused with retinoic acid receptor alpha (RAR $\alpha$ ) and transformed into PLZF-RAR $\alpha$  oncogene. In this situation, 455 amino acids from N-terminus of PLZF

is fused with RAR $\alpha$  (76). Normally, PLZF acts as a transcriptional repressor which is able to bind to the promoters of its target genes such as cyclin A and interleukin 3 (IL3) receptor  $\alpha$  chain with the help of its ZFs (77, 78). Transcriptional repression is performed by the recruitment of corepressor proteins such as NCOR, SMRT and Sin3A through BTB domain. This eventually brings HDACs to the corresponding promoter region. This complex leads to repression of the genes which basically control mammalian embryonic development and myeloid differentiation (79).

When PLZF is expressed in the hematopoietic cell lines, it performs several physiological functions such as suppressing growth, arresting cell cycle in the G<sub>1</sub>/S phase and blocking the differentiation (80). According to the recent studies, PLZF acts as a crucial regulator of innate T cell lineages. Its expression is elevated in immature CD1d-restricted invariant natural killer T (iNKT) cells. When there was PLZF deficiency in the mice studied, their cells could not undergo thymic expansion and be reduced in the thymus, liver and spleen. The iNKT cells of these mice also behaved like conventional naïve T cells and exhibited a reduction in their cytokine (IL-4 and IFN gamma) secretion level when stimulated. When ectopic expression of PLZF took place, the acquisition of effector or memory T cell phenotype and functions was obtained (81). Besides, PLZF might have some effects on NK cell function either in a direct or indirect way. One example for this assumption is that the deficiency in PLZF interferes with the protection against infection of Semliki Forest virus and this susceptibility was attributed to the decrease level of IFN-induced NK cell cytotoxicity (82). Furthermore, since the expression level of PLZF is high in multipotential precursors of hematopoietic cells and low in their differentiated versions, PLZF is speculated to be involved in the contribution of embryonic stem cell maintenance in the germline (83). Moreover, PLZF is responsible for the patterning of limb and skeleton formation by regulating the expression of bone morphogenic proteins and *Hox* gene family whose function is controlling the limb morphogenesis. This patterning is modulated by apoptosis and cell proliferation processes in structures of limb (25). The structure and functions of the domains of PLZF are shown in figure 1.8.



**Figure 1. 8 Structure of PLZF protein and its physiological functions**

The diagram exhibits the overall architecture of PLZF protein. BTB domain is responsible for protein protein interactions, a proline rich region, and ZF motifs are able to bind to DNA specifically. When PLZF homodimerization (or heterodimerization for some cases) occurs, the recruitment of corepressors takes place and large corepressor complex is formed. Eventually, certain physiological functions are carried out. The crystal structure of PLZF homodimer is visualized by using VMD program.

#### 1.4.2.9. ZBTB4

ZBTB4 is composed of 1013 amino acids. It has an N-terminal BTB domain which is 175 amino acid in length but it is interrupted by 60 amino acid-long stretch which is found between  $\alpha$  helix 3 and beta sheet 4 so that this region is not in the dimerization interface. It was firstly discovered as a methyl-DNA binding protein when a BLAST experiment was carried out on the human genome against KAISO. ZBTB4 has a bimodal specificity to bind DNA as in the case for KAISO, which is able to bind both TCCTGCNA consensus sequence and methylated CGCG sequences. However, there is a variation related to their binding pattern: while ZBTB4 can bind to a single methylated CpG, KAISO needs at least two consecutives methylated CpGs to bind. ZBTB4 is expressed highly in the brain and here it is estimated to control the gene expression pattern of different neurons that can be involved in olfactory, motor or hippocampal functions (84). In addition to these, ZBTB4 is able to heterodimerize with MIZ1, which together represses *P21CIP1* expression and thus leads to inhibition in the cell cycle arrest in response to the activation of p53. On the contrary, when there is loss of ZBTB4 in the cellular context, apoptosis is inhibited, cell cycle arrest and long-term survival are facilitated in response to the activation of p53 (85).



### 1.5. BACH1 and BACH2 Proteins

BTB and CNC homology 1 and 2 (BACH1 and BACH2) proteins are members of basic region-leucine zipper family (bZip) of transcription factors. They have an N-terminal BTB domain and a C-terminal bZip domain for DNA binding. They are only found in the vertebrates and able to bind to Maf-recognition elements (MAREs) (86). BACH2 is essential for both innate and acquired immunity and has critical roles in the fundamental events of early B cell development such as immunoglobulin class switching, affinity maturation of immunoglobulin-encoding genes, the checkpoint of pre-B cell antigen receptor, the activation of tissue resident macrophages and the development of effector and regulatory T cells (87). On the other hand, BACH1 proteins are responsible for producing reactive oxygen species, providing heme homeostasis, involving in cell cycle and hematopoiesis as a regulator, the differentiation of erythrophagocytic and inflammatory macrophages (88).

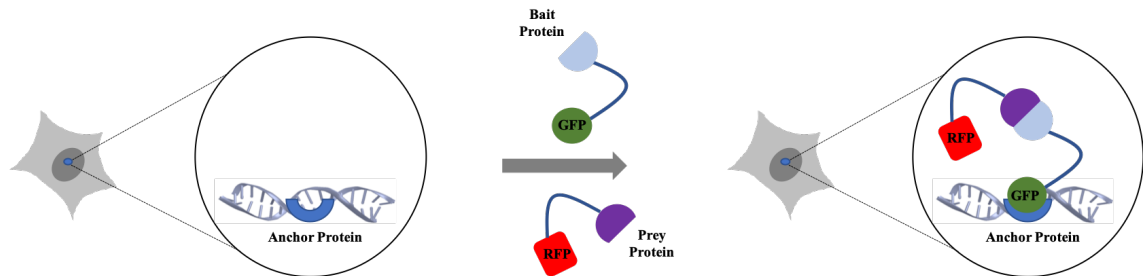
The BACH1 protein is able to homodimerize in such a way that it has a novel homodimer interaction surface. This homodimerization surface was discovered to contain a novel hydrogen bond network and an interaction between hydrophobic surfaces belonging to the kinked N-terminus (N-hook) and C-terminal residues of the partner. When N-hook was deleted, the conversion of homodimer into monomer in solution was the result and this suggests that the presence of N-hook contributes to the homodimerization of BACH1 BTB domain (89). On the other hand, the BACH2 protein is able to interact with its target genes by using its basic leucine-zipper region. The BTB domain part of it is responsible for the recruitment of corepressors and further HDACs. The BTB dimer of BACH2 resembles the BTB dimers of BTB-ZF transcription factors, this dimerization is independent from the N-hook region which is required for the dimerization of BACH1 protein. The BACH2 protein has been crystallized in two forms: the difference between them was the presence of an inter-subunit disulfide bond. This disulfide bond formation might be considered as a reversible regulation mechanism during the activity of proteins found in oxidative stress responses. Also, the stabilization of the interactions among subunits in a protein can be achieved with this bond formation. Furthermore, it can be

helpful for the mediation of protein-protein interactions but not required for the stabilization of the dimerization surface of BACH2 (90).

### **1.6. Fluorescent Two Hybrid (F2H) Assay**

Fluorescent two-hybrid (F2H) assay is a novel method to detect and visualize protein-protein interactions more accurately in the natural environment of living mammalian cells. The result of this method is obtained during real time as a simple optical readout. The obtained optical readout can be analyzed to acquire the high-quality data for the screening of corresponding protein-protein interactions in response to any external stimuli or chemical compounds such as inhibitors. This system is basically dependent on the fact that a fluorescently labeled bait protein is immobilized on a distinct subcellular structure, generally nucleus of the cells, and the detection of interactions between proteins is performed by checking the colocalization of another fluorescently labeled prey protein, which should be different in terms of its fluorophore, at this defined structure (91). In other words, if the proteins, which are freely drifting within the cells, interact with the certain components of the cells, which are immobilized and enriched at a specific structure in a transient way, colocalization might be eventually observed. In the F2H assay system that we used for this study, the BHK cell line clone number 2 which have been stably integrated with about 200-1000 copies of a plasmid each possessing 256 copies of the *lac* operator sequence was used (92). On this *lac* operator, the GFP binding protein (GBP)-Lac repressor (LacI) fusion protein sits via its lac repressor part. GBP is a nanobody, which is able to bind to GFP and some GFP variants such as YFP with high affinity, and it is suitable for expression and localization *in vivo* conditions. Its molecular weight is 13 kDa and it is a soluble protein (93, 94). The GFP-tagged bait protein is immobilized by binding of GBP to GFP. If there is an interaction between GFP-tagged bait protein and RFP-tagged prey protein, the colocalization of green and red foci is observed. This interaction is easily visualized with a conventional fluorescent microscopy. F2H assay might give some false positive or negative results thus from the beginning it should be controlled. If prey proteins are able to bind to *lac* operator in the absence of bait protein, then they will be only used as baits for further experiments. The

most significant advantage of this system is that it is fairly simple because there is no need for costly instrumentation or advanced technical expertise (92). The summary of F2H assay is seen in figure 1.9.



**Figure 1. 9 Fluorescent Two Hybrid (F2H) assay**

In the genetically modified BHK cells, *lac* operators are stably integrated into the genome. On this region, anchor protein, which is also known as GBP-Lac repressor fusion protein, is tethered. GFP-tagged bait protein is bound to this region and this initial localization is mediated by GBP-GFP binding, which is visible as a green fluorescent spot in the nuclei of transfected cells. If RFP-tagged prey protein is able to interact with the bait protein, it will become enriched at the same spot and this results in the colocalization of green and red foci. If there is no interaction, only green focus colocalization is seen (not shown).

## 2. AIM OF THE STUDY

The BTB domains found in BTB-zinc finger transcription factors exhibit how a family of fundamental protein domains can form a variety of interactions and eventually acquire several distinct functions. These interactions and their networks should be revealed properly to understand the mechanisms of related biological processes at a molecular level. Previously conducted studies have shown the presence of several BTB homodimers but only a few BTB heterodimers. Furthermore, these studies have also revealed that certain BTB homodimers are necessary for the repression activity of the BTB-ZF transcription factors. Simply, these homodimers form an interface that is essential for the interactions with some corepressors such as NCOR, BCOR, and SMRT which are members of large histone deacetylase-containing complexes. Therefore, to get an overall representation of how BTB domains interact, a more credible and effective way of interaction mapping is required. In this study, we aimed to develop an assay for screening the interactions between various BTB-ZF transcription proteins and their networks with other proteins in a systematic way.

In the first part of the study, we wanted to express and purify the BTB domains of selected proteins from the bacterial system. For protein expression, we followed cytoplasmic expression protocol by using the Rosetta DE3 pLYSs expression strain of *E.coli*. The purification of these expressed proteins was carried out by immobilized metal affinity chromatography (IMAC) and size exclusion chromatography (SEC) respectively. After these purification steps, we designed a surface plasmon resonance (SPR) experiment with the obtained proteins to screen their homodimerization, heterodimerization, homotetramerization and heterotetramerization potentials.

In the second part of the study, we set up a fluorescent two-hybrid assay to identify potential homodimers and heterodimers of BTB domains and their interaction networks with other corepressor proteins such as NCOR and SMRT. In this assay, BTB domains of selected proteins were tagged with two different fluorescent proteins, TagGFP and TagRFP. When there was homo/heterodimerization between the BTB domains with different tags, two distinguishable fluorescent foci at the same location within the nuclei of BHK cells were formed. Moreover, NCOR and SMRT proteins were tagged with BFP protein and the interaction between BTB dimers and these corepressors was checked with the designed system. If there was an interaction among them, green and blue foci (TagGFP-TagGFP homodimers and corepressor) or green, red and blue foci (TagGFP-TagRFP homodimers and corepressor) formation at the same spot was the end result. In conclusion, our aim for this study was to come up with a high-throughput interaction assay to analyze BTB domain interaction networks systematically. This interaction network can be further used to identify key residues of BTB interaction interfaces, reveal the rules of BTB domain interactions and understand the structure-function relationship of BTB-ZF transcription factors.

### **3. MATERIALS & METHODS**

#### **3.1. Materials**

##### **3.1.1. Chemicals**

All the chemicals used in this thesis are shown in Appendix A.

##### **3.1.2. Equipment**

All the equipment used in this thesis is shown in Appendix B.

##### **3.1.3. Solutions and Buffers**

Calcium Chloride (CaCl<sub>2</sub>) Solution: 60 mM CaCl<sub>2</sub> (from 1 M stock), 15% glycerol and 10 mM PIPES (pH 7.0) were mixed and volume of mixture was completed to 500 ml with ddH<sub>2</sub>O. The solution was sterilized with 0.22 µm filter and stored at 4°C.

Agarose Gel: In order to prepare 100 ml 1% w/v agarose gel, 1 g of agarose powder was weighed and dissolved in 100 ml 0.5X TBE buffer by heating in a microwave. 0.002% (v/v) ethidium bromide was added to the final solution.

Tris-Borate-EDTA (TBE) Buffer: In order to prepare 1 L 5X stock solution, 54 g Tris-Base, 27.5 g boric acid, and 20 ml 0.5 M EDTA (pH 8.0) were dissolved in 1 L ddH<sub>2</sub>O.

The solution is stored at room temperature and diluted 1 to 10 with ddH<sub>2</sub>O to obtain 0.5X working solution.

Polyethyleneimine (PEI) Solution: In order to prepare 1 mg/ml (w/v) working solution, 100 mg polyethyleneimine powder was dissolved in 100 ml ddH<sub>2</sub>O by heating at 80°C. The pH was adjusted to 7.0 with 33% hydrochloric acid (HCl). The final solution was filter-sterilized, aliquoted as 1 ml in each 1.5 tube and kept at -20°C.

SDS Separating Gel: In order to prepare 10 ml 10% separation gel, 3.34 ml Acrylamide: Bis-acrylamide (37.5:1), 2.5 ml Tris (1.5 M pH 8.8), 100 µl 10% (w/v) SDS, 100 µl 10% (w/v) APS and 10 µl TEMED were mixed and the volume was completed to 10 ml with ddH<sub>2</sub>O.

SDS Stacking Gel: In order to prepare 5 ml 4% stacking gel, 1.25 ml Tris (0.5M pH 6.8), 1 ml Acrylamide: Bis-acrylamide (37.5:1), 50µl 10% SDS (w/v), 15µl 10% APS (w/v), and 7.5µl TEMED were mixed and the volume was completed to 5ml with ddH<sub>2</sub>O.

SDS Running Buffer: Initially, 1 L 10X Tris-Glycine stock solution was prepared by dissolving 40 g Tris-Base and 144 g Glycine in ddH<sub>2</sub>O while arranging the pH to 8.3. Then, in order to prepare 1X SDS running buffer, 100 ml Tris-Glycine solution was mixed with 895 ml ddH<sub>2</sub>O and 5 ml 20% SDS solution.

Protein Loading Buffer: In order to prepare 4X protein loading buffer, 2.4 ml Tris (1 M pH 6.8), 0.8 g SDS, 4 ml 100% glycerol, 0.01% bromophenol blue, and 2 ml β-mercaptoethanol were mixed and then the volume was completed to 10 ml.

Lysis Buffer: In order to prepare 50 ml 1X lysis buffer, 50 mM HEPES, 250 mM NaCl, 0.5 mM TCEP, 10 mM imidazole, EDTA-free protease inhibitor cocktail (Roche), and 10 µl DNase I (100U/ µl) were mixed. The volume was completed to 50 ml with ddH<sub>2</sub>O.

Buffer IMAC-A: In order to prepare 1 L of IMAC-A solution, 50 mM HEPES, 250 mM NaCl, and 10 mM imidazole were mixed. The volume was completed to 1 L with ddH<sub>2</sub>O.

The solution was filter-sterilized and kept at 4°C. 0.5 mM TCEP was added freshly before using the solution.

Buffer IMAC-B: In order to prepare 1 L of IMAC-B solution, 50 mM HEPES, 250 mM NaCl, and desired concentration of imidazole were mixed. The solution was filter-sterilized and 0.5 mM TCEP was added fresh before using the solution. The IMAC-B solution was used as elution buffer of His-Tagged Affinity Chromatography. In this study, 100 mM and 300 mM imidazole concentrations were used.

Gel Filtration Buffer: In order to prepare 1 L gel filtration buffer, 20 mM HEPES, and 250 mM NaCl were mixed. 5 mM TCEP (or 0.05%  $\beta$ -mercaptoethanol) was added to the solution. The volume was completed to 1 L with ddH<sub>2</sub>O.

### **3.1.4. Growth Media**

Luria Broth (LB): In order to prepare 1 L 1X LB medium, 20 g LB powder was completed to 1 L with ddH<sub>2</sub>O. The medium was autoclaved at 121°C for 15 minutes. After cooling the medium, kanamycin at final concentration of 50  $\mu$ g/ml, ampicillin at final concentration of 100 $\mu$ g/ml or chloramphenicol at final concentration of 34 $\mu$ g/ml was added to the liquid medium just before use for antibiotic selection.

LB-Agar: In order to prepare 1 L 1X agar medium, 35 g LB-Agar powder was completed to 1 L with ddH<sub>2</sub>O. The medium was autoclaved at 121°C for 15 minutes. After cooling down the medium to 50°C, the corresponding antibiotic was added into the medium for selection. The final concentrations of used antibiotics were kanamycin 50  $\mu$ g/ml, ampicillin 100  $\mu$ g/ml and chloramphenicol 34  $\mu$ g/ml. 15 ml of LB-Agar solution was poured into a sterile petri dish under fume hood. The plates were kept at 4°C.

DMEM: BHK cells were maintained in DMEM growth medium which is supplemented with 10% heat-inactivated fetal bovine serum (FBS) and 1% Pen-Strep (100 U/ml Penicillium and 100  $\mu$ g/mL Streptomycin).



Freezing Medium: The cells were frozen in heat-inactivated fetal bovine serum containing 10% DMSO (v/v).

### **3.1.5. Molecular Biology Kits**

All the used commercial molecular biology kits in this thesis are given in Appendix C.

### **3.1.6. Enzymes**

Restriction and DNA modifying enzymes, polymerase enzymes, and their corresponding buffers were obtained from either New England Biolabs (NEB) or Fermentas.

### **3.1.7. Bacterial Strains**

*Escherichia coli* (*E. coli*) DH-5 $\alpha$  was used for general transformation and cloning applications. *E. Coli* Rosetta2 DE3 pLysS expression strain was used for mammalian protein production and purification.

### **3.1.8. Mammalian Cell Lines**

BHK: BHK21 cell line was derived from the kidneys of Syrian hamsters. The BHK cell line version we used (ChromoTek) was modified in such a way that cells have Lac operator repeats in their genomes.

### **3.1.9. Plasmid and Oligonucleotides**

All the plasmids used in this thesis are listed in Table 3.1.

**Table 3. 1 List of plasmids**

<b>PLASMID NAME</b>	<b>PURPOSE OF USE</b>	<b>SOURCE</b>
pET-47b (+)	The bacterial expression plasmid to express BTB domains with an N-terminal His-tag	Merck Millipore (71461)
pET-47b (+)-BCL6-BTB	The bacterial expression plasmid to express BCL6-BTB domain with an N-terminal His-tag	Lab construct
pET-47b (+)-FAZF-BTB	The bacterial expression plasmid to express FAZF BTB domain with an N-terminal His-tag domain with an N-terminal His-tag	Lab construct
pET-47b (+)-KAISO-BTB	The bacterial expression plasmid to express KAISO-BTB domain with an N-terminal His-tag	Lab construct
pET-47b (+)-LRF-BTB	The bacterial expression plasmid to express LRF-BTB domain with an N-terminal His-tag	Lab construct
pET-47b (+)-MIZ1-BTB	The bacterial expression plasmid to express MIZ1-BTB domain with an N-terminal His-tag	Lab construct
pET-47b (+)-PATZ2-BTB	The bacterial expression plasmid to express PATZ2-BTB domain with an N-terminal His-tag	Lab construct

pET-47b (+)-PLZF-BTB	The bacterial expression plasmid to express PLZF-BTB domain with an N-terminal His-tag	Lab construct
pCDNA3.1/ myc- His (-) B	Mammalian expression plasmid with CMV promoter	Thermo Fischer Scientific, (V85520)
pcDNA3.1/myc-His (-) B-TagGFP	The mammalian expression plasmid to express. N-terminal TagGFP	Lab construct
pcDNA3.1/myc-His (-) B-TagRFP	The mammalian expression plasmid to express N-terminal TagRFP	Lab construct
pcDNA3.1/myc-His (-) B-TagGFP-BACH1-BTB	The mammalian expression plasmid to express BACH1-BTB domain with N-terminal TagGFP tag	Lab construct
pcDNA3.1/myc-His (-) B-TagGFP-BACH2-BTB	The mammalian expression plasmid to express BACH2-BTB domain with N-terminal TagGFP tag	Lab construct
pcDNA3.1/myc-His (-) B-TagGFP-BCL6-BTB	The mammalian expression plasmid to express BCL6-BTB domain with N-terminal TagGFP tag	Lab construct
pcDNA3.1/myc-His (-) B-TagGFP-KASIO-BTB	The mammalian expression plasmid to express KASIO-BTB	Lab construct

	domain with N-terminal TagGFP tag	
pcDNA3.1/myc-His (-) B-TagGFP-LRF-BTB	The mammalian expression plasmid to express LRF-BTB domain with N-terminal TagGFP tag	Lab construct
pcDNA3.1/myc-His (-) B-TagGFP-MIZ1-BTB	The mammalian expression plasmid to express MIZ1-BTB domain with N-terminal TagGFP tag	Lab construct
pcDNA3.1/myc-His (-) B-TagGFP-PATZ1-BTB	The mammalian expression plasmid to express PATZ1-BTB domain with N-terminal TagGFP tag	Lab construct
pcDNA3.1/myc-His (-) B-TagGFP-PATZ2-BTB	The mammalian expression plasmid to express PATZ2-BTB domain with N-terminal TagGFP tag	Lab construct
pcDNA3.1/myc-His (-) B-TagGFP-PLZF-BTB	The mammalian expression plasmid to express PLZF-BTB domain with N-terminal TagGFP tag	Lab construct
pcDNA3.1/myc-His (-) B-TagGFP-ZBTB4-BTB	The mammalian expression plasmid to express ZBTB4-BTB domain with N-terminal TagGFP tag	Lab construct

pcDNA3.1/myc-His (-) B-TagRFP-BACH1-BTB	The mammalian expression plasmid to express BACH1-BTB domain with N-terminal TagRFP tag	Lab construct
pcDNA3.1/myc-His (-) B-TagRFP-BACH2-BTB	The mammalian expression plasmid to express BACH2-BTB domain with N-terminal TagRFP tag	Lab construct
pcDNA3.1/myc-His (-) B-TagRFP-BCL6-BTB	The mammalian expression plasmid to express BCL6-BTB domain with N-terminal TagRFP tag	Lab construct
pcDNA3.1/myc-His (-) B-TagRFP-FAZF-BTB	The mammalian expression plasmid to express FAZF-BTB domain with N-terminal TagRFP tag	Lab construct
pcDNA3.1/myc-His (-) B-TagRFP-KAISO-BTB	The mammalian expression plasmid to express KAISO-BTB domain with N-terminal TagRFP tag	Lab construct
pcDNA3.1/myc-His (-) B-TagRFP-LRF-BTB	The mammalian expression plasmid to express LRF-BTB domain with N-terminal TagRFP tag	Lab construct
pcDNA3.1/myc-His (-) B-TagRFP-MIZ1-BTB	The mammalian expression plasmid to express MIZ1-BTB	Lab construct

	domain with N-terminal TagRFP tag	
pcDNA3.1/myc-His (-) B-TagRFP-PATZ1-BTB	The mammalian expression plasmid to express PATZ1-BTB domain with N-terminal TagRFP tag	Lab construct
pcDNA3.1/myc-His (-) B-TagRFP-PATZ2-BTB	The mammalian expression plasmid to express PATZ2-BTB domain with N-terminal TagRFP tag	Lab construct
pcDNA3.1/myc-His (-) B-TagRFP-PLZF-BTB	The mammalian expression plasmid to express KAISO-BTB domain with N-terminal TagRFP tag	Lab construct
pcDNA3.1/myc-His (-) B-GBP-LacI	The mammalian expression plasmid to express GBP-LacI fusion protein for F2H assay	Lab construct
pcDNA3-GFP	GFP expressing plasmid for transfection control	Lab construct
pCDNA3.1/myc-His (-) B-BFP-oligo1-NCOR	The mammalian expression plasmid to express oligo1-Ncor with N-terminal TagBFP tag	Lab construct
pCDNA3.1/myc-His (-) B-BFP-oligo1-SMRT	The mammalian expression plasmid to express oligo1-SMRT with N-terminal TagBFP tag	Lab construct

pcDNA3.1/myc-His (-) B-BFP-NLS	The mammalian expression plasmid to express N-terminal TagBFP	Lab construct
--------------------------------	---	---------------

All the oligonucleotides used in this thesis are listed in Table 3.2.

**Table 3. 2 List of oligonucleotides**

<b>OLIGONUCLEOTIDE NAME</b>	<b>SEQUENCE</b>	<b>PURPOSE OF USE</b>
BCL6-BTB-SmaI-Forward	TGGACTCGAGATGGCCTCGCCGGC TGACAG	pET-47(b)+ cloning
BCL6-BTB-NotI-Reverse	GGACGCGGCCGCTTATTCAGTGGC CTTAATAAACTTCCGGCAAG	pET-47(b)+ and F2H cloning
FAZF-BTB-SmaI-Forward	TGGACCCGGGATGTCCCTGCCCCC CATAAGACTGC	pET-47(b)+ cloning
FAZF-BTB-NotI-Reverse	GGACGCGGCCGCTTAAGCCCTGTC CCCTCGAGCCCTC	pET-47(b)+ and F2H cloning
KAISO-BTB-SmaI-Forward	TGGACCCGGGATGGAGAGTAGAA AACTGATTTCTGC	pET-47(b)+ cloning
KAISO-BTB-NotI-Reverse	GGACGCGGCCGCTTACTGTGACAA TGGGACACCAA	pET-47(b)+ and F2H cloning
LRF-BTB-SmaI-Forward	TGGACCCGGGATGGCCGGCGGCGT GGA	pET-47(b)+ cloning
LRF-BTB-NotI-Reverse	GGACGCGGCCGCTTAGATCTGCCG GTCCAGGAGGTCG	pET-47(b)+ and F2H cloning

MIZ1-BTB-SmaI-Forward	TGGACCCGGGATGGACTTTCCCA GCACAGCCAGC	pET-47(b)+ cloning
MIZ1-BTB-NotI-Reverse	GGACGCGCCGCTTAAGCAAGTGA CTTGAGGGCATGGCAG	pET-47(b)+ and F2H cloning
PATZ2-BTB-SmaI-Forward	TGGACCCGGGATGGCAGAAACATC GCCAGAG	pET-47(b)+ cloning
PATZ2-BTB-NotI-Reverse	GGACGCGCCGCTTAGCTATGATT ATTTTGGAAGTCTGTGTAAGC	pET-47(b)+ and F2H cloning
PLZF-BTB-SmaI-Forward	TGGACCCGGGATGGATCTGACAAA AATGGGCATGA	pET-47(b)+ cloning
PLZF-BTB-NotI-Reverse	GGACGCGCCGCTTACTGGATGGT CTCCAGCATCTTCAG	pET-47(b)+ and F2H cloning
PATZ1-BTB-XhoI-Forward	TGGA CTCGAGGGATGGAGCGGGTC AACGACGCTTC	F2H cloning
PATZ1-BTB-NotI-Reverse	GGACGCGCCGCTTAGGACTGTTT GATTACTTCCTGGCAGATC	F2H cloning
PATZ2-BTB-XhoI-Forward	TGGA CTCGAGGGATGGCAGAAAC ATCGCCAGAG	F2H cloning
PLZF-BTB-XhoI-Forward	TGGA CTCGAGGGATGGATCTGACA AAAATGGGCATGA	F2H cloning
LRF-BTB-XhoI-Forward	TGGA CTCGAGGGATGGCCGGCGGC GTGGA	F2H cloning
KAISO-BTB-XhoI-Forward	TGGA CTCGAGGGATGGAGAGTAG AAACTGATTTCTGC	F2H cloning
ZBTB4-BTB-XhoI-Forward	TGGA CTCGAGGGATGCCCCCCCCT GCAGAGGTGACG	F2H cloning
ZBTB4-BTB-NotI-Reverse	GGACGCGCCGCTTAACCAGGCAG TGCGAGCCGGGCGCT	F2H cloning
BCL6-BTB-XhoI-Forward	TGGA CTCGAGGGATGGCCTCGCCG GCTGACAG	F2H cloning



BACH1-BTB-SmaI- Forward	TGGACCCGGGATGTCTCTGAGTGA GAACTCGGTTTTT	F2H cloning
BACH1-BTB-XhoI- Forward	TGGACTCGAGGGATGTCTCTGAGT GAGAACTCGGTTTTT	F2H cloning
BACH1-BTB-NotI- Reverse	GGACGCGGCCGCTTAAAATTTTCAG AAACTGAAAGCAGGATTCCTC	F2H cloning
BACH2-BTB-SmaI- Forward	TGGACCCGGGATGTCTGTGGATGA GAAGCCTGACT	F2H cloning
BACH2-BTB-XhoI- Forward	TGGACTCGAGGGATGTCTGTGGAT GAGAAGCCTGACT	F2H cloning
BACH2-BTB-NotI- Reverse	GGACGCGGCCGCTTACAGGAAGCT GAAGCAGGAGTCCT	F2H cloning
CMV Forward	CGC AAA TGG GCG GTA GGC GTG	F2H cloning
TagGFP-XhoI&SmaI- Reverse	GGACCTCGAGGGACCCCGGGAGA ACCGCTGTACAGCTCGTCCATGCC	F2H cloning

### 3.1.10. DNA and Protein Molecular Weight Markers

DNA and protein ladders which were used in this thesis are given in Appendix E.

### 3.1.11. DNA Sequencing

DNA sequencing services were provided by MCLAB, CA, USA. (<https://www.mclab.com/home.php>).

### 3.1.12. Software, Computer-based Programs, and Websites

Software, computer-based programs, and websites used in this thesis are given in Table 3.3

**Table 3. 3 List of software and computer-based programs and websites**

<b>SOFTWARE, PROGRAM, WEBSITE NAME</b>	<b>COMPANY/WEBSITE</b>	<b>PURPOSE OF USE</b>
CLC Main Workbench v7.9.4	QIAGEN Bioinformatics	Molecular cloning, analysis of sequence, data, DNA sequence alignment
NCBI BLAST	<a href="https://blast.ncbi.nlm.nih.gov/Blast.cgi">https://blast.ncbi.nlm.nih.gov/Blast.cgi</a>	Tool for basic local alignment to examine the similarities between biological sequences
NCBI PRIMER- BLAST	<a href="https://www.ncbi.nlm.nih.gov/tools/primer-blast/">https://www.ncbi.nlm.nih.gov/tools/primer-blast/</a>	Primer design
Addgene	<a href="https://www.addgene.org/">https://www.addgene.org/</a>	Information for plasmid map
ExPASy	<a href="https://www.expasy.org/">https://www.expasy.org/</a>	Protein parameters and translation tool
Ensembl Genome Browser	<a href="https://www.ensembl.org/index.html">https://www.ensembl.org/index.html</a>	Information for Human genome
UNICORN 7.1	GE Healthcare Life Sciences	Chromatography operation
BIACORE T200 software v3.0	GE Healthcare Life Sciences	Operation and Evaluation of SPR experiments
Visual Molecular Dynamic (VMD)	<a href="https://www.ks.uiuc.edu/Research/vmd/">https://www.ks.uiuc.edu/Research/vmd/</a>	Analysis of PDB files

## **3.2. Methods**

### **3.2.1. Bacterial Cell Culture**

#### **3.2.1.1. The growth of Bacteria**

*E.coli* DH5 $\alpha$  and Rosetta DE3 pLYSs strains were cultured in LB medium with corresponding antibiotics for selection, overnight around 12-16 hours at 37°C with vigorous shaking (221rpm). To obtain single bacterial colony, the culture was spread with autoclaved glass beads on LB-Agar plates containing the suitable antibiotics for selection and these plates were incubated overnight at 37°C. In order to prepare glycerol stock, 10% (v/v) glycerol was added to the bacterial culture to get 1 ml final volume under the fume hood. Cryovials were used to maintain glycerol stocks and they are kept at -80 °C.

#### **3.2.1.2. Preparation of Competent Bacteria**

Previously prepared competent *E.coli* DH5 $\alpha$  was added to 40 ml LB in a 250 ml flask without adding any antibiotics due to the absence of resistance in this strain. The culture was incubated overnight at 37°C by shaking at 221 rpm (For Rosetta2 DE3 pLYSs, chloramphenicol with a final concentration of 34 $\mu$ l/ml was added at this stage.). The next day, 4 ml of overnight-grown culture was taken from 40 ml initial culture and inoculated into 400 ml LB in 2 L flask without the addition of any antibiotic. This final culture was incubated at 37°C with vigorous shaking (221 rpm) until the optical density of the culture at 590 nm (OD<sub>590nm</sub>) has reached to 0.375. After this point, 400 ml culture was divided into eight sterile 50 ml tubes and they were incubated on ice for 10 minutes. Then, this chilled bacterial culture was centrifuged at 1600 g for 10 minutes at 4°C. The supernatant was removed and each bacterial pellet was resuspended in 10 ml ice-cold CaCl<sub>2</sub> solution and then centrifuged at 1100 g for 5 minutes at 4°C. Again, the supernatant was discarded and each pellet was resuspended in 10 ml ice-cold CaCl<sub>2</sub> solution. The cells were incubated on ice for 30 minutes. Then, they were centrifuged at 1100 g for 5 minutes at

4°C. The supernatant was discarded and each pellet was resuspended in 2 ml pre-chilled CaCl<sub>2</sub> solution. All the suspensions were put together in one 50 ml tube and aliquoted as 200 µl volume for each ice-cold microcentrifuge tube. They were immediately flash-frozen in liquid nitrogen at -80°C and kept at -80°C. The transformation efficiency of prepared competent cells was calculated by transforming different concentrations of pUC19 plasmid (Efficiency should be between 10<sup>7</sup>-10<sup>8</sup> cfu/µg).

### **3.2.1.3. Transformation of Competent Bacteria**

For all transformation experiments, heat-shock transformation was carried out. Flash frozen aliquots of chemically competent bacteria were thawed on ice until they turned into viscous form. Then, desired concentration of DNA (for pure plasmid transformation, 1pg-1ng; for ligated product transformation, 5-20 µl ligation mix) was added into competent bacteria. The mixture was incubated on ice for 30 minutes. After this incubation, the cells were heat-shocked at 42°C for 90 seconds and placed on ice for 1 minute. 800 µl LB (without addition of any antibiotic) was put on the heat-shocked cells and this final culture was incubated at 37°C for 45 minutes. After this incubation, the cells were centrifuged at 13,200 rpm for 30 seconds and bacterial pellet was resuspended in 100 µl of LB coming from the supernatant. Finally, this suspension was spread onto LB-agar plate containing the corresponding antibiotic for selection and the plates were incubated overnight at 37°C.

### **3.2.1.4. Plasmid DNA Isolation**

In order to isolate plasmid DNA from *E.coli* DH5α, alkaline lysis protocol as described in Molecular Cloning: A Laboratory Manual (Sambrook et al.) was carried out. Furthermore, Macherey Nagel Midiprep commercially available kit was performed according to protocol of manufacturer for midiprep protocol. The obtained concentration and purity of DNA were measured by a NanoDrop spectrophotometer.

### **3.2.2. Mammalian Cell Culture**

#### **3.2.2.1. Maintenance of Cell Lines**

For maintenance of BHK cells, complete DMEM was used. This maintenance was performed in 10 cm sterile tissue culture plates and those plates were incubated in the incubator whose temperature and CO<sub>2</sub> level were set to 37 °C and 5% CO<sub>2</sub> respectively. When cell confluency reached to about 80%, the cells were split in such a way that cells were firstly washed with serum-free DMEM, trypsin was added afterwards and they were waited in trypsin for 5 minutes within the incubator. Then, they were suspended in complete DMEM and split to a new 10 cm sterile tissue plate at 1:10 ratio. This process should be repeated for every 2-3 days.

#### **3.2.2.2. Cryopreservation of Cells**

Cells were frozen within the freezing medium for later use or storage purposes. They were split a day before freezing to become 30-40% confluent. The next day, cell were counted to obtain  $1-5 \times 10^6$  cells. Then, they were centrifuged at 300 g for 5 minutes. Pelleted cells were resuspended in 1 ml freezing medium and kept in the cryovials. The cryovials were put into a freezing container which has isopropanol and stored at -80°C for at least 24 hours and then transferred to liquid nitrogen tank for long-term storage.

#### **3.2.2.3. Thawing Frozen Mammalian Cells**

Cryovials were initially taken out from nitrogen tank. Then, cells were immediately thawed by addition of 9 ml complete growth medium (DMEM for this study) in 15 ml centrifuge tube to dilute DMSO found in the freezing medium. The cells were centrifuged at 300 g for 5 minutes to remove DMSO. The supernatant was taken out, pellet was resuspended in 10 ml complete growth medium and suspension was placed in 10 cm tissue culture plate. Plate was incubated at 37°C and 5% CO<sub>2</sub>.

### 3.2.2.4. Transient Transfection of Mammalian Cell Lines Using Polyethyleneimine (PEI)

The day before transfection, the necessary number of cells were split onto 6-well tissue culture plate. On the transfection day, desired amount of DNA (2 µg for this study) was mixed with 200 µl serum-free phenol-free DMEM in a sterile microcentrifuge tube. Then, PEI (1 µg/µl) solution was vortexed well and added to DNA-DMEM mix at a 2:1 ratio of PEI (µg) to total plasmid DNA (µg). Immediately after addition of PEI, the mixture was vortexed and incubated at room temperature for 15 minutes. After incubation, the mixture was added onto the cells in a dropwise manner. The list of PEI transfection ingredients and conditions for 6 well plate is shown in Table 3.4.

**Table 3. 4. List of PEI transfection ingredients and conditions**

<b>Plate Type</b>	<b>Seeded cell number</b>	<b>DMEM amount for cell seeding</b>	<b>Total DNA amount</b>	<b>DMEM amount for transfection</b>	<b>PEI:DNA ratio</b>
6 well plate	1.5x10 <sup>5</sup>	2 ml	2 µg	200 µl	2:1

### 3.2.3. Vector Construction

Restriction enzyme digestion: Digestion reactions were carried out by mixing desired amount of DNA, corresponding enzymes and their compatible buffers in PCR tubes. It was followed by incubation in Thermal Cycler for 1-3 hours at the optimum temperature of corresponding enzymes.

Klenow fragment application: Klenow fragment was used for blunting of DNA via filling the 5'-overhangs created by XhoI restriction enzyme digestion in cloning steps of BTB-domains to pcDNA3.1/myc-His (-) B-TagRFP-BTB domains.

Dephosphorylation of 5' phosphate groups: When the plasmid DNA is digested with a single enzyme or compatible enzymes and further aimed to be used in a ligation reaction,

5' phosphate groups of linearized plasmids are removed by alkaline phosphatase enzyme (calf intestinal alkaline phosphatase, (CIAP)) in order to prevent self-ligation.

Agarose gel electrophoresis and DNA purification from the gel: PCR products, products of digestion reactions and other DNA samples are separated and visualized with the help of agarose gel electrophoresis. Agarose gels were prepared by dissolving the required amount of agarose which is determined according to the size of DNA fragment, ranging from 0.7 to 2 g, in 100 ml 0.5X TBE. The prepared mixture was heated in a microwave to dissolve the agarose completely. Then, it was cooled down and 2 µl ethidium bromide (0.0002% v/v) was added to this final solution. DNA samples were mixed with DNA loading dye and loaded to the already solidified agarose gel. Electrophoresis was carried out at 100 V for 45-90 minutes in 0.5X TBE buffer. As a next step, gel extraction is performed to obtain the corresponding DNA band which was cut from the gel under UV light quickly to minimize the harmful effects of UV light. DNA was then purified with the help of a commercially available gel purification kit according to the manufacturer's protocol.

Ligation: Ligation reactions are carried out by the use of T4 DNA Ligase (NEB) with its suitable buffer. For all ligation experiments, 1:3 vector to insert ratio was chosen. 100 ng vector DNA was used with the required insert amount for ligation reactions. Ligation was carried out either at room temperature for 2 hours or at 16°C for 16 hours. For each cloning, vector-only ligation was additionally done as a control to check whether there was re-ligation of the vector on itself or not. Finally, the ligation mixture was transformed into *E. coli* DH5α competent cells.

#### **3.2.4. Protein Purification**

##### **3.2.4.1. Bacterial Expression Vector Construction**

As a backbone, pET-47b (+) bacterial expression vector with an N-terminal His-tag was used. The BTB domains of selected proteins were obtained as in the form of PCR products

by using Q5 High-Fidelity DNA Polymerase (NEB) according to its suggested conditions for PCR. In order to amplify these inserts, the forward primers with SmaI and the reverse primers with NotI restriction sites were designed. SmaI and NotI-HF enzymes do not work in Q5 Reaction Buffer hence NucleoSpin Gel and PCR Clean-up protocol was carried out just before digestion of PCR products. The suitable annealing temperature for PCR was determined by performing gradient PCR. Reactions were carried out in a thermal cycler by using Q5 High Fidelity DNA Polymerase according to following recipe;

5X Q5 Reaction Buffer	5 µl
10 mM dNTPs	0.5 µl
10 µM Forward Primer (SmaI-BTB Domain Forward)	1.25 µl
10 µM Reverse Primer (BTB Domain- NotI- Reverse)	1.25 µl
Template DNA (1 ng)	1 µl
Q5 High-Fidelity DNA Polymerase (2,000 units/ml)	0.25 µl
ddH <sub>2</sub> O	To 25 µl

In order to construct the desired vector, the vector backbone and inserts were digested with SmaI at 25°C for 2 hours then with NotI-HF at 37°C for 1 hour.

	Insert	pET-47b (+)
DNA	PCR product	2 µg
10X CutSmart Buffer (NEB)	5 µl	5 µl
SmaI (20,000 U/ml) (NEB)	1 µl	1 µl
NotI-HF (20,000 U/ml) (NEB)	1 µl	1 µl
ddH <sub>2</sub> O	To 50 µl	To 50 µl

Then, CIAP enzyme (Fermentas) treatment was applied to the digested pET-47(+) vector backbone, which was PCR cleaned-up after digestion (elution to 30 µl), to prevent re-ligation of vector on itself.

SmaI and NotI-HF digested pET-47b (+)	30 µl
CIAP Enzyme (20,000U/ml) (Fermentas)	3 µl
10X CIAP Buffer (Fermentas)	5 µl



ddH <sub>2</sub> O	To 50 µl
--------------------	----------

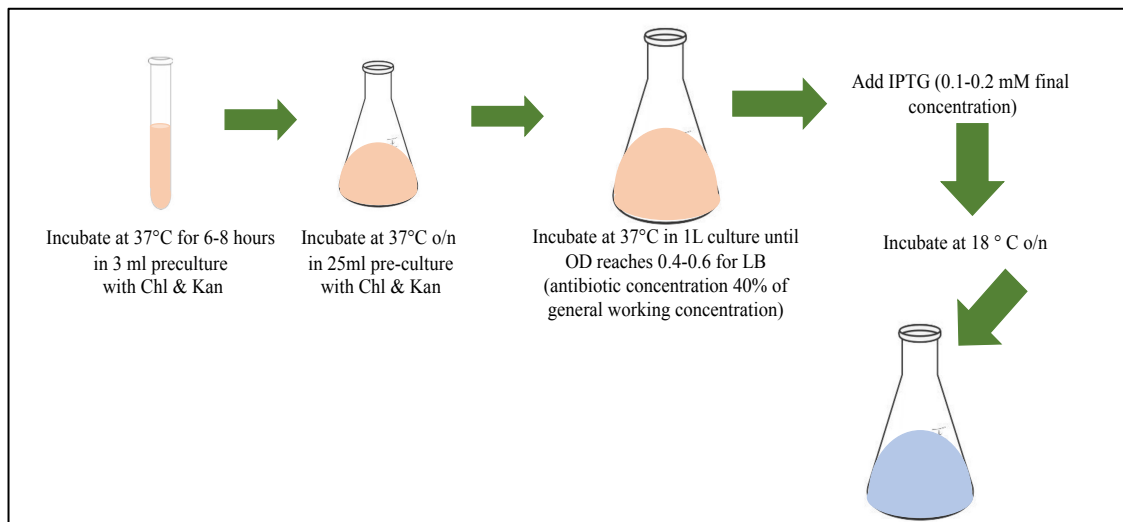
The CIAP enzyme was applied at 37°C for 30 minutes. Then, the obtained vector was run on a 1% agarose gel to separate the double-digested vector from the uncut vector. The corresponding band was extracted from the agarose gel and the DNA was purified. To obtain the digested insert, the reaction mixture was purified with NucleoSpin Gel and PCR Clean-up kit. The ligation reaction was performed according to 3:1 insert to vector ratio. After ligation, transformation into *E. coli* DH5 $\alpha$  competent cells was performed. Single bacterial colonies were picked from LB-Agar plate and their plasmid DNAs were isolated with miniprep protocol. The accuracy of ligation was controlled by performing diagnostic digestions and possible correct candidates were sent to sequencing.

#### 3.2.4.2. His-tagged Protein Expression

pET-47b (+) plasmid has all the necessary features for protein expression and purification such as the presence of T7 promoter, lac operator, LacI gene, N-terminal His-tag, 3C protease recognition site, and kanamycin resistance gene for selection. LacI protein binds to the lac operator in such a way that it eventually prevents the transcription from the T7 promoter. However, when the addition of IPTG to the medium happens, this IPTG competes with LacI protein and inhibits the prevention of transcription. N-terminal His-tag is necessary to perform affinity chromatography. 3C protease recognition site is important if N-terminal His-tag is necessary to be removed.

Initially, pET-47b (+)-BTB domain (for BCL6, FAZF, KAISO, LRF, MIZ1, PATZ2, and PLZF BTBs) plasmids were transformed into *E. coli* Rosetta2 DE3 pLYSs competent cells. Rosetta2 DE3 strains are derived from the BL21 strain. They are specifically designed to express eukaryotic proteins that contain rarely used codons in bacteria. In this strain, extra tRNAs for rare codons and their corresponding promoters are available. The backbone of the rare tRNA-coding vector also has a chloramphenicol resistance gene. Furthermore, the presence of DE3 indicates this strain is a  $\lambda$ DE3 lysogen which refers that a prophage is found as DNA expressing the T7 RNA polymerase gene under the lacUV5 promoter control and protein production happens with the help of IPTG

induction. pLYSs strains produce T7 lysozyme which provides protein purification in a controllable way by preventing T7 RNA polymerase basal expression. Thanks to this, leakage in protein production can be reduced.

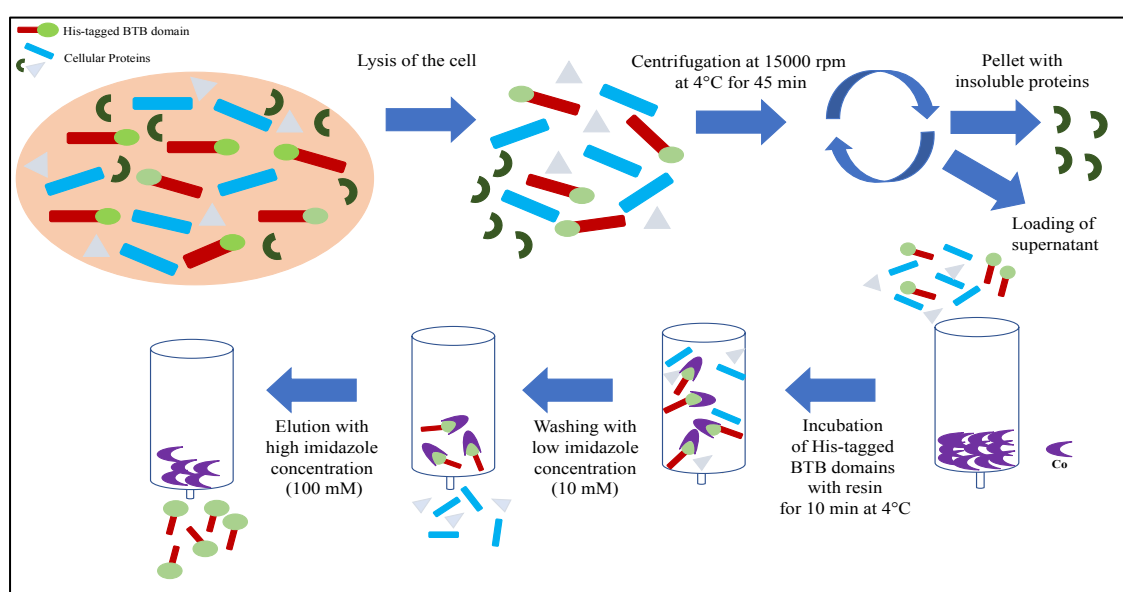


**Figure 3. 1 Bacterial induction and expression of His-tagged proteins**

After transformation, a single colony was randomly picked and inoculated into 3 ml LB medium which was added with 3  $\mu$ l of Chl and Kan antibiotics. This preculture was incubated at 37°C for 6-8 hours with vigorous shaking (221 rpm). Then, it was transferred to 25 ml LB culture in which 25  $\mu$ l Chl and Kan were also supplemented. This culture was incubated overnight at 37°C with vigorous shaking (221 rpm). Finally, 25 ml preculture was transferred to 1 L LB medium. This time, antibiotic concentration dropped to 40% of the general working concentration to decrease resistance effect on cells, promote cell growth and production of protein. This last culture was incubated at 37°C with vigorous shaking (221 rpm) until its optical density at 600 nm (OD<sub>600nm</sub>) was in between 0.4-0.6. When this range was reached, culture was incubated on ice to cool down and then IPTG was added in such a way that final concentration should be 0.1-0.2 mM. Induction of protein expression was performed with the help of IPTG addition by incubating the culture overnight at 18°C in a shaker incubator (180 rpm). (Figure 3.1).

### 3.2.4.3. Affinity Chromatography of His-tagged Proteins

Harvesting of cells was performed at 4000 rpm for 10 minutes and the supernatant was discarded. Then, the pellet was dissolved in 25 ml lysis buffer which should be freshly prepared. The cells were lysed by sonication using Qsonica Q500 at 4°C in a box filled with ice. For sonication, total elapsed time was arranged to 4 minutes and 30 seconds, and pulse was on for 5 seconds and off for 10 seconds. The final cell lysate was spun at 15000 rpm for 45 minutes at 4°C. Meanwhile, the affinity column was washed with ddH<sub>2</sub>O and checked whether it is plugged or not. For cell lysate of 1 L culture, 3 ml HisPur Cobalt Superflow Agarose resin was loaded to the column. The resin solution is diluted 1:1 in ethanol thus the actual volume of resin added was 1.5 ml. The resin was washed with ddH<sub>2</sub>O two times to get rid of ethanol and then washed with 10 ml of IMAC-A two times to equilibrate the column. When centrifugation was completed, the supernatant containing soluble proteins was loaded to the column and the protein-resin mixture was incubated with end-to-end rotation at 4°C for about 30 minutes. After this incubation, flow through was collected in a 50 ml tube. This collected fraction includes the proteins without His-tag. Then, the resin-protein complex was washed with 10 ml of IMAC-A for three times. Finally, the His-tagged protein was eluted by the use of IMAC-B solutions with different concentrations. Starting from the lowest imidazole concentration, IMAC-B solutions were loaded to column and fractions were collected in 15 ml tubes at 4 °C (Figure 3.2).



**Figure 3. 2 Steps of immobilized metal affinity chromatography (IMAC)**

#### **3.2.4.4. SDS-PAGE gel and Coomassie Blue Staining**

Preparation of 14% separating gel and 4% stacking gels was performed and the samples from each protein purification step, which can be listed as cell lysate, after sonication, pellet, non-retained fraction and elutes, were mixed with 4X protein loading buffer. Denaturation of those samples were carried out at 95 °C for 10 minutes. When the samples were loaded to the wells, they were run with 1X running buffer for about 2-2.5 hours. After running, the gel was separated from the glasses carefully and the stacking gel was removed as well. Then the remaining gel was placed into the staining solution for 2-3 hours and then into the destaining solution overnight.

#### **3.2.4.5. Concentrating Proteins**

When the protein is too diluted, it is concentrated with the help of concentrator tubes which have a specific molecular weight cut-off value. If size of protein is smaller than this cut-off value, the protein will pass to the bottom. Otherwise, it will stay at the top. Initially, ddH<sub>2</sub>O was put into the concentrator tube and spun at 3000 g until all the water went down. Then, the protein of interest was added, spun for 1 minute and protein concentration was measured by NanoDrop. For this measurement, the liquid passed to the bottom of the tube was used as a blank. Concentrator falcon was spun for several times at 3000 g until concentration or volume of protein reached to desired values. For this study, the used concentrator tubes had 10 kDa or 5 kDa molecular weight cut-off.

#### **3.2.4.6. Size-exclusion Chromatography**

When there are some other non-specific proteins in the eluted version of total protein sample after His-tag affinity chromatography, size exclusion chromatography is carried out to remove non-specific proteins from the desired protein according to their size differences. AKTA pure was used as size exclusion chromatography. Superdex 200 Increase 5/150 GL and Superdex 200 Increase 10/300 GL columns were used during the procedure. Gel filtration buffer was used for the equilibration of the column. Before this

equilibration, washing of the pumps and column with autoclaved filtered ddH<sub>2</sub>O was performed. For the washing, at least 1 column volume (CV) was used in terms of water amount. Then, before starting the experiment, the column and whole system were equilibrated with gel filtration buffer whose volume should be at least 1.5 CV. For the injection of protein sample to AKTA pure, sample volume should be equal or lower than 50 µl for Superdex 200 Increase 5/150 GL column; 500 µl for Superdex 200 Increase 10/300 GL column. The protein was injected into the corresponding loop for each column type with a syringe and the experiment was initiated. When protein completed its passage from in front of a UV detector, it was collected in a 96-well collector plate. Depending on UV absorbance at 280 nm, the location of desired protein within the plate was found. When the samples from different peak positions of UV-absorbance graph were selected, they were loaded to SDS gel to perform SDS-PAGE for determination of our desired protein in the pure form and its boundaries of purity.

### **3.2.5. Surface Plasmon Resonance**

For surface plasmon resonance (SPR) experiments, BIACORE T200 was applied. SPR is a technique used to identify protein-protein interactions quantitatively. Also, kinetic parameters of the interactions among these proteins can be studied with the help of SPR. The logic behind this technique is based on the changes in refractive indices when polarized light hits to a gold film. With the help of a prism, the light coming from a light source is focused on the gold film. The reflected light is collected with a detector. When there is a change in the mass attached to the gold surface, there will be a change in the refractive index of the medium at the interface as well. According to mass change on the surface of gold film, the refractive index differs proportionally and absorbance of some light part happens. All these events give information about the quantification of binding taking place on the surface. It is represented as a resonance unit (RU).

In this method, ligand is known as the attached molecule on the gold surface. Analyte is known as the molecule found in the mobile phase that flows on the surface of the chip with the running buffer. pH scouting, ligand immobilization on the surface, ligand injection and surface generation are some of the basic steps in SPR. For this study,

PATZ1-BTB, PATZ2-BTB and MIZ1-BTB were immobilized covalently on the Sensor Chip CM5. CM-series sensor chips have a carboxymethylated dextran matrix attached to the gold surface. Ligand is covalently bound to sensor surface with amine coupling. To do immobilization, surface of the gold chip should initially be activated. Activation is performed in such a way that mixture of 1-ethyl-3-(3-dimethylaminopropyl) carbodiimide (EDC) and N-hydroxysuccinimide (NHS) is passed on the surface and while being passed, they react with carboxyl groups of the dextran. Eventually, succinimide esters are formed on the surface. These reactive ester groups are able to interact with amino groups of the ligand and thus form covalent bonds between dextran surface and ligand. In order to result in successful reaction, electrostatic interactions among ligand and dextran should be strong. The dextran matrix has negative charge when pH is above 3.5. pH of immobilization buffer, which is acetate buffer, should be above 3.5 and below the isoelectric point of the ligand (it means that ligand should be positively charged and matrix should be positively charged) so that efficient electrostatic interactions of the ligand to the surface can be achieved. For determining the suitable pH of acetate buffer for coupling, pH scouting step was performed. Acetate buffers with different pH values, 4, 4.5, 5, 5.5, were used for pH scouting and the interaction among the surface and ligand was examined by checking differences in their RU values.

After pH scouting was done, immobilization with chosen acetate buffer (pH 4 for MIZ1-BTB, pH 5 for PATZ1 and pH 4 for PATZ2) was performed as a next step. Then, deactivation of unbound surface was carried out with the help of ethanolamine (pH 8.5). Different concentrations of analytes, MIZ1-BTB, PATZ1-BTB and PATZ2-BTB, passed on the surface separately. Dilutions for analytes were done with HBS-EP + running buffer. After this step, regeneration of the surface was performed to take away analyte bound to the ligand on the surface. This is one of the most crucial steps because it influences the binding activity of the surface for upcoming experiments and chip life-time. In order to regenerate the surface, glycine pH 3 was used. Thanks to regeneration, chip is prepared for other experiments.

### 3.2.6. Fluorescent Two- Hybrid (F2H) Assay

#### 3.2.6.1. Vector Construction for pcDNA 3.1/ myc-His (-) B- TagGFP-BTB Domain and pcDNA 3.1/ myc-His (-) B-TagRFP-BTB Domain

pcDNA 3.1/ myc-His (-) B is a vector used for construction of mammalian expression systems. It was selected for cloning due to the presence of NheI, XhoI and NotI cut sites in its multiple cloning site. Initially, TagGFP was taken from TagGFP-p53 plasmid via PCR amplification followed by PCR clean-up and NheI and XhoI digestion. TagRFP was obtained from TagRFP-MDM2 plasmids via its digestion with NheI and XhoI (TagGFP-p53 and TagRFP-MDM2 plasmids were supplied from F2H Assay Chromotek). pcDNA 3.1/ myc-His (-) B vector was also digested with these two enzymes to create compatible ends for ligation. These digestions were performed in thermocycler at 37°C for 2 hours.

5X Q5 reaction buffer	5 µl
10 mM dNTP	0.5 µl
10 µM forward primer (CMV Forward)	1.25 µl
10 µM reverse primer (TagGFP-XhoI&SmaI-Reverse)	1.25 µl
Template DNA (1 ng)	1 µl
Q5 HF DNA Polymerase	0.25 µl
ddH <sub>2</sub> O	To 25 µl

	TagGFP	TagRFP	Vector
DNA	PCR Product	1 µg	2 µg
CutSmart Buffer (NEB)	5 µl	5 µl	5 µl
NheI-HF (20,000 U/ml) (NEB)	0.5 µl	0.5 µl	0.5 µl
XhoI (20,000 U/ml) (NEB)	0.5 µl	0.5 µl	0.5 µl
ddH <sub>2</sub> O	To 50 µl	To 50 µl	To 50 µl

After digestions, inserts were cleaned by NucleoSpin Gel and PCR Clean-up kit. Digested vector was dephosphorylated and then run on 1% agarose gel to separate digested DNA from undigested one. Digested part was gel extracted and purified by NucleoSpin Gel and

PCR Clean-up kit. Insert to vector molar ratio was adjusted to 3:1 for each cloning and ligation was performed according to this setting. Transformation of ligation mixture into DH5 $\alpha$  competent cells was followed and single colonies were taken for isolation of their plasmid DNA. These plasmids were controlled via diagnostic digestion with suitable enzymes and their corresponding conditions and buffers. Positive colonies were selected and sent for sequencing.

When pcDNA 3.1/ myc-His (-) B- TagGFP and pcDNA 3.1/ myc-His (-) B- TagRFP constructs were obtained, next step was the addition of selected BTB domains to the ends of these tags. This step was performed differently for each construct. For pcDNA 3.1/ myc-His (-) B- TagGFP, BTB domains were initially PCR amplified by using their corresponding forward primers with XhoI and reverse primers with NotI cut sites. Then, PCR products were cleaned up by NucleoSpin Gel and PCR Clean-up kit. Inserts and vectors were digested with XhoI and NotI enzymes for 2 hours at 37°C.

5X Q5 reaction buffer	5 $\mu$ l
10 mM dNTP	0.5 $\mu$ l
10 $\mu$ M forward primer (XhoI-BTB Domain)	1.25 $\mu$ l
10 $\mu$ M reverse primer (BTB Domain-NotI)	1.25 $\mu$ l
Template DNA (1 ng)	1 $\mu$ l
Q5 HF DNA Polymerase	0.25 $\mu$ l
ddH <sub>2</sub> O	To 25 $\mu$ l

	BTB Domain	Vector
DNA	PCR Product	2 $\mu$ g
CutSmart Buffer (NEB)	5 $\mu$ l	5 $\mu$ l
Not-HF (20,000 U/ml) (NEB)	1 $\mu$ l	1 $\mu$ l
XhoI (20,000 U/ml) (NEB)	1 $\mu$ l	1 $\mu$ l
ddH <sub>2</sub> O	To 50 $\mu$ l	To 50 $\mu$ l

After digestion, inserts were PCR cleaned-up, vector was dephosphorylated, run on the gel to obtain only the digested part and purified. The molar concentration ratio of insert to vector (3:1) was calculated for each insert and vector and ligation reaction was set up



accordingly. After ligation; transformation, picking of colonies for plasmid DNA isolation, diagnostic digestion and sequencing steps were performed in the given order. For pcDNA 3.1/ myc-His (-) B- TagRFP, BTB domains were taken from pET-47b (+)-BTB Domain constructs by digestion of them with SmaI and NotI enzymes. Meanwhile, pcDNA 3.1/ myc-His (-) B- TagRFP vector was digested with XhoI enzyme for 2 hours at 37°C first, then it was treated with Klenow fragment for 15 minutes at 37°C. In order to stop the reaction, heating at 65°C for 15 minutes was performed. This treatment was carried out to blunt the 5' overhang created after XhoI digestion. By blunting, 5' end was aimed to make compatible with the 5' end of BTB domain insert created by SmaI digestion.

	pcDNA 3.1/ myc-His (-) B- TagRFP
DNA	5 µg
10X Buffer R (Fermentas)	3 µl
XhoI (Fermentas)	1 µl
ddH <sub>2</sub> O	To 30 µl

	pcDNA 3.1/ myc-His (-) B- TagRFP
Linear DNA	30 µl
10X Reaction Buffer for Klenow	5 µl
10 mM dNTP	1.25 µl
Klenow fragment (Fermentas)	1 µl
ddH <sub>2</sub> O	To 50 µl

After Klenow fragment treatment, vector was digested with NotI enzyme. After SmaI and NotI digestions, the inserts were cleaned up. The digested vector was run on the gel, double digested part of it was extracted and purified. 3:1 molar concentration ratio of insert to vector was calculated and according to this calculation, ligation mixture was prepared. After ligation; transformation, colony selection, plasmid DNA isolation, diagnostic digestion and sequencing parts were carried out respectively.

### 3.2.6.2. PEI Transfection of F2H Assay Plasmids

The day before transfection, BHK cells were seeded in 6 well plate in such a way that each well should have 150,000 cells. For transfection, 10  $\mu$ l PEI was used for all conditions. Combinations of plasmids used and their amounts are shown in Table 3.4.

**Table 3. 5 Combination of plasmids and their amounts**

	GBP- LacI	TagGFP- BTB	TagRFP- BTB	TagGFP	TagRFP	BFP- NCOR	BFP- SMRT	BFP- Only
#1	500 ng	500 ng	1000 ng	-	-	-	-	-
#2	1000 ng	1000 ng	-	-	-	-	-	-
#3	1000 ng	-	1000 ng	-	-	-	-	-
#4	500 ng	-	1000 ng	500 ng	-	-	-	-
#5	500 ng	500 ng	-	-	-	1000 ng	-	-
#6	500 ng	500 ng	-	-	-	-	1000 ng	-
#7	500 ng	500 ng	-	-	-	-	-	1000 ng
#8	500 ng	-	-	500 ng	-	1000 ng	-	-
#9	500 ng	-	-	500 ng	-	-	1000 ng	-
#10	500 ng	-	-	500 ng	-	-	-	1000 ng
#11	500 ng	500 ng	500 ng	-	-	500 ng	-	-
#12	500 ng	500 ng	500 ng	-	-	-	500 ng	-

#13	1000 ng	-	-	-	-	1000 ng	-	-
#14	1000 ng	-	-	-	-	-	1000 ng	-
#15	-	1000 ng	-	-	-	1000 ng	-	-
#16	-	1000 ng	-	-	-	-	1000 ng	-
#17	-	-	1000 ng	-	-	1000 ng	-	-
#18	-	-	1000 ng	-	-	-	1000 ng	-
#19	-	500 ng	750 ng	-	-	-	-	750 ng
#20	500 ng	-	750 ng	-	-	750 ng	-	-
#21	500 ng	-	750 ng	-	-	-	750 ng	-
#22	2000 ng	-	-	-	-	-	-	-

### 3.2.6.3. Live Cell Imaging

After 24 hours from transfection, BHK cells were examined with live cell imaging microscope (ZEISS Axio Observer Z1) and their photographs were taken.

## 4. RESULTS

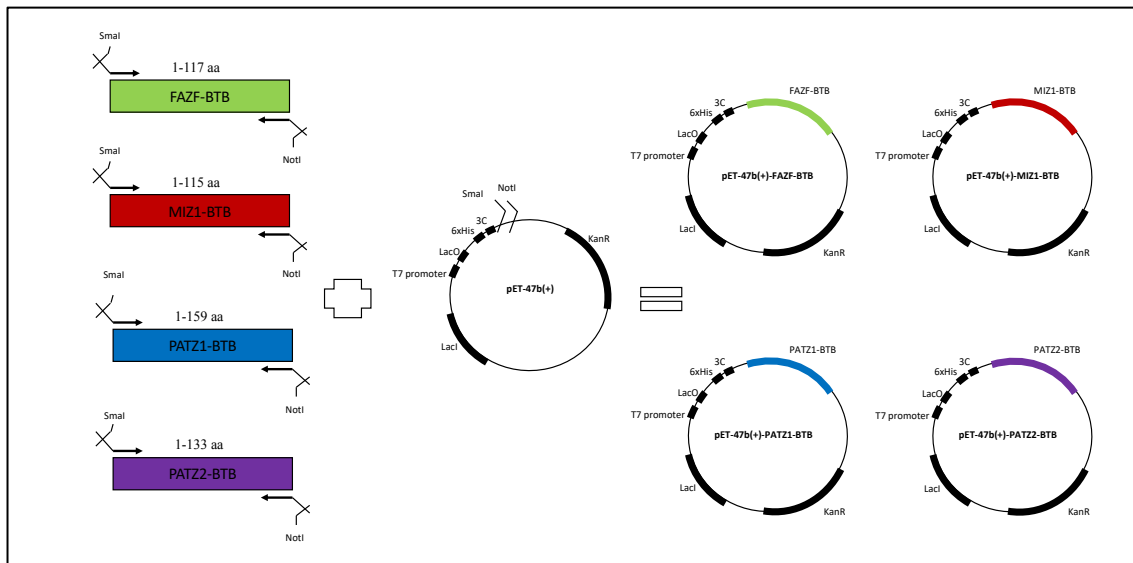
### 4.1. Protein Purification of FAZF-BTB, MIZ1-BTB, PATZ1-BTB and PATZ2-BTB domains

In this study, we aimed to develop an assay for screening the interactions between various BTB domain transcription factors and systematically analyze the networks of these interactions with the help of this assay. Because BTB domains are the responsible unit of the interactions between these proteins, only this part of the whole protein was used during all experimental procedures. Previous studies have shown the presence of many BTB homodimers but only the limited numbers of heterodimers. To obtain a better representation of how BTB domains interact, a robust interaction matrix is required. Thus, we first analyzed *in vitro* interactions between BTB domains using surface plasmon resonance. In this experiment, His-tagged BTB-domains were attached to the surface of a CM5 chip and other His-tagged BTB-domains were passed over this chip. With this experimental set-up, we were able to examine the homodimerization and heterodimerization partners of selected BTB domains. The selected BTB domains and their estimated molecular weights for SPR are shown in Table 4.1.

**Table 4. 1 Estimated molecular weights of selected BTB domains in this part of the study**

BTB Domain	Molecular Weight (kDa) for monomers
FAZF-BTB	14.86
MIZ1-BTB	14.97
PATZ1-BTB	19.20
PATZ2-BTB	17.07

To begin with, we constructed four bacterial expression plasmids which were expected to express His-tagged FAZF-BTB, MIZ1-BTB, PATZ1-BTB and PATZ2-BTB domains. Sequences of FAZF-BTB, MIZ1-BTB, PATZ1-BTB and PATZ2-BTB domains were PCR-amplified from cDNA of WT HCT116 colon cancer cell lines. These amplifications were performed by using a forward primer with a SmaI cut site and reverse primer with a NotI cut site. SmaI and NotI digested PCR products were cloned into a pET-47B (+) vector backbone digested with the same enzymes as well (Figure 4.1).



**Figure 4. 1 Construction of bacterial expression plasmids for selected BTB domains**

Sequences of FAZF-BTB, MIZ1-BTB, PATZ1-BTB and PATZ2-BTB domains were amplified by using the corresponding primers which were provided with suitable SmaI and NotI restriction enzyme cut sites. There were stop codons after each BTB domain sequence. The digested PCR products were cloned into the SmaI-NotI digested pET-47b (+) plasmid which is the bacterial expression vector.

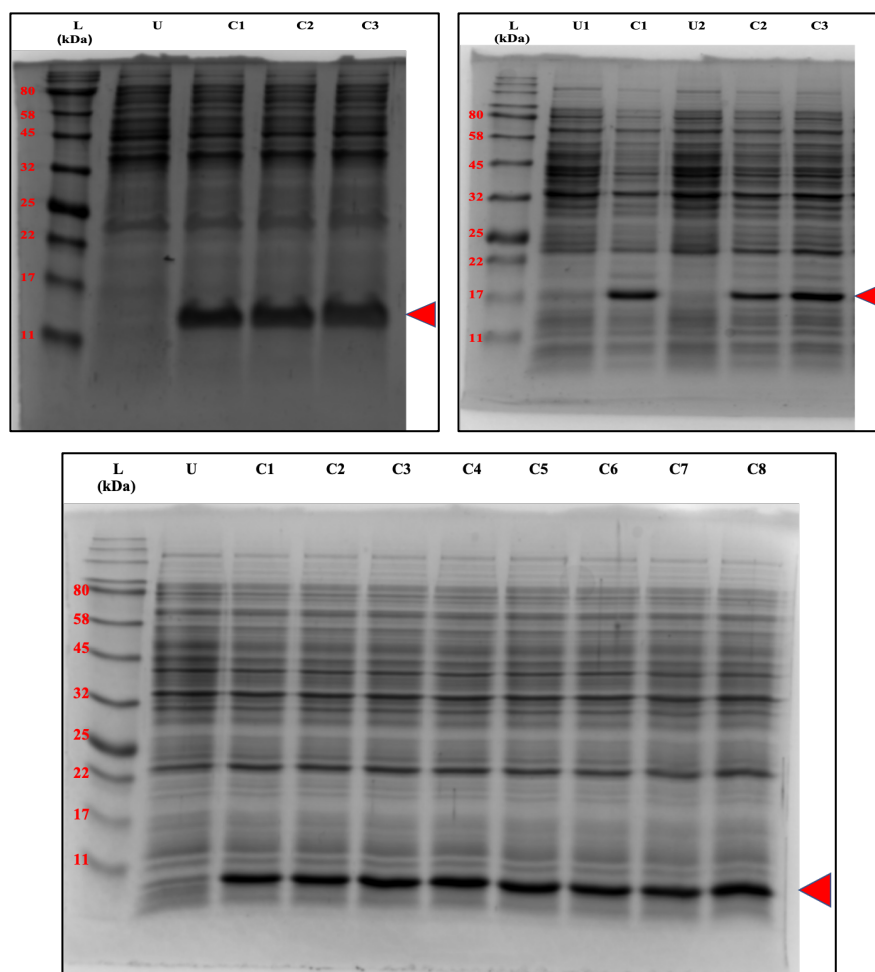
Next, we transformed pET-47b (+)-FAZF-BTB, pET-47b (+)-MIZ1-BTB, pET-47b (+)-PATZ1-BTB and pET-47b (+)-PATZ2-BTB constructs into the Rosetta2 DE3 pLysS *E. coli* expression strain. This strain was chosen to express our eukaryotic proteins expressed from pET plasmids with the help of a chloramphenicol-resistant plasmid from which tRNAs for rare codons are expressed. The designed pET47b (+) plasmids expressed BTB domain proteins with an N-terminal His-tag used for purification by affinity chromatography. In these plasmids, protein expression from the T7 promoter is inhibited due to the expression of the LacI protein which is expressed from the same plasmid. This protein binds to Lac operator sites situated next to the T7 promoter and blocks the activity of this promoter by preventing the binding of T7 RNA polymerase to it. When cells are

treated with IPTG, an inducer that binds to LacI and prevents its binding to the Lac operator site, releasing LacI mediated repression. In the absence of LacI/Lac operator binding, T7 RNA polymerase can associate with the T7 promoter to initiate transcription.

Before starting with large scale protein production, we performed a colony screening assay by picking random colonies after transformation and checked their protein expression capabilities in a small-scale. Induction of expression was performed by the addition of 0.1 mM IPTG to each culture. The results of all colony screening trials were positive (Figure 4.2) and confirmed that the BTB domain expression constructs in fact were capable of expressing these proteins in *E.coli*.

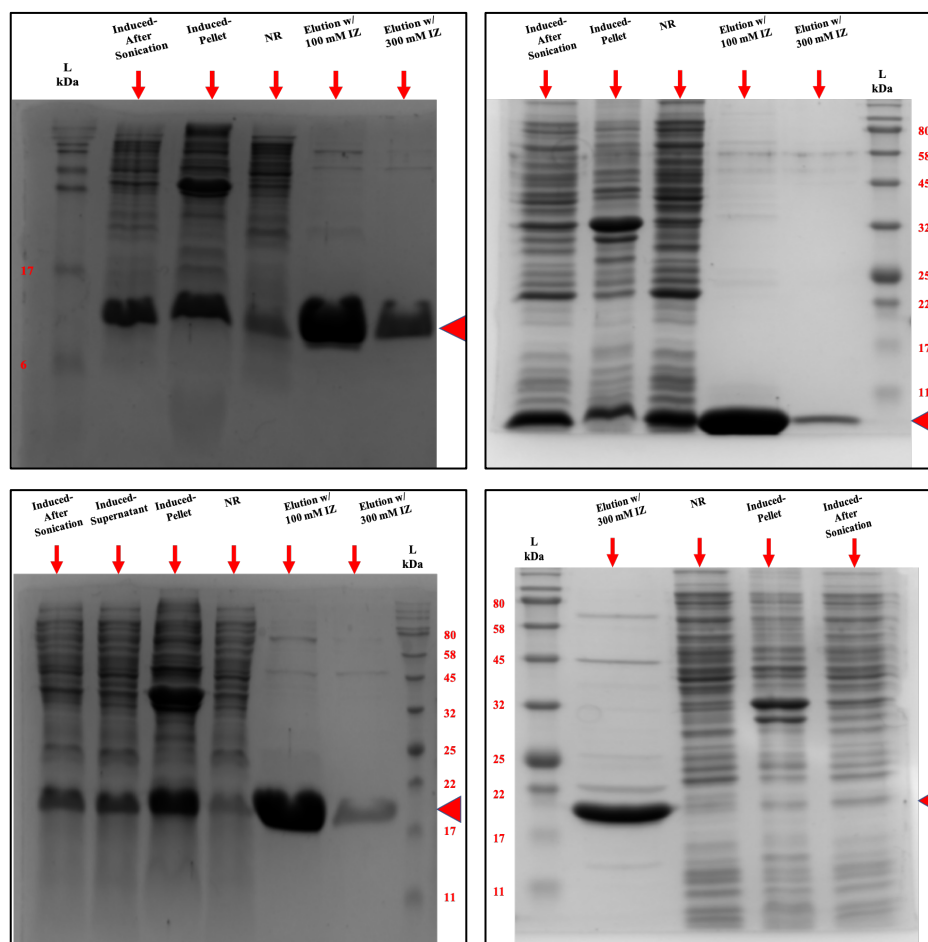
For the large-scale protein production and purification, we continued with one of the positive colonies. For PATZ1-BTB, we used a construct in the same bacterial strain that was previously shown to express, thus we directly purified it in a large scale. We prepared 1 L LB medium with corresponding antibiotics to culture the transformed bacteria. This culturing was carried out at 37°C (221rpm) until optical density at 600 nm reached to a value between 0.4 and 0.6. Then, we added 0.1 mM IPTG to each culture and put the cultures to shaker incubator overnight at 18°C for IPTG induction. The next day, we carried out affinity chromatography purification to obtain purified His-tagged BTB domains (see section 3.2.6.3.) and visualized our samples by SDS-PAGE. The expected molecular weights of FAZF-BTB, MIZ1-BTB, PATZ1-BTB and PATZ2-BTB were 14.86, 14.97, 19.20 and 17.07 kDa respectively and we obtained these values (except for MIZ1-BTB) at 100 mM imidazole (IZ) elution (except for PATZ1-BTB). The band we got at 100 mM IZ elution for MIZ1-BTB was lower than expected in terms of molecular weight and PATZ1-BTB domain band was obtained at 300 mM IZ elution. Moreover, the eluted BTB domains contained contaminant proteins, which were larger than our BTB domains (Figure 4.3). Furthermore, bands for same proteins were seen in fractions of sonicated lysate, non-retained (NR) and pellet samples. This means that our proteins were not 100% soluble because the parts in the pellet shows the insoluble fractions. Obtaining proteins in the NR fraction was not desired because it shows that we were not able to collect all the expressed proteins to completion.

Next, we concentrated our proteins with the help of a concentrator that has 10 kDa molecular weight cutoff (MWCO) to a volume of approximately 1 ml. This was necessary to load our samples to the AKTA pure size exclusion chromatography purification and also for removing the contaminant proteins. The final concentrations of our samples were 8.15 mg/ml for FAZF-BTB, 12.64 mg/ml for MIZ1-BTB, 6.67 mg/ml for PATZ2-BTB and 20 mg/ml for PATZ1-BTB.



**Figure 4. 2 Colony screening for FAZF-BTB, PATZ2-BTB and MIZ1 BTB domains**

FAZF-BTB (on the top-left), PATZ2-BTB (on the top-right) and MIZ1-BTB (at the bottom) domains were expressed in Rosetta2 DE3 pLysS in a small scale. 14% SDS gel was used for SDS-PAGE and expected sizes of proteins are around 14.86, 17.07 and 14.97 kDa respectively.



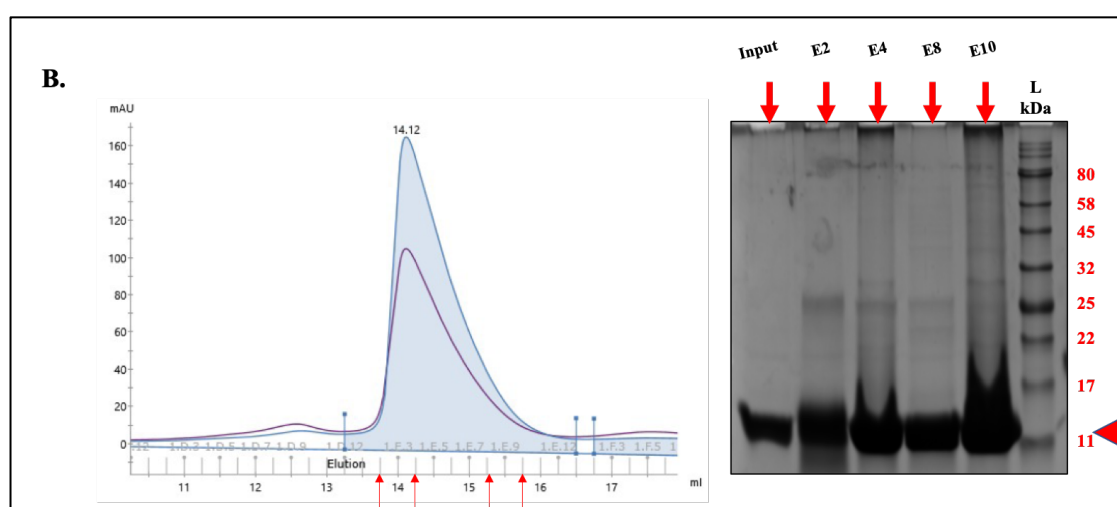
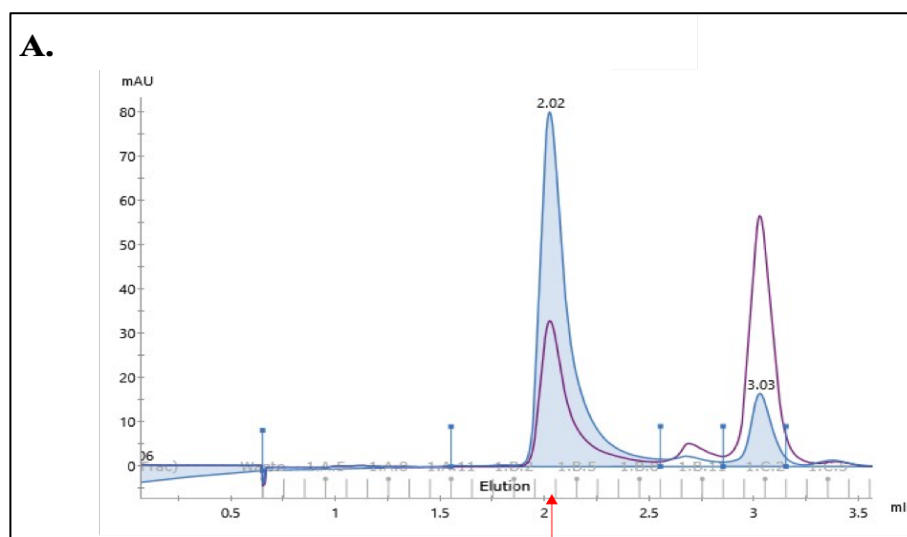
**Figure 4. 3 Affinity purification of His-tagged FAZF-BTB, MIZ1 BTB, PATZ1-BTB and PATZ2-BTB domains**

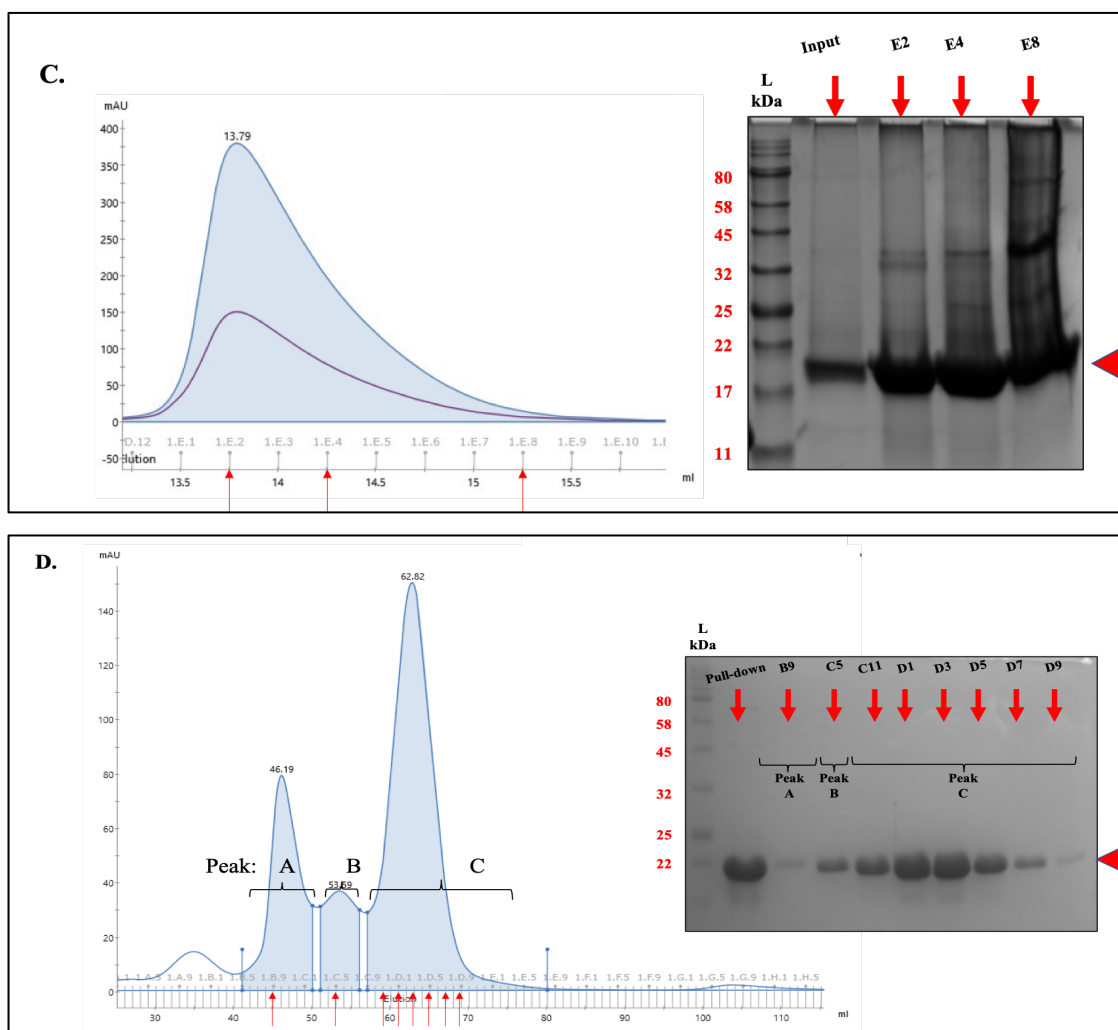
FAZF-BTB (on the top-left), MIZ1-BTB (on the top-right) and PATZ2-BTB (at the bottom-left) and PATZ1-BTB (at the bottom-right) domains were purified with affinity purification by using HisPur Cobalt Superflow Agarose resin (Thermo Fisher Scientific). The collected samples from each step were visualized by 14% SDS-PAGE and expected sizes of proteins are around 14.86, 14.97, 19.20 and 17.07 kDa respectively.

As a next step, we performed size exclusion chromatography (SEC) according to the guidelines in section 3.2.6.6. Before sample injection, we calibrated the column (Superdex 200 Increase 5/150 GL) used for the FAZF-BTB domain sample because it required calibration before use. For this purpose, low molecular weight (LMW) kit was used and a calibration curve was calculated (Figure 4.5). For MIZ1-BTB and PATZ2-BTB domains, Superdex 200 Increase 10/300 GL column was used, which was already calibrated. For the PATZ1-BTB domain, a HiLoad16/60-SD75 column was used and no calibration was performed for this already-calibrated column. After SEC was completed, we collected the purified protein from the peaks measured by absorbance at 280 nm for MIZ1-BTB, PATZ1-BTB and PATZ2-BTB (Figure 4.4.A, B, C and D). For FAZF-BTB,



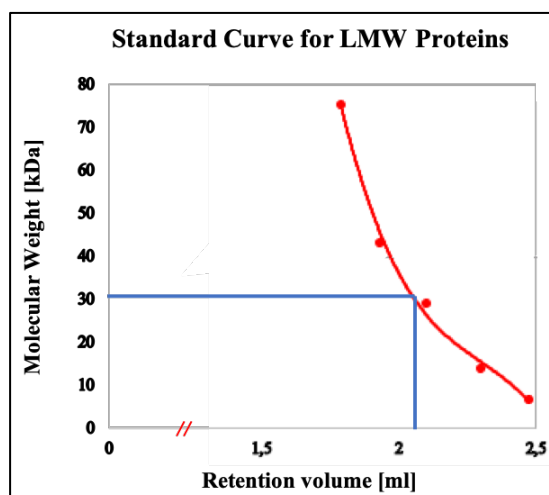
we only checked the accuracy of molecular weight of the dimer from the graph we obtained. The expected molecular weight of FAZF-BTB homodimer was 29.72 kDa. When we examined the graph (Figure 4.5.A), we could see that the peak at 280 nm absorbance was obtained when the retention volume was 2.02, which corresponds to the MW around 30 kDa according to the calibration curve (Figure 4.4). This means that theoretically calculated MW of FAZF-BTB dimer shows high concordance with the experimental value. Moreover, there was another peak whose retention volume was 3.03 ml most likely due to the presence of imidazole in the sample. Literature review confirmed that this peak arises to the absorbance properties of the ring structure of imidazole.





**Figure 4. 4 Size exclusion chromatography result of FAZF-BTB, MIZ1-BTB, PATZ2-BTB and PATZ1-BTB domains**

We carried out size exclusion chromatography by the use of AKTA Pure for removal of contaminant proteins. The blue graph exhibited absorbance at 280 nm which represents the presence of proteins. On the other hand, purple graph showed absorbance at 254 nm which represents the presence of DNA contamination. (A) The graph showed the curve of absorbance (mAU) versus elution volume (ml) of His-tagged FAZF-BTB domain. The peak at elution volume of 2.02 ml was the point where His-tagged FAZF-BTB domain was expected to come. (B), (C) and (D) On the left sides, absorbance versus elution volume graphs of His-tagged MIZ1-BTB (part B), PATZ2-BTB (part C) and PATZ1-BTB (part D) domains were available. The elution fractions around the peak of each protein were collected and visualized with SDS-PAGE to analyze their purities. Expected sizes of His-tagged MIZ1-BTB, PATZ2-BTB and PATZ1-BTB are around 14.97, 17.07 and 19.20 kDa respectively. Obtained results were compatible with these expected values. Input was the initial sample taken before the injection.



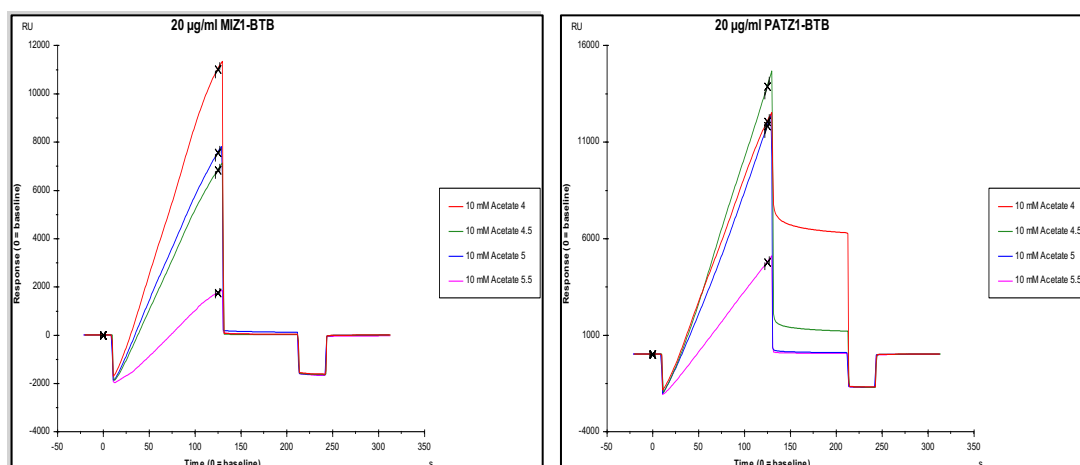
**Figure 4. 5 Standard curve for low molecular weight proteins**

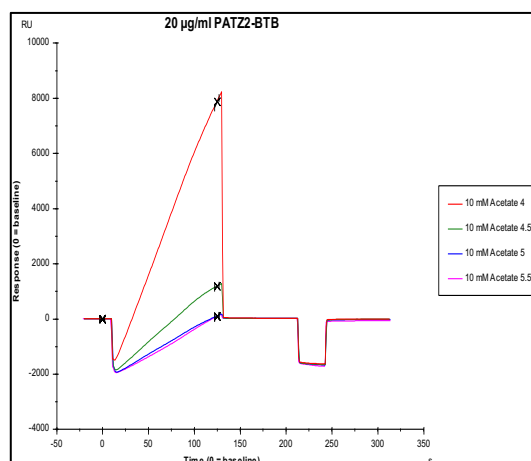
For the calibration of Superdex 200 Increase 5/150 GL column, low molecular weight (LMW) kit was used. It contains five proteins with their molecular weights ranging from 6.5 kDa to 75 kDa. The retention volume of the peak of FAZF-BTB was 2.02 ml. This value approximately corresponds to the MW between 30 and 33 kDa.

For His-tagged MIZ1-BTB, PATZ2-BTB and PATZ1-BTB, we collected samples from elution fractions. E2, E4, E8 and E10 were the samples for MIZ1-BTB. E2, E4 and E8 were the samples for PATZ2-BTB. B9, C5, C11, D1, D3, D5, D7 and D9 were the collected samples for PATZ1-BTB. We selected these fractions around the peaks obtained in order to understand the boundaries of pure proteins. Then, we analyzed them with SDS-PAGE and we ended up with the fact that for MIZ1-BTB, desired protein was found between E2 and E8 fractions; for PATZ2-BTB, it was available between E2 and E7; for PATZ1-BTB it was found between C11 and D9. After this decision, from E2 to E8 for MIZ1-BTB; from E2 to E7 for PATZ2-BTB and from C11 to D9 for PATZ1-BTB were pooled and their concentrations were measured individually. They were 1.95 mg/ml, 1.50 mg/ml and 1.67 mg/ml respectively. The final versions of the samples were flash-frozen in liquid nitrogen. In conclusion, the SEC step is important to remove most impurities that were present after affinity chromatography. These double purified samples were used in SPR experiments.

#### 4.2. Screening the interactions of MIZ1-BTB, PATZ1-BTB and PATZ2-BTB domains *in vitro* by surface plasmon resonance (SPR)

We used the surface plasmon resonance assay to determine the interaction affinities of selected purified BTB domains and their capability for homodimerization, heterodimerization, homotetramerization and heterotetramerization by the use of Biacore T200 machine. The first step of this experiment was pH scouting to find an appropriate surface immobilization pH for BTB domains. For this purpose, ligands were diluted in sodium acetate buffers with different pH values (pH 4, pH 4.5, pH 5 and pH 5.5) to reach a final concentration of 20  $\mu\text{g/ml}$  for each sample. The contact time was 120 seconds and the flow rate was 30  $\mu\text{l/min}$ . The response unit (RU) corresponds to the change in refractive index. The binding to the surface was plotted in terms of function of time. In order to select the best pH, we identified the pH at which the highest signal was obtained and where the signal returned to baseline completely. In the light of this information, we chose the pH 4 for MIZ1-BTB, pH 5 for PATZ1-BTB and pH 4 for PATZ2-BTB as immobilization pH (Figure 4.6). pH of immobilization buffer should be higher than 3.5 and lower than isoelectronic point (pI) of ligands to achieve efficient immobilization to the surface. For MIZ1-BTB, PATZ1-BTB and PATZ2-BTB pI values are 5.87, 5.89 and 5.29 respectively. Therefore, we met all the requirements for immobilization step.





**Figure 4. 6 pH scouting experiment for MIZ1-BTB, PATZ1-BTB and PATZ2-BTB**  
20 µg/ml sample was used for each experiment. pH 4, pH 5 and pH 4 were chosen as immobilization pH respectively.

As a next step, we performed immobilization of ligands to the surface of the CM5 chip. We used the same contact time and flow rate and also the corresponding pH values for each sample. Instead of 20 µg/ml protein samples, we decided to use 10 µg/ml and arrange our concentrations by diluting the samples with suitable buffers. We aimed to immobilize 80 RU of protein onto the surface of the chip. We performed the necessary steps according to section 3.2.5. Finally, we immobilized 77.2 RU of MIZ1-BTB, 66.5 RU of PATZ1-BTB and 86.0 RU of PATZ2-BTB ligands. The results for pH scouting and immobilization are shown in Table 4.2.

**Table 4. 2 Overall information and immobilization results related to selected BTB domains**

Protein	MW (Da)	Theoretical pI	pH scouting for immobilization	RUs immobilized & final RUs		Initial concentration (nM)	Flow-cell
MIZ1	29946	5.87	pH 4	77.2	197.0	65100	2
PATZ1	38400	5.89	pH 5	66.5	200.9	43500	3
PATZ2	34148	5.29	pH 4	86.0	196.3	43900	4

After immobilization of selected His-tagged BTB domain protein ligands to the CM5 chip, we carried out a tetramerization test for these proteins. As an analyte, we used MIZ1-BTB, PATZ1-BTB and PATZ2-BTB domains. These three BTB domains were separately passed over the CM5 chip which had been bound by MIZ1-BTB, PATZ1-BTB and PATZ2-BTB domains. For each analyte, we used 7 different concentrations; 0,

15.625 nM, 62.5 nM, 250 nM, 500 nM, 1000 nM and 2000 nM. For all dilutions to get correct concentrations, we used the running buffer, HBS- EP +.

The results were analyzed based on the binding using multiple cycle kinetics (according to the 1:1 binding model) which are shown in Table 4.3, 4.4 and 4.5 and visualized in Figure 4.7. In the table, the U value was also available. This is a parameter which represents the uniqueness of the Rmax value (represents analyte binding capacity theoretically calculated by  $(\text{Analyte MW}/\text{Ligand MW}) \times R_L \times S_m$  in which  $R_L$  is the immobilized ligand and  $S_m$  is the stoichiometric ratio). When the U value is small, the confidence in the results becomes greater. A U value, higher than 25, indicates that the calculated kinetic constant is inaccurate. According to these preliminary experiments, it is possible that MIZ1-BTB and PATZ1-BTB can homo-tetramerize. Also, there was a possible interaction between MIZ1-BTB and PATZ1-BTB which may be interpreted as the presence of MIZ1-PATZ1 heterodimers or homodimers. These interactions were concentration-dependent; the higher the concentration the better the binding we got at the end. We did not observe any interaction between PATZ1 and PATZ2 dimers or PATZ2 and MIZ1 dimers. Unfortunately, the SPR results were not as clean as expected, most likely due to the impurities and imidazole in our protein samples. Normally the SPR curve should be above the baseline while in our experiments the application of analyte resulted in a dip of the RU values, most likely due to solvent and impurity effects.

**Table 4. 3 The obtained results for MIZ1-BTB ligand; MIZ1-BTB, PATZ1-BTB and PATZ2-BTB analytes**

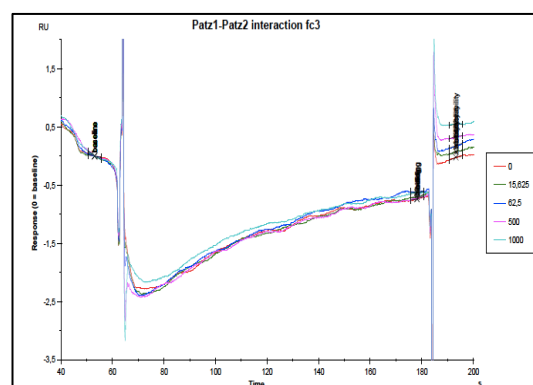
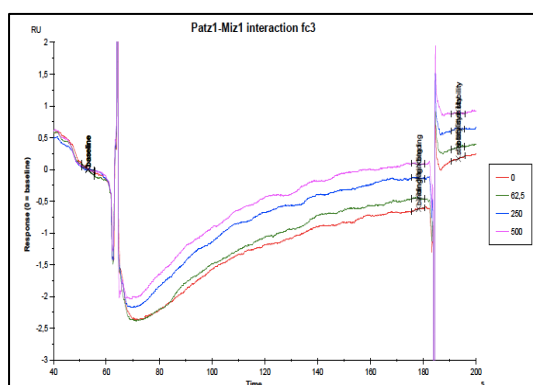
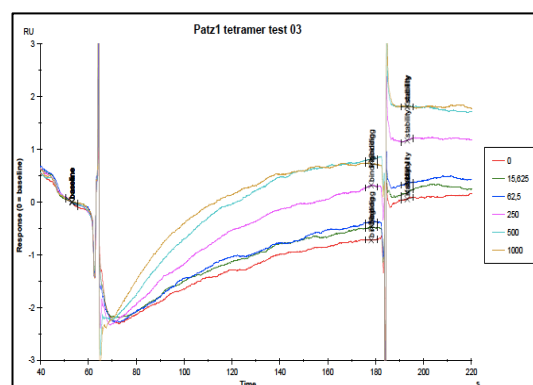
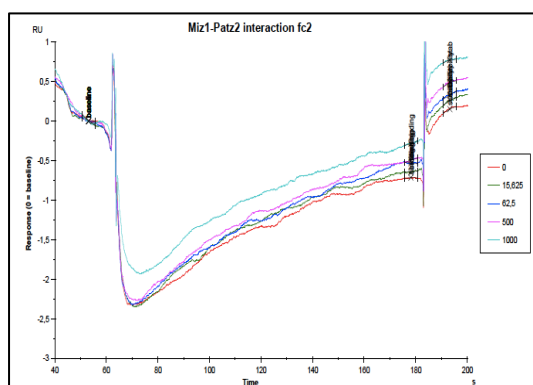
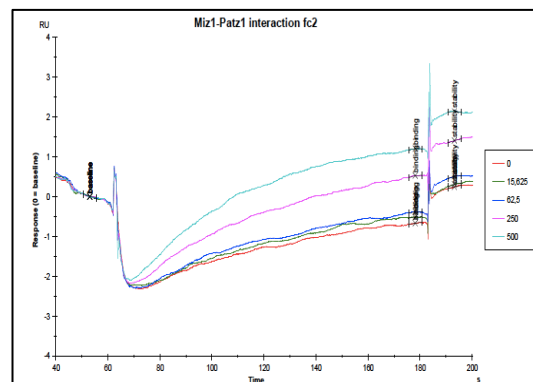
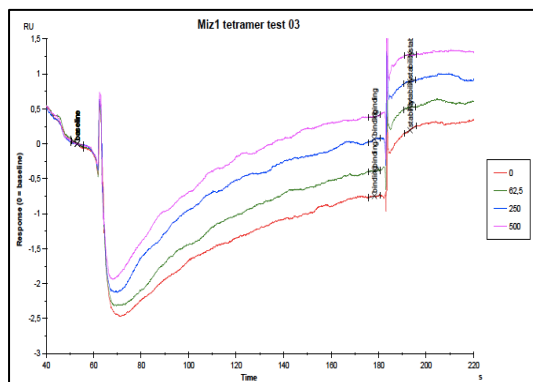
Analyte	Ligand	Analyte MW	Ligand MW	Rmax (theoretical)	Rmax	KD (M)	Chi2 (RU <sup>2</sup> )	U-value
Miz1	Miz1	29946	29946	77.2	1.239	5.387E-8	0.00503	5
Patz1	Miz1	38400	29946	98.9	2.236	3.376E-8	0.00541	4
Patz2	Miz1	34148	29946	88.0	0.4540	2.442E-9	0.0117	43

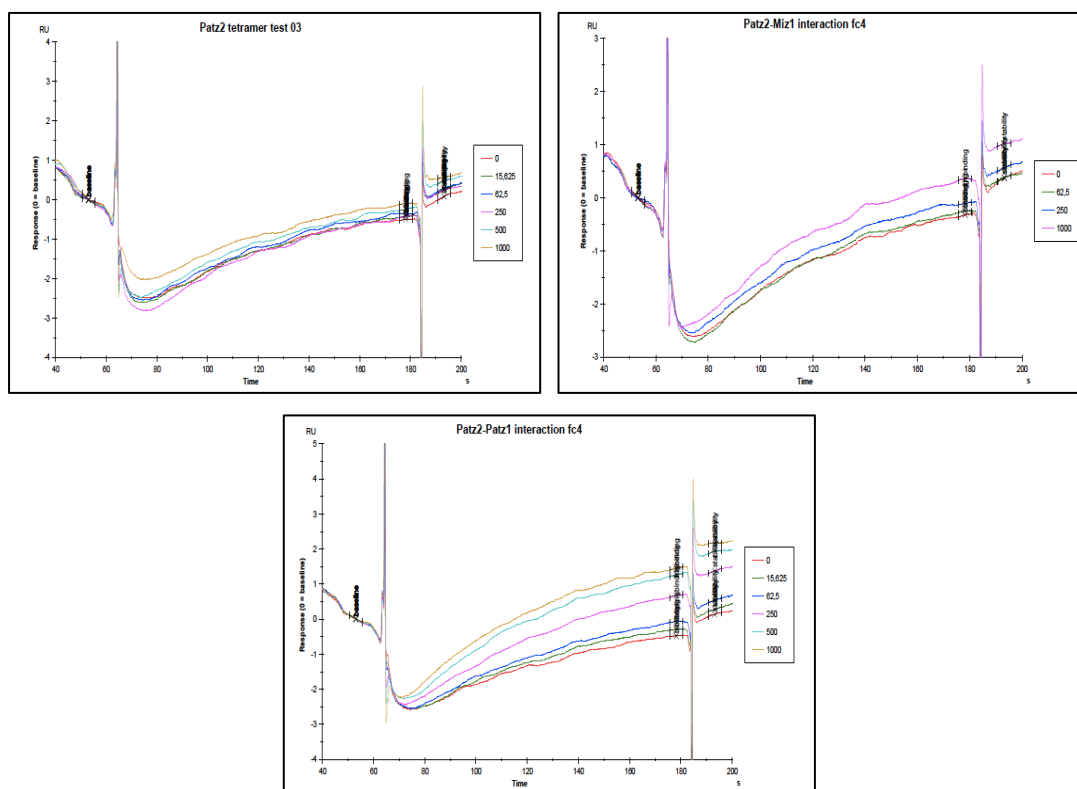
**Table 4. 4 The obtained results for PATZ1-BTB ligand; MIZ1-BTB, PATZ1-BTB and PATZ2-BTB analytes**

Analyte	Ligand	Analyte MW	Ligand MW	Rmax (theoretical)	Rmax	KD (M)	Chi2 (RU <sup>2</sup> )	U-value
Miz1	Patz1	29946	38400	51.8	1.903	3.378E-7	0.0233	33
Patz1	Patz1	38400	38400	66.5	1.950	3.578E-8	0.133	20
Patz2	Patz1	34148	38400	59.1	0.5401	8.744E-10	0.149	95

**Table 4. 5 The obtained results for PATZ2-BTB ligand; MIZ1-BTB, PATZ1-BTB and PATZ2-BTB analytes**

Analyte	Ligand	Analyte MW	Ligand MW	Theoretical Rmax (RU)	Rmax (RU)	KD (M)	Chi2 (RU <sup>2</sup> )	U-value
Miz1	Patz2	29946	34148	75.4	29.42	2.845E-5	0.0966	43
Patz1	Patz2	38400	34148	96.7	1.943	2.010E-8	0.208	26
Patz2	Patz2	34148	34148	86.0	0.3603	2.396E-11	0.163	95





**Figure 4. 7 Binding assay for MIZ1-BTB, PATZ1-BTB and PATZ2-BTB**

After activation and immobilization of His-tagged MIZ1-BTB, PATZ1-BTB and PATZ2-BTB domains, different concentrations of analytes (His-tagged MIZ1-BTB, PATZ1-BTB and PATZ2-BTB domains) were passed over the chip. In the right part of each graph, the concentrations used, 0, 15.625 nM, 62.5 nM, 250 nM, 500 nM, 1000 nM and 2000 nM, were found. The ones that did not follow the regular fashion were excluded from the graphs.

#### **4.3. Fluorescent two-hybrid assay for assessing the rules of dimerization of BTB domains with each other and with NCOR/SMRT corepressors**

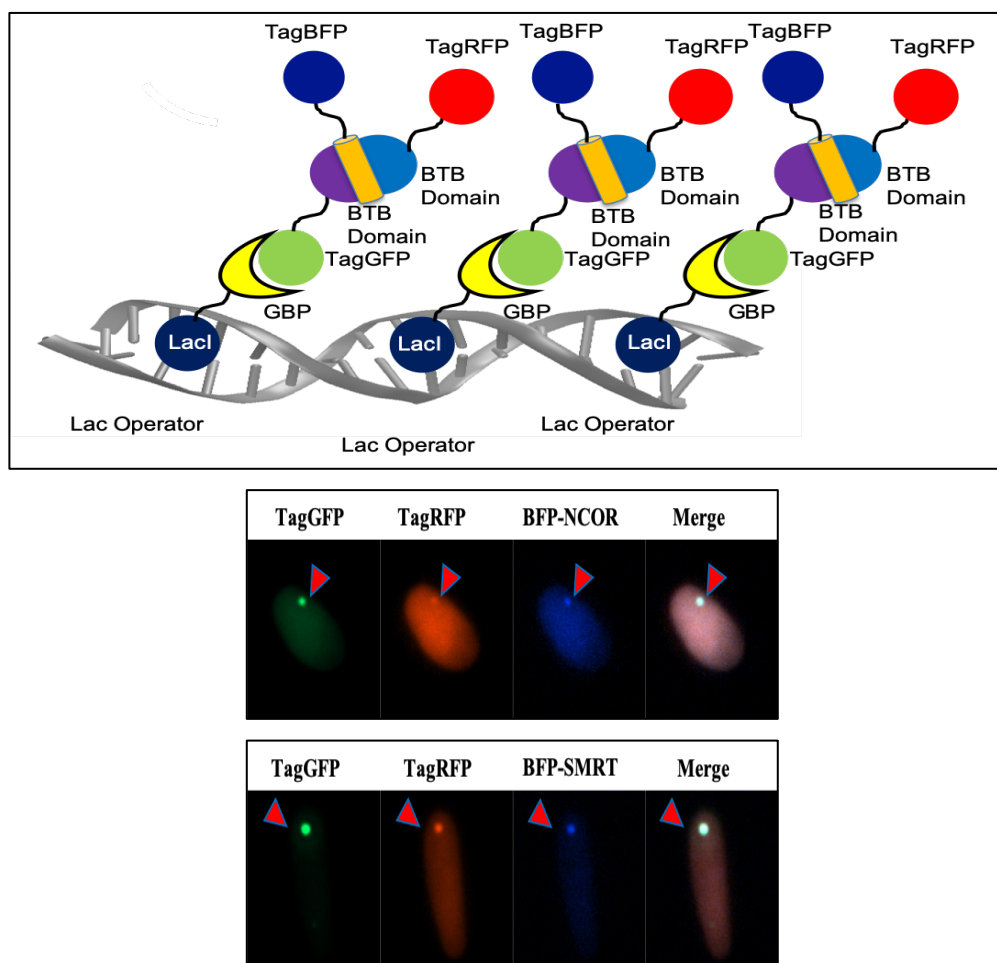
Fluorescent two-hybrid (F2H) assay is a technique used to investigate protein-protein interactions by the use of fluorescent live-cell microscopy. This system is based on tethering strategy which is applied by the use of lac operator sequence. The lac operator sequences are repeatedly and randomly integrated into the genome of baby hamster kidney (BHK) cells. In this system, we tagged our selected BTB domains with green (TagGFP) and red (TagRFP) fluorescent proteins separately and transfected them into these BHK cells together with green fluorescent binding protein (GFP nanobody)-LacI construct (Figure 4.8). Green fluorescence tagged BTB domains have the potential to be



localized on the lac operator site by the use of GBP-LacI construct because the LacI part can bind to this operator site and GBP part can recruit GFP-tagged BTB domains by binding to their GFP sides. Eventually, green focus formation occurs in the nucleus. Red fluorescent-tagged BTB domains have the potential to bind to the GFP-tagged BTB domains from BTB sides and red focus formation takes place. Eventually, colocalization of these two colors happens and it gives the information about the presence of interaction or dimerization among those BTB domains (91). We also checked the interactions of NCOR and SMRT corepressors which were tagged with blue fluorescent protein (BFP) with BTB dimers by using the same system (Figure 4.9). The selected BTB domains for this experimental set up were BACH1-BTB, BACH2-BTB, BCL6-BTB, FAZF-BTB, KAISO-BTB, LRF-BTB, MIZ1-BTB, PATZ1-BTB, PATZ2-BTB, PLZF-BTB and ZBTB4-BTB. BFP-SMRT and BFP-NCOR constructs were already available so that we directly used them for transfection.

Initially, we seeded BHK cells on the 10 cm culture dish and co-transfected our plasmids in different combinations to check the functionality of the system (see Table 3.4). Among all transfection combination candidates, we chose BCL6-BTB as our positive control because it has been known that BTB domain of BCL6 must homodimerize for correct folding of the final functional protein and upon this obligate dimerization, the recruitment of corepressor proteins such as NCOR, SMRT and BCOR takes place, which eventually represses target genes (95). In other words, all the possible interactions should be seen in BCL6-BTB transfection combinations that we aimed to perform and we saw all of them as we expected (Figure 4.9).



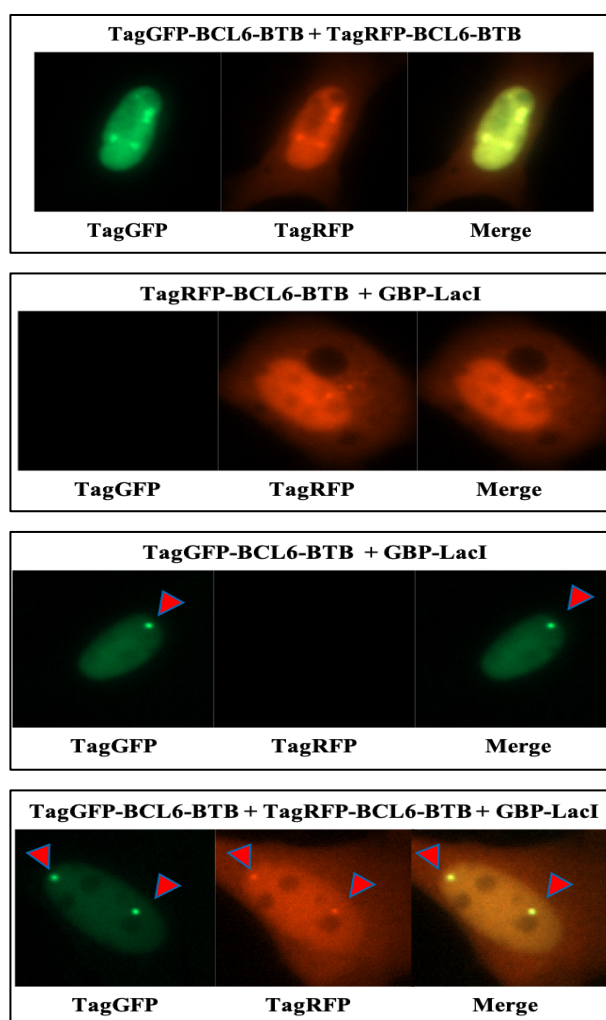


**Figure 4. 9 Experimental approach of fluorescent two-hybrid (F2H) assay for this study and positive controls**

In the first picture, we see that there are lac operator sites integrated into the genome of BHK cells and GBP-LacI fusion protein binds to these regions. When there is an interaction chain between GBP and TagGFP proteins and also BTBs of TagGFP fused and TagRFP fused proteins, the formation of green and red foci in the nucleus should be the result. In the second picture, we saw the result of the same experiment for TagGFP-BCL6-BTB and TagRFP-BCL6 constructs. In the third picture, in addition to same experimental set-up, BFP-NCOR and BFP-BCOR fused proteins are added to check their interactions with BTB dimers. The experimental results for this design could be seen in picture 4 and 5 for TagGFP-BCL6-BTB and TagRFP-BCL6 constructs.

To verify this designed system, we performed the transfection of different combinations of the F2H plasmids which were considered as positive controls for this study. When we transfected the TagRFP-BCL6-BTB and TagGFP-BCL6-BTB plasmids, there was no focus formation because of absence of GBP-LacI fusion protein in the system. Secondly, we performed transfection of TagRFP-BCL6-BTB and GBP-LacI plasmids and again we did not see any focus formation due to absence of GFP protein. Thirdly, we carried out transfection of TagGFP-BCL6-BTB and GBP-LacI fusion protein and eventually we

observed green focus formation only. This shows that GBP-LacI fusion protein is responsible for localization of TagGFP-BCL6-BTB on the lac operator sites in the nucleus. Finally, we transfected all three plasmids together and obtained both green and red foci at the same place in the nucleus (Figure 4.10)

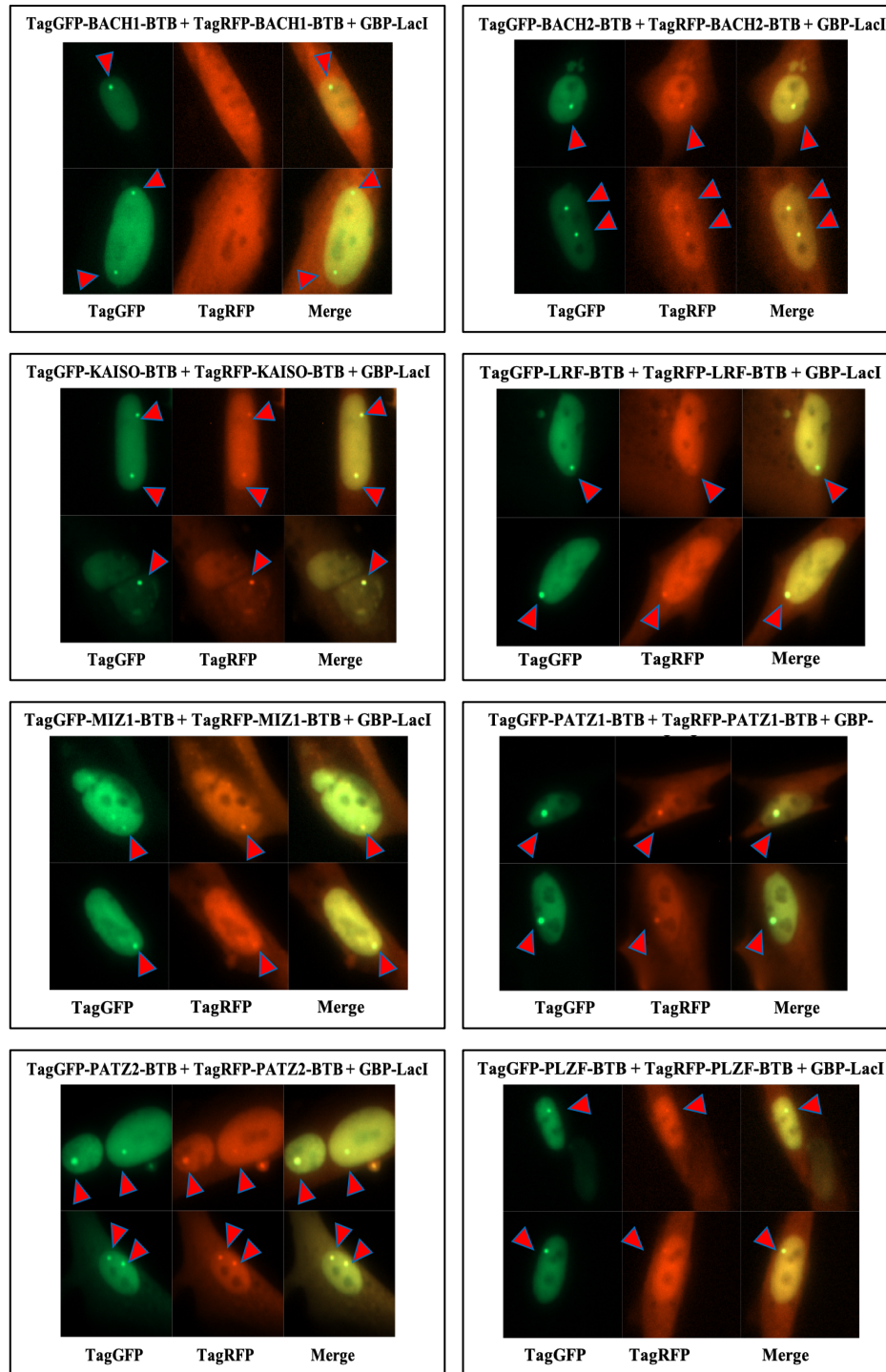


**Figure 4. 10 F2H assay verification**

TagGFP-BCL6-BTB, TagRFP-BCL6-BTB and GBP-LacI-GBP plasmids were transfected to BHK cells with different combinations. Red and green foci were only formed at the same place when all three plasmids were transfected together. Overall, system worked as in the expected way.

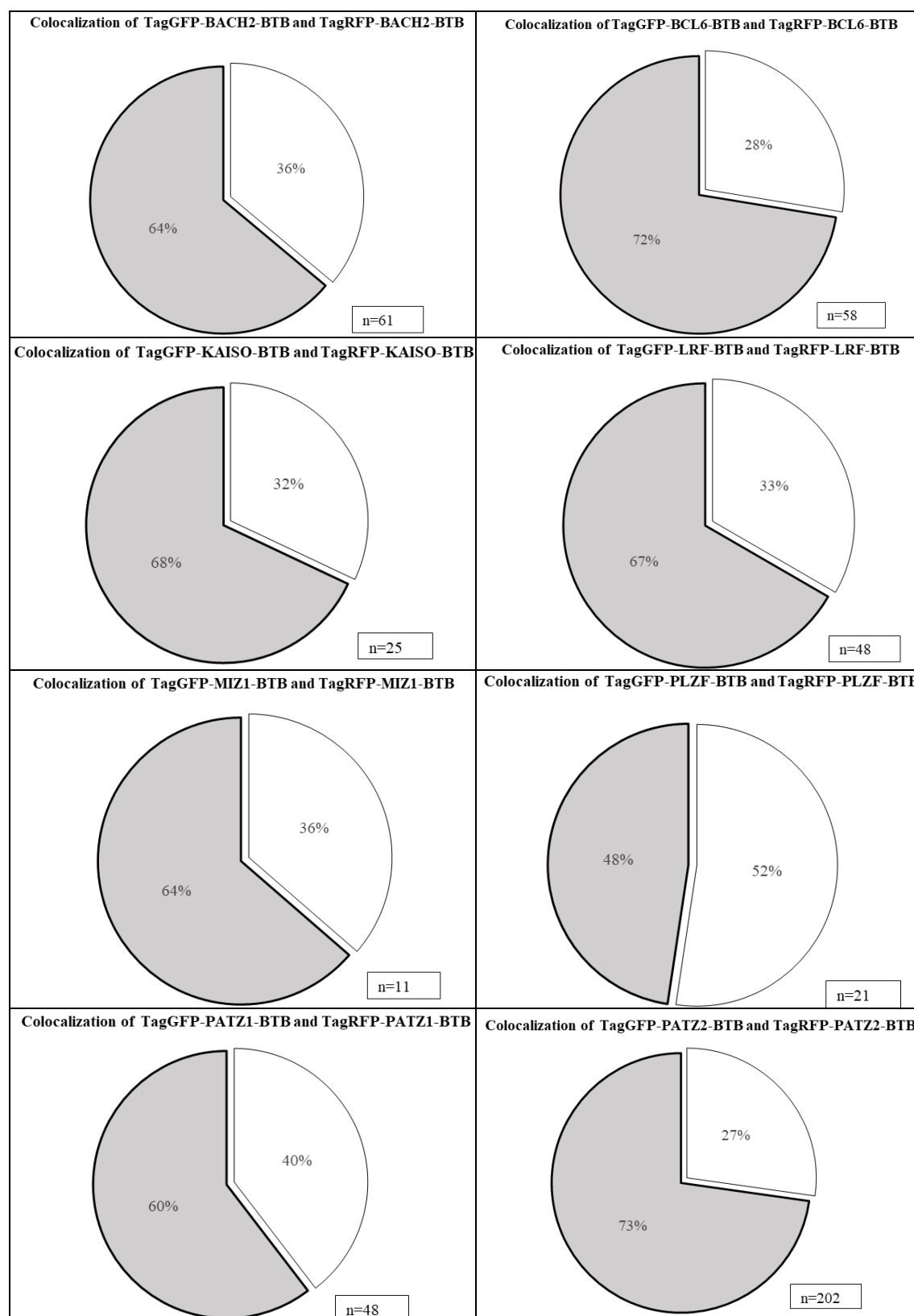
In the second part of the experiment, we checked availability of homodimerization among the other selected BTB domains. For this purpose, all three plasmids for each BTB domain were transfected into BHK cells. According to the observations we made after transfection, we could say that BACH2 BTB, KAISO-BTB, LRF-BTB, MIZ1-BTB, PATZ1-BTB, PATZ2-BTB and PLZF-BTB domains homodimerized and gave the same

result which was obtained for BCL6-BTB, our positive control. On the contrary, we did not get the same results for BACH1-BTB domain; it only formed green foci within the context of this experimental set-up (Figure 4.11). The quantifications of all these dimerizations that we observed are seen in Figure 4.12.



**Figure 4. 11 Homodimerization patterns for selected BTB domains**

All three plasmids with corresponding BTB domains were transfected into BHK cells and their homodimerization statuses were visualized. Except BACH1-BTB; BACH2-, KAISO-, LRF-, MIZ1-, PATZ1-, PATZ2- and PLZF-BTB domains could homodimerize and colocalization of green and red foci are the sign of this homodimerization.

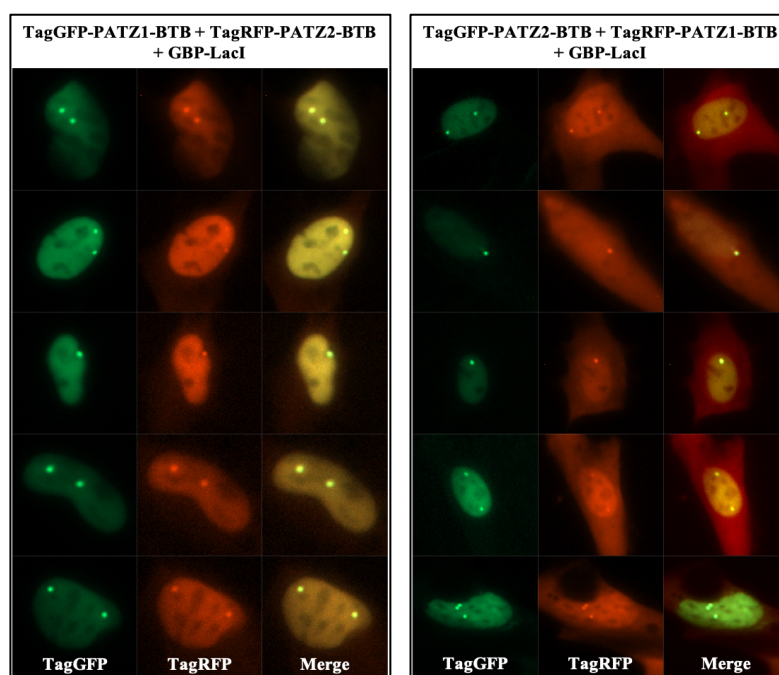




**Figure 4. 12 The pie charts for the colocalization of green and red foci in the homodimerizations of selected BTB domains**

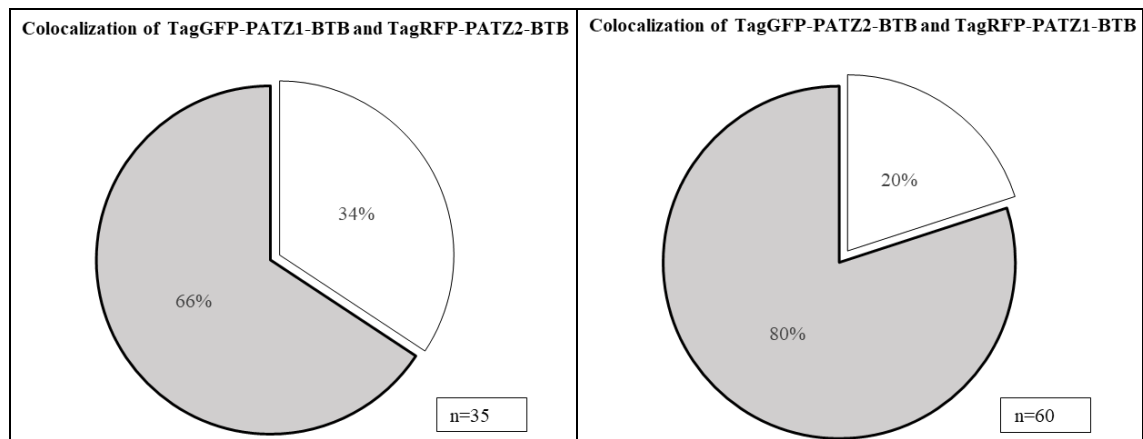
The percentages of green and red foci colocalization among all green foci for each homodimerization experiment are represented as in the form of pie charts above. The gray slices correspond to the colocalization of green and red foci, whereas white slices represent the green foci only. n is the number of cells having all green foci observed after corresponding transfections.

In the third part of the experiment, we checked the availability of heterodimerization for selected BTB domains. For this purpose, we performed several transfection experiments in different combinations (see Table 3.4). Among all candidates (Figure 4.15), only PATZ1-BTB and PATZ2-BTB could heterodimerize (Figure 4.13). The quantifications for this heterodimerization are shown in Figure 4.14.



**Figure 4. 13 Heterodimerization experiment for PATZ1-BTB and PATZ2-BTB domains**

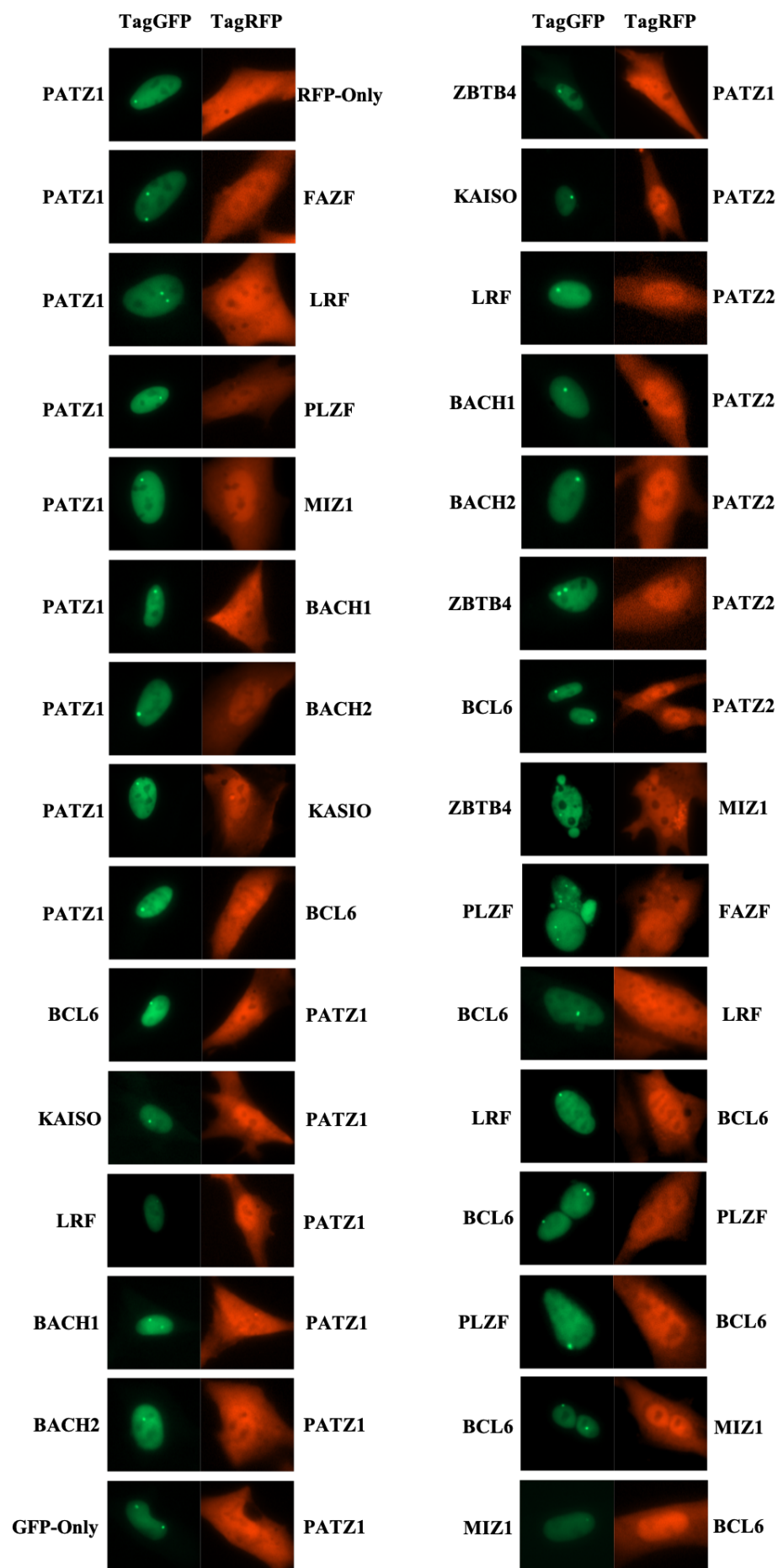
Among all combinations we tried, only PATZ1-BTB and PATZ2-BTB were able to heterodimerize in both conditions, TagGFP-PATZ1-BTB & TagRFP-PATZ2-BTB; TagGFP-PATZ2-BTB & TagRFP-PATZ1-BTB. This heterodimerization was inferred from the colocalization of green and red foci.



**Figure 4. 14 The pie charts for the colocalization of green and red foci in the heterodimerizations of PATZ1 and PATZ2 BTB domains**

The percentages of green and red foci colocalization among all green foci for PATZ1 and PATZ2 BTB heterodimerization are represented as in the form of pie charts above. The gray slices correspond to the colocalization of green and red foci, whereas white slices represent the green foci only. n is the number of cells having all green foci observed after corresponding transfections.





#### Figure 4. 15 Heterodimerization experiment for selected BTB domains

Except PATZ1-BTB and PATZ2-BTB combinations, we did not observe any other interactions and thus heterodimerization of selected BTB domains because only green foci were visible and there was no colocalization of green foci and red foci in these partners.

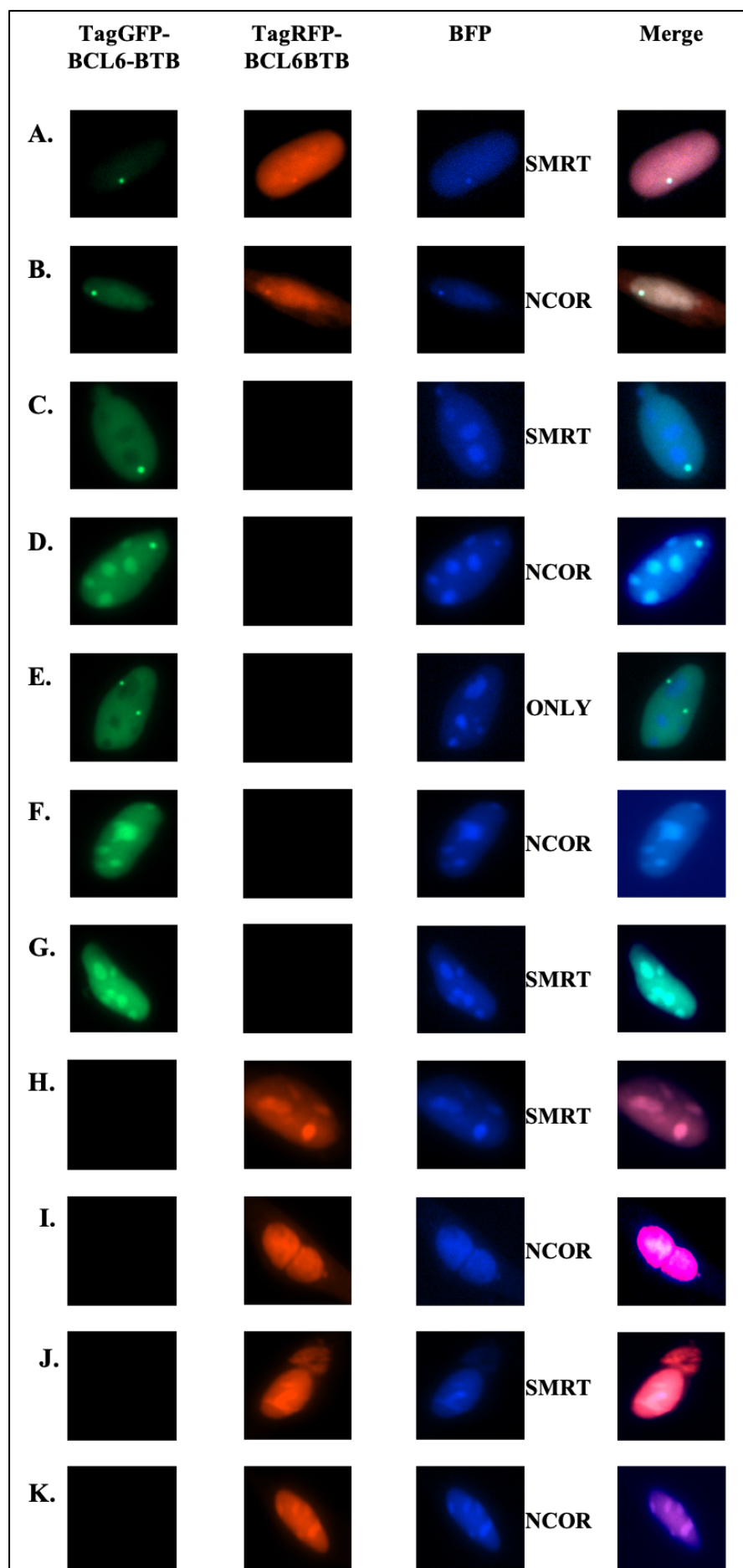
The overall interaction matrix which we obtained after these experiments is seen in Figure 4.16. According to this matrix, we can say that heterodimerization might not take place between the selected BTB domain partners seen in the matrix; only exception was PATZ1-BTB and PATZ2-BTB in our study.

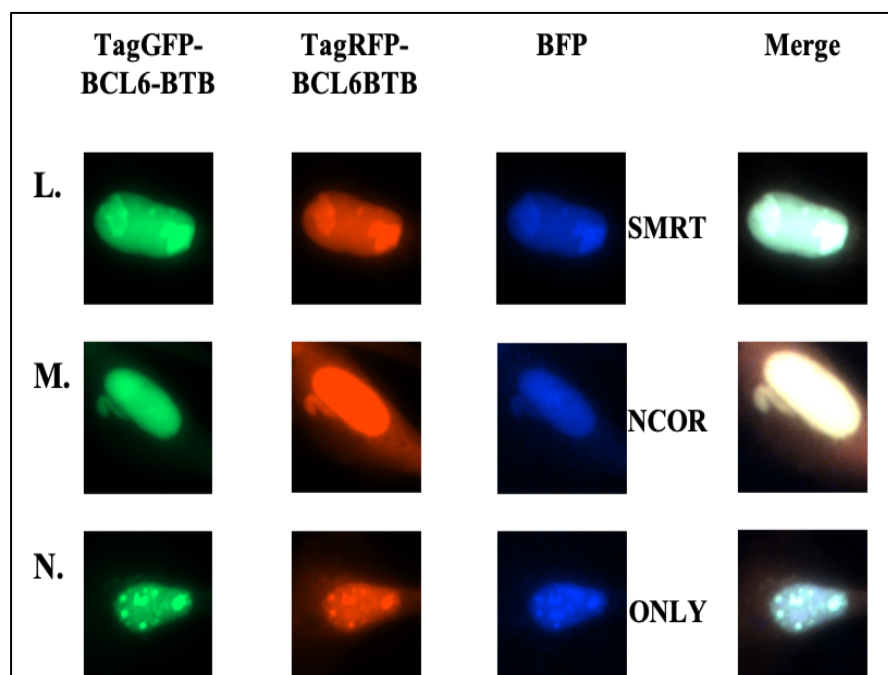
		TagGFP-BTB									
		BACH1	BACH2	BCL6	KAISO	LRF	MIZ1	PATZ1	PATZ2	PLZF	ZBTB4
TagRFP-BTB	BACH1	×						×			
	BACH2		✓					×			
	BCL6			✓		×	×	×			
	FAZF							×		×	
	KAISO				✓			×			
	LRF			×		✓		×			
	MIZ1			×			✓	×			×
	PATZ1	×	×	×	×	×	×	✓	✓	×	×
	PATZ2	×	×	×	×	×		✓	✓		×
	PLZF			×				×		✓	

Figure 4. 16 An interaction matrix for the selected BTB-domains

In the last part of this study, we wanted to check the availability of interactions of BTB dimers with NCOR and SMRT corepressor proteins. For this purpose, we started with BCL6-BTB domain to analyze its behaviors within the context of different transfection combinations. When TagGFP-BCL6, TagRFP-BCL6, BFP-SMRT/NCOR and GBP-LacI plasmids were all transfected into BHK cells, we saw the formations of green, red and blue foci at the same spots. As a next step, we performed transfection of TagGFP-BCL6, BFP-SMRT/NCOR and GBP-LacI plasmids into the cells and examined the results under the live-cell imaging microscope. Again, we saw colocalization of green and blue foci within the nucleus. In the first case, the dimerization of BCL6-BTBs happened between TagGFP and TagRFP tagged versions. In the second case, TagGFP tagged BTB domains homodimerized in themselves. In both cases, we can say that there might be some interactions between BCL6-BTB dimers and NCOR/SMRT corepressors. Then, we

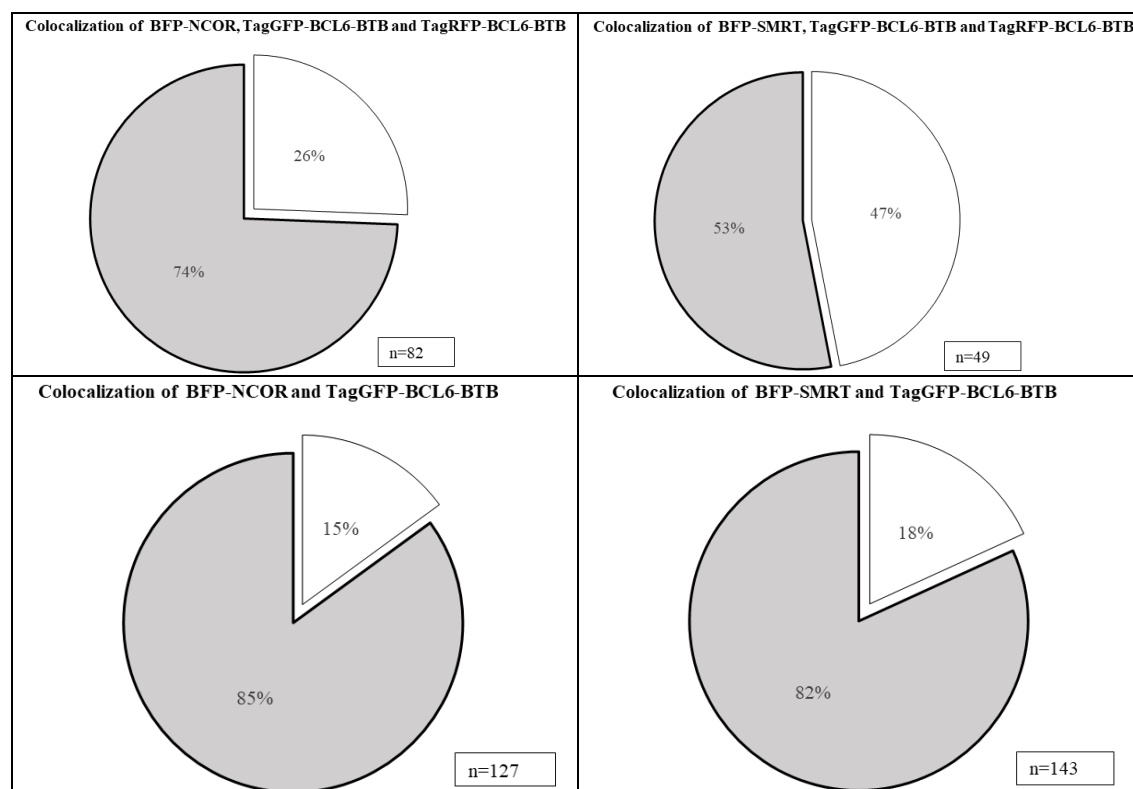
carried out another transfection in which TagGFP-BCL6, BFP-Only and GBP-LacI plasmids were available and we saw that there was only green focus formation; no blue foci were available. This might be an indication of the necessity of NCOR/SMRT peptides for the interaction to occur. Next, we transfected TagGFP-BCL6, BFP-NCOR/SMRT plasmids only and obtained no focus formations, which means that for the green focus to appear, the presence of GBP-LacI is necessary and without green foci formation, blue foci cannot be formed as well due to the absence of the interactions between BCL6-BTB dimers. Furthermore, we carried out the transfections of TagRFP-BCL6, BFP-SMRT/NCOR and GBP-LacI plasmids; and TagRFP-BCL6, BFP-SMRT/NCOR separately. Still, we did not get any focus formation in both conditions due to absence of TagGFP-BCL6 and GBP-LacI constructs which are crucial for green focus formation. Moreover, we did TagGFP-BCL6, TagRFP-BCL6 and BFP-SMRT/NCOR; TagGFP-BCL6, TagRFP-BCL6 and BFP-Only transfections and we did not obtain any focus formation (Figure 4.17). The quantifications of positive data for these experiments are shown in Figure 4.18.





**Figure 4. 17 The interaction table for BCL-BTB dimers and BFP-NCOR/BFP-SMRT and BFP-Only proteins**

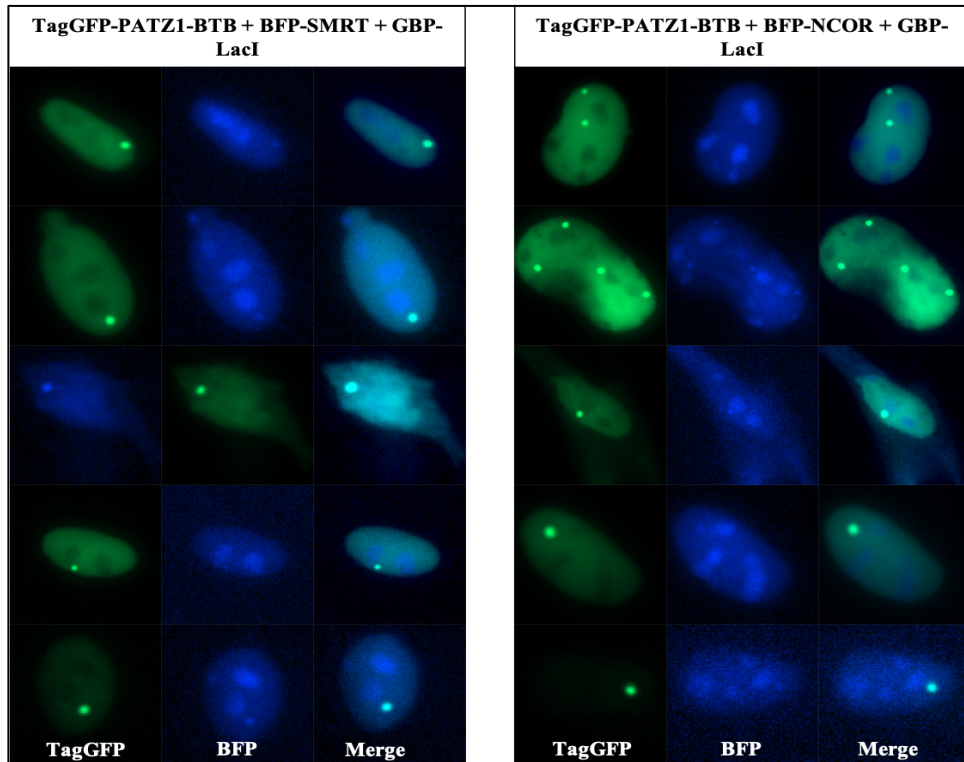
From A to E and H to I, the transfection conditions contained GBP-LacI fusion protein as well. From F to G and J to M, there was no addition of GBP-LacI into the transfection conditions.



**Figure 4. 18 The pie charts for the colocalization of green, blue and red foci for interactions between TagGFP-BCL6-TagRFP-BCL6 dimers and NCOR/SMRT corepressors; and the colocalization of green and blue foci for interactions between TagGFP-BCL6 dimers and NCOR/SMRT corepressors**

The gray slices correspond to the colocalization of green blue/red foci, whereas white slices represent the green foci only. n is the number of cells having all green foci observed after corresponding transfections.

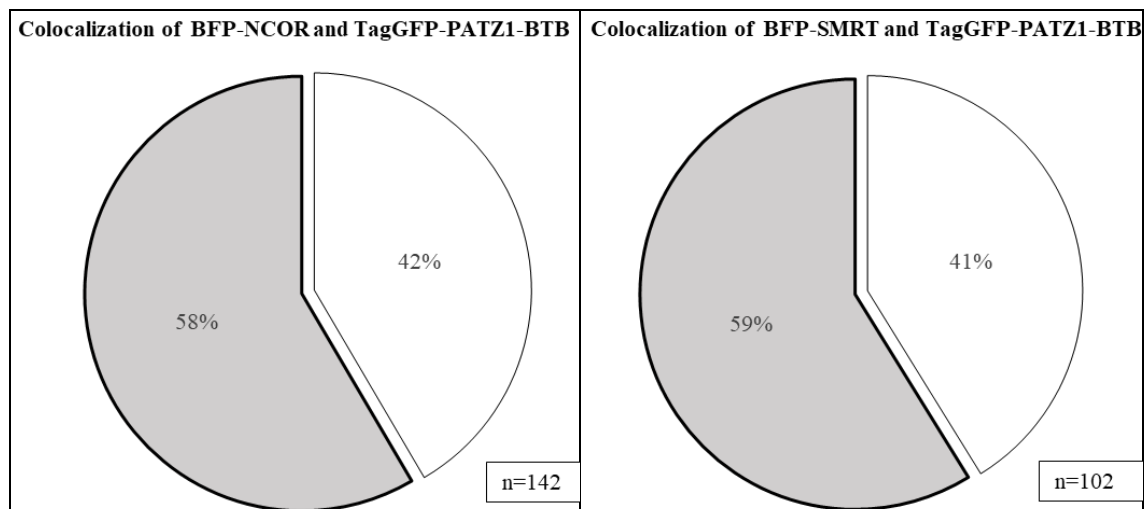
According to the conducted studies, we know that BCL6-BTB dimers interacts with NCOR and SMRT corepressors (95) and our F2H systems confirmed this information. As a next step, we wanted to check whether these interactions are also valid for PATZ1-BTB dimers. For this purpose, we carried out three different transfection combinations. In the first scenario, we transfected TagGFP-PATZ1-BTB, BFP-NCOR and GBP-LacI plasmids. In the second scenario, we performed TagGFP-PATZ1-BTB, BFP-SMRT and GBP-LacI plasmids. Finally, TagGFP-PATZ1-BTB, BFP-Only and GBP-LacI were transfected into the BHK cells. For the first two cases, we saw that both green and blue foci were visible at the same spots which might be interpreted as colocalization. However, blue foci were too faint comparing with the green foci (Figure 4.19). As a result of third case, we observed that only green focus formation was available. No blue foci were seen in the areas where green foci were localized (Figure 4.21), which might be interpreted as the presence of NCOR/SMRT peptides are required for interactions to take place.



**Figure 4. 19 F2H assay to check the availability of interaction between PATZ1-BTB dimers and NCOR/SMRT corepressor**

Our preliminary data show that there might be an interaction between PATZ1-BTB dimers and NCOR/SMRT corepressor proteins.

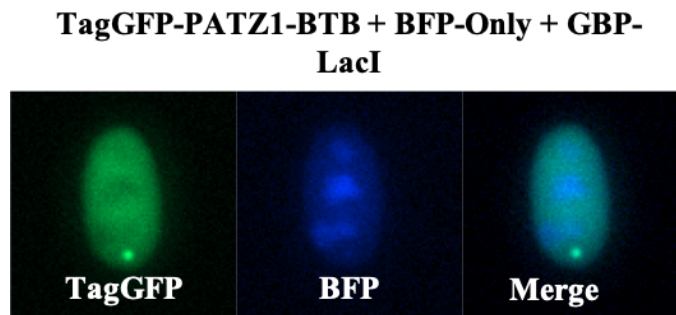
The quantification of these data is represented in Figure 4.20.



**Figure 4. 20 The pie charts for the colocalization of green and blue foci in interactions between PATZ1 homodimers and NCOR/SMRT corepressors**

The percentages of green and blue foci colocalization among all green foci for interactions between PATZ1 homodimers and NCOR/SMRT corepressors are represented as in the

form of pie charts above. The gray slices correspond to the colocalization of green and blue foci, whereas white slices represent the green foci only. n is the number of cells having all green foci observed after corresponding transfections.



**Figure 4. 21 F2H assay to check the necessity of NCOR/SMRT proteins for interaction.**

Our preliminary data show that there was no interaction in the absence of NCOR/SMRT peptide.

The overall results for positive interactions are clarified in terms of numbers in Table 4.6.



**Table 4. 6 The quantification table for all positive interactions**

Transfection partners	# of cells without foci	# of cells having green foci	# of cells having green and red foci	# of cells having green and blue foci	# of cells having green, red and blue foci	% of colocalization among green foci containing cells
TagGFP-BCL6-BTB & TagRFP-BCL6-BTB & GBP-LacI	11	58	42	-	-	72.4
TagGFP-PATZ2-BTB & TagRFP-PATZ2-BTB & GBP-LacI	49	202	147	-	-	72.8
TagGFP-PATZ1-BTB & TagRFP-PATZ1-BTB & GBP-LacI	25	48	29	-	-	60.4
TagGFP-KAISO-BTB & TagRFP-KAISO-BTB & GBP-LacI	7	25	17	-	-	68
TagGFP-LRF-BTB & TagRFP-LRF-BTB & GBP-LacI	13	48	32	-	-	66.7
TagGFP-MIZ1-BTB & TagRFP-MIZ1-BTB & GBP-LacI	16	11	7	-	-	63.6
TagGFP-PLZF-BTB & TagRFP-PLZF-BTB & GBP-LacI	2	21	10	-	-	47.6
TagGFP-BACH2-BTB & TagRFP-BACH2-BTB & GBP-LacI	20	61	39	-	-	63.9
TagGFP-PATZ2-BTB & TagRFP-PATZ1-BTB & GBP-LacI	9	60	48	-	-	80
TagGFP-PATZ1-BTB & TagRFP-PATZ2-BTB & GBP-LacI	8	35	23	-	-	65.7
BFP-NCOR & TagGFP-BCL6-BTB & TagRFP-BCL6-BTB & GBP-LacI	28	82	-	-	61	74.4
BFP-SMRT & TagGFP-BCL6-BTB & TagRFP-BCL6-BTB & GBP-LacI	22	49	-	-	26	53.1
BFP-NCOR & TagGFP-BCL6-BTB & GBP-LacI	53	127	-	-	108	85
BFP-SMRT & TagGFP-BCL6-BTB & GBP-LacI	43	143	-	-	117	81.8
BFP-NCOR & TagGFP-PATZ1-BTB & GBP-LacI	62	142	-	-	83	58.5
BFP-SMRT & TagGFP-PATZ1-BTB & GBP-LacI	19	102	-	-	60	58.8

## 5. DISCUSSION

The broad complex, tramtrack, bric-a-brac, and zinc finger (BTB-ZF) proteins are a family of transcriptional factors which are evolutionarily well-conserved. There are 49 known members of this family encoded in human genome and these members have common characteristics such as the presence of one or more C-terminal C<sub>2</sub>H<sub>2</sub> *Krüppel*-type zinc finger DNA binding domain and an N-terminal BTB/POZ domain responsible for the mediation of protein-protein interactions. These transcriptional factors regulate the expression pattern of target genes generally in a repressive way by binding to the regulatory regions in target genes through their ZF domain in a sequence specific manner. This binding is coupled with the recruitment of corepressor proteins which have roles in the chromatin remodeling and transcriptional silencing/activation depending on the cellular context. The formation of cofactor complexes is mainly achieved by the BTB domain that is able to interact directly with the corepressors and histone modifying enzymes such as SMRT, NCOR, BCOR, Sin3A and HDAC. Furthermore, this domain mediates the homodimerization and heterodimerization between different members of the family. One ZBTB family protein, BCL6 is a good example: BCL6 is able to homodimerize in the proper cellular conditions. Also, it can heterodimerize with other BTB-ZF proteins such as PLZF, LRF and MIZ1 (26). The members of this family is responsible for the regulation of normal and proper development of lymphocytes, fertility, skeletal morphogenesis, embryonic and neurological development (21). Apart from these BTB-ZF transcription factors, we studied two other proteins, BACH1 and BACH2 which are members of both BTB and CNC homology and the Cap'n'Collar type of the basic region-leucine zipper factor family. They are able to form heterodimers with small MAF proteins and this heterodimerization results in the repression of target gene expression. They also possess an N-terminal BTB/POZ domain necessary for the interactions with other proteins (96). The identification of BTB domain mediated interactions and their

networks important to understand their structure-function relationship. In this study, we aimed to come up with a systematic assay to screen the interactions among several BTB containing transcription factors and the corepressors which are in connection with BTB domain containing proteins.

Firstly, we expressed and purified the BTB domains of selected proteins, FAZF-BTB, MIZ1-BTB, PATZ1-BTB and PATZ2-BTB, by the use of a bacterial protein expression system. For this, a cytoplasmic protein expression protocol was followed. Initially, to be sure whether our constructs for these BTB domains express the desired protein or not, we performed colony screening method in a small scale and we saw that all tested clones were able to express the desired BTB domains accurately. Next, we continued with the large-scale protein expression and purification steps. For purifications, IMAC (immobilized metal affinity chromatography) and SEC (size exclusion chromatography) protocols were performed respectively. Although cytoplasmic expression was carried out, we saw some portions of our proteins in the pellet as well. Fortunately, we obtained enough amount of our soluble proteins for the further experimental steps. At this point, when we compared the molecular weights of our purified proteins with the expected values, we saw that the experimental results were compatible with the calculated versions except for MIZ1-BTB, whose molecular weight was lower than expected. This might be because of proteolytic modification of this protein during experimental conditions, certain physical features of the proteins such as having acidic pI that causes faster migration under SDS-PAGE conditions or non-specific protein degradation during experimental steps. Furthermore, after IMAC and SEC experiments for PATZ1-BTB, we obtained a graph (Figure 4.4D) which has three different peaks. The first peak likely corresponds to the homotetramer version of PATZ1 because its molecular weight is compatible with the calculated tetramer MW. The second peak likely corresponds to a transitional state between possible tetramer and dimer forms of PATZ1. The third peak corresponds to homodimeric PATZ1 because its MW is compatible with the calculated MW. For the other proteins, there was only one peak and the obtained MWs from these peaks show high concordance with the calculated values for homodimeric BTB domains.

Secondly, we wanted to screen homodimerization, heterodimerization, homotetramerization and heterotetramerization behaviors of our purified MIZ1-BTB,

PATZ1-BTB and PATZ2-BTB proteins and measure their potential interaction affinities with surface plasmon resonance (SPR). We covalently immobilized our MIZ1-BTB, PATZ1-BTB and PATZ2-BTB domains on the CM5 chip. On this chip, they might be anchored either in dimer form or monomer form. Over them, same proteins were passed to see possible homodimer/heterodimer/homotetramer/heterotetramer formations. We observed intramolecular interactions between MIZ1 dimers or monomers and PATZ1 dimers or monomers, but not between PATZ2 dimers or monomers. These interactions indicate that MIZ1 and PATZ1 can homotetramerize or homodimerize. Also, preliminary results show the presence of an interaction between MIZ1 and PATZ1 dimers, indicating the possibility of the presence of MIZ1-PATZ1 heterodimers or heterotetramers. We did not observe an interaction between PATZ1 and PATZ2 dimers or monomers, or PATZ2 and MIZ1 dimers or monomers. The results seem to show concentration-dependent interactions; higher the concentration, better the binding. However, the obtained signals were not high enough to draw an absolute conclusion about these interactions. The chip structure, immobilization methods and multiple cycle kinetic steps should be optimized to obtain more representative results and different BTB domains should be used to get a picture about these behaviors.

Finally, we set up a fluorescent two hybrid (F2H) assay to assess the homodimerization and heterodimerization patterns of selected BTB domains and their interactions with the NCOR and SMRT corepressor proteins. For this purpose, we used 11 different BTB domains. These BTB domains were tagged with two different fluorescent tags; TagGFP and TagRFP. According to this experimental set up, if there is homodimerization or heterodimerization among two differently labelled BTB domains, we will expect to see the colocalization of green and red foci at the same spot. Furthermore, the parts of the NCOR and SMRT proteins which are responsible for binding to the BTB dimers were tagged with BFP fluorescent protein. If there is an interaction between BTB dimers and one of these proteins, we will see the colocalization of green, red and blue (or green and blue, depending on the type of BTB dimers) foci at the same location.

For these experiments, we used BCL6-BTB as a positive control because according to the literature, BCL6 protein is able to homodimerize and the presence of BTB domain is sufficient and necessary for homodimerization to take place. Moreover, BCL6 interacts

with NCOR and SMRT proteins when a BTB dimer can form (95). Our preliminary results related to BCL6-BTB confirmed this; we saw the corresponding colocalization patterns for homodimerization and also for interactions with NCOR and SMRT. Next, we checked whether BACH1-BTB, BACH2-BTB, KAISO-BTB, LRF-BTB, MIZ1-BTB, PATZ1-BTB, PATZ2-BTB and PLZF-BTB domains can homodimerize. We observed that all of these except the BACH1-BTB were able to homodimerize. The homodimerization patterns were compatible with both the patterns of BCL6-BTB, our positive control, and with the literature (97, 98, 51, 66, 90, 71). In the BACH1-BTB case, for dimerization to take place, the kinked N-terminal region (N-hook) at the BTB domain is required (89). In our expression system, it is possible that this structure is not formed because of the fused fluorescent protein to the N-terminus.

For BTB pairs that interacted, we quantified if the interaction was observed in multiple cells/samples. In multiple images acquired from transfected cells, we counted all the cells containing green foci. Among these, we identified the ones in which red and green foci were colocalized. Using these values, we calculated the percentage of green-foci containing cells that also showed colocalization and plotted these values in pie-charts. Next, we checked the ability of selected BTB domain proteins to heterodimerize. From the literature, we already knew that FAZF and PLZF could heterodimerize and the presence of a BTB domain is sufficient for this heterodimerization (43). In our system, we did not observe any heterodimerization for these BTB domains, which was not compatible with the literature. It is likely that further regions of the BTB domain or modifications thereof are required for these interactions. Furthermore, full length LRF and BCL6 (with BTB domains and ZF motifs) were shown to associate (32). We did not observe any interaction between the BTB domains of these two proteins in our system. This failure is likely due to the absence of the DNA binding domains of these proteins that likely creates the cellular context of the interaction on the DNA. Moreover, it has been observed that, PLZF and BCL6 proteins can heterodimerize and this depends on both the interactions between BTB domains and ZF motifs (34). We again did not observe any heterodimerization among these two proteins, most likely because our interaction system only assesses the interactions of BTB domains. Also, MIZ1 and BCL6 can interact to form heterodimers which is only mediated by their BTB domains (62). In our system, we did not observe any heterodimerization for these two proteins.

Further experiments showed that PATZ1-BACH1 (65) and ZBTB4-MIZ1 (85) can interact, dependent on the BTB domains, and also between PATZ1-BACH2, which requires both BTB domain and ZF motifs (65). In our experimental set up, we did not observe any interactions. For PATZ1-BACH2, this is expected. However, for the rest, the results were not compatible with the literature. Due to the restriction of the F2H system to test the interaction of only BTB domains, this system may not recapitulate all biological interactions between BTB-ZF proteins (see Figure 4.16). Also, there might be additional components such as certain regulatory proteins and post-translational modifications required for mediating the dimerization process. The only heterodimerization we observed was between PATZ1-BTB and PATZ2-BTB. This interaction was documented before (71).

Finally, we checked the interactions of the BCL6-BTB and PATZ1-BTB dimers with NCOR and SMRT proteins. We could identify the interactions between BCL6-BTB dimers and NCOR/SMRT peptides, which we use as a positive control. Next, we assessed the interaction between PATZ1-BTB dimers and NCOR/SMRT peptides. Previously, PATZ1-BTB and NCOR interactions were demonstrated (66). However, the PATZ1-SMRT interaction has not yet been documented. Our preliminary results show that PATZ1-BTB dimers may interact with both NCOR and SMRT peptides.

For the further identification of the protein-protein interactions of BTB-containing transcription factors, other methods can be used as well. For example, Förster resonance energy transfer (FRET) is a powerful technique for the detection of protein-protein interactions both *in vivo* and *in vitro* conditions in a direct way. It is based on the fact that the bait and prey proteins are fused with compatible donor and acceptor fluorophores and there is an energy transition from donor fluorophore to acceptor one when two proteins of interest are located 10 nm away from each other and when the donor fluorophore is excited. This transfer of photons between donor and acceptor proteins results in the fluorescence of the acceptor, calculated as a FRET signal (99). TagBFP-TagGFP2 (improved version of TagGFP) and TagGFP2-TagRFP pairs give the most efficient FRET results among tested Tag fluorescent proteins. In our system, BTB domains were tagged with TagGFP and TagRFP and we can use this technology to determine the presence of homodimerization/heterodimerization among BTB domains. Furthermore, availability of

tetramerization can be checked by our F2H assay. For this purpose, we can tag our BTB domains with four different fluorescent proteins such as mTagBFP, TagGFP, TagRFP and mRFP1. By transfecting all necessary plasmids into BHK cells, we can observe the colocalization of four foci with different colors with the help of live-cell imaging microscope and make deductions about their ability to tetramerize.

In conclusion, we generated two different assays to screen for the dimerization and tetramerization of BTB domains. Our F2H system is also capable of testing the interaction between BTB domains and the corepressors interaction partners. Our interaction systems can assess binding both in vitro and in vivo. As a next step, we aim to test the remaining BTB domain interactions to complete the interaction matrix of these proteins.

## 6. BIBLIOGRAPHY

1. Koonin E V., Senkevich TG, Chernos VI. A family of DNA virus genes that consists of fused portions of unrelated cellular genes. *Trends Biochem Sci.* 1992;17(6):213-214. doi:10.1016/0968-0004(92)90379-N
2. Godt D, Couderc JL, Cramton SE, Laski FA. Pattern formation in the limbs of *Drosophila*: bric a brac is expressed in both a gradient and a wave-like pattern and is required for specification and proper segmentation of the tarsus. *Development.* 1993;119(3):799-812.
3. Zollman S, Godt D, Prive GG, Couderc JL, Laski FA. The BTB domain, found primarily in zinc finger proteins, defines an evolutionarily conserved family that includes several developmentally regulated genes in *Drosophila*. *Proc Natl Acad Sci.* 1994;91(22):10717-10721. doi:10.1073/pnas.91.22.10717
4. Bardwell VJ, Treisman R. The POZ domain: A conserved protein-protein interaction motif. *Genes Dev.* 1994;8(14):1664-1677. doi:10.1101/gad.8.14.1664
5. Perez-Torrado R, Yamada D, Defossez PA. Born to bind: The BTB protein-protein interaction domain. *BioEssays.* 2006;28(12):1194-1202. doi:10.1002/bies.20500
6. Miller J, McLachlan AD, Klug A. Repetitive zinc-binding domains in the protein transcription factor IIIA from *Xenopus* oocytes. *EMBO J.* 1985;4(6):1609-1614.
7. Klug A. The discovery of zinc fingers and their development for practical applications in gene regulation and genome manipulation. *Q Rev Biophys.* 2010;43(1):1–21. doi:10.1017/S0033583510000089
8. Stogios PJ, Downs GS, Jauhal JJS, Nandra SK, Privé GG. Sequence and structural analysis of BTB domain proteins. *Genome Biol.* 2005;6(10):R82. doi:10.1186/gb-2005-6-10-r82
9. Bradley JR, Pober JS. Tumor necrosis factor receptor-associated factors (TRAFs). *Oncogene.* 2001;20(44):6482-6491. doi:10.1038/sj.onc.1204788
10. Adams J, Kelso R, Cooley L. The kelch repeat superfamily of proteins: Propellers of cell function. *Trends Cell Biol.* 2000;10(1):17-24. doi:10.1016/S0962-8924(99)01673-6
11. Robinson DN, Cooley L. *Drosophila* kelch is an oligomeric ring canal actin



- organizer. *J Cell Biol.* 1997;138(4):799-810. doi:10.1083/jcb.138.4.799
12. Hara T, Ishida H, Raziuddin R, Dorkhom S, Kamijo K, Miki T. Novel kelch-like protein, KLEIP, is involved in actin assembly at cell-cell contact sites of Madin-Darby canine kidney cells. *Mol Biol Cell.* 2004;15(3):1172-1184. doi:10.1091/mbc.e03-07-0531
  13. Sakai T, Wada T, Ishiguro S, Okada K. RPT2: A Signal Transducer of the Phototropic Response in Arabidopsis. *Plant Cell.* 2000;12(2):225-236. doi:10.1105/tpc.12.2.225
  14. Strang C, Cushman SJ, DeRubeis D, Peterson D, Pfaffinger PJ. A Central Role for the T1 Domain in Voltage-gated Potassium Channel Formation and Function. *J Biol Chem.* 2001;276(30):28493-28502. doi:10.1074/jbc.M010540200
  15. Ahmad KF, Melnick A, Lax S, et al. Mechanism of SMRT Corepressor Recruitment by the BCL6 BTB Domain. *Mol Cell.* 2003;12(6):1551-1564. doi:10.1016/S1097-2765(03)00454-4
  16. Barish GD, Yu RT, Karunasiri MS, et al. The Bcl6-SMRT/NCoR Cistrome Represses Inflammation to Attenuate Atherosclerosis. *Cell Metab.* 2012;15(4):554-562. doi:https://doi.org/10.1016/j.cmet.2012.02.012
  17. Kreusch A, Pfaffinger PJ, Stevens CF, Choe S. Crystal structure of the tetramerization domain of the Shaker potassium channel. *Nature.* 1998;392(6679):945-948. doi:10.1038/31978
  18. Horn M, Collingro A, Schmitz-Esser S, et al. Illuminating the Evolutionary History of Chlamydiae. *Science* (80- ). 2004;304(5671):728-730. doi:10.1126/science.1096330
  19. Thomas JH. Adaptive evolution in two large families of ubiquitin-ligase adapters in nematodes and plants. *Genome Res.* 2006;16(8):1017-1030. doi:10.1101/gr.5089806
  20. Vogel C, Bashton M, Kerrison ND, Chothia C, Teichmann SA. Structure, function and evolution of multidomain proteins. *Curr Opin Struct Biol.* 2004;14(2):208-216. doi:10.1016/j.sbi.2004.03.011
  21. Siggs O, Beutler B. The BTB-ZF transcription factors. *Cell cycle.* 2012;11(18):3358-3369.
  22. Wieschaus E, Nusslein-Volhard C, Kluding H. Krüppel, a gene whose activity is required early in the zygotic genome for normal embryonic segmentation. *Dev*

- Biol.* 1984;104(1):172-186. doi:10.1016/0012-1606(84)90046-0
23. Huynh KD, Bardwell VJ. The BCL-6 POZ domain and other POZ domains interact with the co-repressors N-CoR and SMRT. *Oncogene*. 1998;17(19):2473-2484. doi:10.1038/sj.onc.1202197
  24. Staller P, Peukert K, Kiermaier A, et al. Repression of p15INK4b expression by Myc through association with Miz-1. *Nat Cell Biol.* 2001;3(4):392-399. doi:10.1038/35070076
  25. Kelly KF, Daniel JM. POZ for effect - POZ-ZF transcription factors in cancer and development. *Trends Cell Biol.* 2006;16(11):578-587. doi:10.1016/j.tcb.2006.09.003
  26. Beaulieu AM, Sant'Angelo DB. The BTB-ZF Family of Transcription Factors: Key Regulators of Lineage Commitment and Effector Function Development in the Immune System. *J Immunol.* 2011;187(6):2841-2847. doi:10.4049/jimmunol.1004006
  27. Melnick A, Carlile G, Ahmad KF, et al. Critical residues within the BTB domain of PLZF and Bcl-6 modulate interaction with corepressors. *Mol Cell Biol.* 2002;22(6):1804-1818. doi:10.1128/mcb.22.6.1804-1818.2002
  28. Linggi BE, Brandt SJ, Sun ZW, Hiebert SW. Translating the histone code into leukemia. *J Cell Biochem.* 2005;96(5):938-950. doi:10.1002/jcb.20604
  29. Chang CC, Ye BH, Chaganti RSK, Dalla-Favera R. BCL-6, a POZ/zinc-finger protein, is a sequence-specific transcriptional repressor. *Proc Natl Acad Sci U S A.* 1996;93(14):6947-6952. doi:10.1073/pnas.93.14.6947
  30. Basso K, Dalla-Favera R. Roles of BCL6 in normal and transformed germinal center B cells. *Immunol Rev.* 2012;247(1):172-183. doi:10.1111/j.1600-065X.2012.01112.x
  31. Dhordain P, Albagli O, Ansieau S, et al. The BTB/POZ domain targets the LAZ3/BCL6 oncoprotein to nuclear dots and mediates homomerisation in vivo. *Oncogene*. 1995;11(12):2689-2697.
  32. Davies JM, Hawe N, Kabarowski J, et al. Novel BTB/POZ domain zinc-finger protein, LRF, is a potential target of the LAZ-3/BCL-6 oncogene. *Oncogene*. 1999;18(2):365-375. doi:10.1038/sj.onc.1202332
  33. Phan RT, Saito M, Basso K, Niu H, Dalla-Favera R. BCL6 interacts with the transcription factor Miz-1 to suppress the cyclin-dependent kinase inhibitor p21

- and cell cycle arrest in germinal center B cells. *Nat Immunol.* 2005;6(10):1054-1060. doi:10.1038/ni1245
34. Dhordain P, Albagli O, Honore N, et al. Colocalization and heteromerization between the two human oncogene POZ/zinc finger proteins, LAZ3 (BCL6) and PLZF. *Oncogene.* 2000;19(54):6240-6250. doi:10.1038/sj.onc.1203976
  35. Okabe S, Fukuda T, Ishibashi K, et al. BAZF, a Novel Bcl6 Homolog, Functions as a Transcriptional Repressor. *Mol Cell Biol.* 1998;18(7):4235-4244. doi:10.1128/mcb.18.7.4235
  36. Jardin F, Ruminy P, Bastard C, Tilly H. The BCL6 proto-oncogene: a leading role during germinal center development and lymphomagenesis. *Pathol Biol.* 2007;55(1):73-83. doi:10.1016/j.patbio.2006.04.001
  37. Kawamata N, Miki T, Fukuda T, Hirosawa S, Aoki N. The organization of the BCL6 gene. *Leukemia.* 1994;8(8):1327-1330.
  38. Ranuncolo SM, Wang L, Polo JM, et al. BCL6-mediated attenuation of DNA damage sensing triggers growth arrest and senescence through a p53-dependent pathway in a cell context-dependent manner. *J Biol Chem.* 2008;283(33):22565-22572. doi:10.1074/jbc.M803490200
  39. Ye BH, Cattoretti G, Shen Q, et al. The BCL-6 proto-oncogene controls germinal-centre formation and Th2-type inflammation. *Nat Genet.* 1997;16(2):161-170. doi:10.1038/ng0697-161
  40. Dent AL, Shaffer AL, Yu X, Allman D, Staudt LM. Control of inflammation, cytokine expression, and germinal center formation by BCL-6. *Science (80- ).* 1997;276(5312):589-592.
  41. Tunyaplin C, Shaffer AL, Angelin-Duclos CD, Yu X, Staudt LM, Calame KL. Direct Repression of prdm1 by Bcl-6 Inhibits Plasmacytic Differentiation . *J Immunol.* 2004;173(2):1158-1165. doi:10.4049/jimmunol.173.2.1158
  42. Ranuncolo SM, Polo JM, Melnick A. BCL6 represses CHEK1 and suppresses DNA damage pathways in normal and malignant B-cells. *Blood Cells, Mol Dis.* 2008;41(1):95-99. doi:10.1016/j.bcmd.2008.02.003
  43. Hoatlin ME, Yu Z, Ball H, et al. A novel BTB/POZ transcriptional repressor protein interacts with the Fanconi anemia group C protein and PLZF. *Blood.* 1999;94(11):3737-3747.
  44. Niedernhofer LJ, Lalai AS, Hoeijmakers JHJ. Fanconi anemia (cross)linked to

- DNA repair. *Cell*. 2005;123(7):1191-1198. doi:10.1016/j.cell.2005.12.009
45. Yoon HS, Scharer CD, Majumder P, et al. ZBTB32 is an early repressor of the CIITA and MHC class II gene expression during B cell differentiation to plasma cells. *J Immunol*. 2012;189(5):2393-2403.
  46. Miaw SC, Choi A, Yu E, Kishikawa H, Ho IC. ROG, repressor of GATA, regulates the expression of cytokine genes. *Immunity*. 2000;12(3):323-333. doi:10.1016/S1074-7613(00)80185-5
  47. Piazza F, Costoya JA, Merghoub T, Hobbs RM, Pandolfi PP. Disruption of PLZF in Mice Leads to Increased T-Lymphocyte Proliferation, Cytokine Production, and Altered Hematopoietic Stem Cell Homeostasis. *Mol Cell Biol*. 2004;24(23):10456-10469. doi:10.1128/mcb.24.23.10456-10469.2004
  48. Daniel JM, Reynolds AB. The catenin p120 ctn interacts with Kaiso, a novel BTB/POZ domain zinc finger transcription factor. *Mol Cell Biol*. 1999;19(5):3614-3623.
  49. Daniel JM. The p120ctn-binding partner Kaiso is a bi-modal DNA-binding protein that recognizes both a sequence-specific consensus and methylated CpG dinucleotides. *Nucleic Acids Res*. 2002;30(13):2911-2919. doi:10.1093/nar/gkf398
  50. Daniel JM. Dancing in and out of the nucleus: p120ctn and the transcription factor Kaiso. *Biochim Biophys Acta - Mol Cell Res*. 2007;1773(1):59-68. doi:10.1016/j.bbamcr.2006.08.052
  51. Van Roy FM, McCrea PD. A role for kaiso-p120ctn complexes in cancer? *Nat Rev Cancer*. 2005;5(12):956-964. doi:10.1038/nrc1752
  52. Rodova M, Kelly KF, VanSaun M, Daniel JM, Werle MJ. Regulation of the Rapsyn Promoter by Kaiso and -Catenin. *Mol Cell Biol*. 2004;24(16):7188-7196. doi:10.1128/mcb.24.16.7188-7196.2004
  53. Prokhortchouk A, Sansom O, Selfridge J, et al. Kaiso-Deficient Mice Show Resistance to Intestinal Cancer. *Mol Cell Biol*. 2006;26(1):199-208. doi:10.1128/mcb.26.1.199-208.2006
  54. Maeda T, Hobbs RH, Morghoub T, et al. Role of the proto-oncogene Pokemon in cellular transformation and ARF repression. *Nature*. 2005;433(7023):278-285. doi:10.1038/nature03203
  55. Pessler F, Hernandez N. Flexible DNA binding of the BTB/POZ-domain protein

- FBI-1. *J Biol Chem.* 2003;278(31):29327-29335. doi:10.1074/jbc.M302980200
56. Morrison DJ, Pendergrast PS, Stavropoulos P, Colmenares SU, Kobayashi R, Hernandez N. FBI-1, a factor that binds to the HIV-1 inducer of short transcripts (IST), is a POZ domain protein. *Nucleic Acids Res.* 1999;27(5):1251-1262. doi:10.1093/nar/27.5.1251
  57. Widom RL, Lee JY, Joseph C, Gordon-Froome I, Korn JH. The hcKrox gene family regulates multiple extracellular matrix genes. *Matrix Biol.* 2001;20(7):451-462. doi:10.1016/S0945-053X(01)00167-6
  58. Lee DK, Kang JE, Park HJ, et al. FBI-1 enhances transcription of the nuclear factor- $\kappa$ B (NF- $\kappa$ B)-responsive E-selectin gene by nuclear localization of the p65 subunit of NF- $\kappa$ B. *J Biol Chem.* 2005;280(30):27783-27791. doi:10.1074/jbc.M504909200
  59. Maeda T, Hobbs RM, Pandolfi PP. The transcription factor Pokemon: A new key player in cancer pathogenesis. *Cancer Res.* 2005;65(19):8575-8578. doi:10.1158/0008-5472.CAN-05-1055
  60. Rodondi N, Den Elzen WPJ, Bauer DC, et al. Subclinical hypothyroidism and the risk of coronary heart disease and mortality. *Jama.* 2010;304(12):1365-1374.
  61. Peukert K, Staller P, Schneider A, Carmichael G, Hänel F, Eilers M. An alternative pathway for gene regulation by Myc. *EMBO J.* 1997;16(18):5672-5686. doi:10.1093/emboj/16.18.5672
  62. Stead MA, Trinh CH, Garnett JA, et al. A Beta-Sheet Interaction Interface Directs the Tetramerisation of the Miz-1 POZ Domain. *J Mol Biol.* 2007;373(4):820-826. doi:10.1016/j.jmb.2007.08.026
  63. Phan RT, Saito M, Basso K, Niu H, Dalla-Favera R. BCL6 interacts with the transcription factor Miz-1 to suppress the cyclin-dependent kinase inhibitor p21 and cell cycle arrest in germinal center B cells. *Nat Immunol.* 2005;6(10):1054-1060. doi:10.1038/ni1245
  64. Wiese KE, Walz S, von Eyss B, et al. The role of MIZ-1 in MYC-dependent tumorigenesis. *Cold Spring Harb Perspect Med.* 2013;3(12):a014290. doi:10.1101/cshperspect.a014290
  65. Kobayashi A, Yamagiwa H, Hoshino H, et al. A Combinatorial Code for Gene Expression Generated by Transcription Factor Bach2 and MAZR (MAZ-Related Factor) through the BTB/POZ Domain. *Mol Cell Biol.* 2000;20(5):1733-1746.

doi:10.1128/mcb.20.5.1733-1746.2000

66. Bilic I, Koesters C, Unger B, et al. Negative regulation of CD8 expression via Cd8 enhancer-mediated recruitment of the zinc finger protein MAZR. *Nat Immunol.* 2006;7(4):392-400. doi:10.1038/ni1311
67. Bilic I, Koesters C, Unger B, Sekimata M. Europe PMC Funders Group Negative regulation of CD8 expression via CD8 enhancer-mediated recruitment of the zinc finger protein MAZR. 2010;7(4):392-400. doi:10.1038/ni1311.Negative
68. He X, Park K, Kappes DJ. The Role of ThPOK in Control of CD4/CD8 Lineage Commitment. *Annu Rev Immunol.* 2010;28(1):295-320. doi:10.1146/annurev.immunol.25.022106.141715
69. Keskin N, Deniz E, Eryilmaz J, et al. PATZ1 Is a DNA Damage-Responsive Transcription Factor That Inhibits p53 Function. *Mol Cell Biol.* 2015;35(10):1741-1753. doi:10.1128/MCB.01475-14
70. Valentino T, Palmieri D, Vitiello M, Pierantoni GM, Fusco A, Fedele M. PATZ1 interacts with p53 and regulates expression of p53-target genes enhancing apoptosis or cell survival based on the cellular context. *Cell Death Dis.* 2013;4(12):e963-8. doi:10.1038/cddis.2013.500
71. Huttlin EL, Ting L, Bruckner RJ, et al. The BioPlex Network: A Systematic Exploration of the Human Interactome. *Cell.* 2015;162(2):425-440. doi:10.1016/j.cell.2015.06.043
72. Hansen RS, Wijmenga C, Luo P, et al. The DNMT3B DNA methyltransferase gene is mutated in the ICF immunodeficiency syndrome. *Proc Natl Acad Sci U S A.* 1999;96(25):14412-14417. doi:10.1073/pnas.96.25.14412
73. Thijssen PE, Ito Y, Grillo G, et al. Mutations in CDCA7 and HELLS cause immunodeficiency-centromeric instability-facial anomalies syndrome. *Nat Commun.* 2015;6:7870. doi:10.1038/ncomms8870
74. Liang J, Yan R, Chen G, et al. Downregulation of ZBTB24 hampers the G0/1- to S-phase cell-cycle transition via upregulating the expression of IRF-4 in human B cells. *Genes Immun.* 2016;17(5):276-282. doi:10.1038/gene.2016.18
75. Wu H, Thijssen PE, de Klerk E, et al. Converging disease genes in ICF syndrome: ZBTB24 controls expression of CDCA7 in mammals. *Hum Mol Genet.* 2016;25(18):4041-4051. doi:10.1093/hmg/ddw243
76. Chen Z, Guidez F, Rousselot P, et al. PLZF-RAR $\alpha$  fusion proteins generated from

- the variant t(11;17)(q23;q21) translocation in acute promyelocytic leukemia inhibit ligand-dependent transactivation of wild-type retinoic acid receptors. *Proc Natl Acad Sci U S A*. 1994;91(3):1178-1182. doi:10.1073/pnas.91.3.1178
77. Yeyati PL, Shaknovich R, Boterashvili S, et al. Leukemia translocation protein PLZF inhibits cell growth and expression of cyclin A. *Oncogene*. 1999;18(4):925-934. doi:10.1038/sj.onc.1202375
  78. Ball HJ, Melnick A, Shaknovich R, Kohanski RA, Licht JD. The promyelocytic leukemia zinc finger (PLZF) protein binds DNA in a high molecular weight complex associated with cdc2 kinase. *Nucleic Acids Res*. 1999;27(20):4106-4113. doi:10.1093/nar/27.20.4106
  79. Melnick A, Ahmad KF, Arai S, et al. In-Depth Mutational Analysis of the Promyelocytic Leukemia Zinc Finger BTB/POZ Domain Reveals Motifs and Residues Required for Biological and Transcriptional Functions. *Mol Cell Biol*. 2000;20(17):6550-6567. doi:10.1128/mcb.20.17.6550-6567.2000
  80. Shaknovich R, Yeyati PL, Ivins S, et al. The Promyelocytic Leukemia Zinc Finger Protein Affects Myeloid Cell Growth, Differentiation, and Apoptosis. *Mol Cell Biol*. 1998;18(9):5533-5545. doi:10.1128/mcb.18.9.5533
  81. Savage AK, Constantinides MG, Han J, et al. The Transcription Factor PLZF Directs the Effector Program of the NKT Cell Lineage. *Immunity*. 2008;29(3):391-403. doi:10.1016/j.immuni.2008.07.011
  82. Xu D, Holko M, Sadler AJ, et al. Promyelocytic Leukemia Zinc Finger Protein Regulates Interferon-Mediated Innate Immunity. *Immunity*. 2009;30(6):802-816. doi:10.1016/j.immuni.2009.04.013
  83. Buaas FW, Kirsh AL, Sharma M, et al. Plzf is required in adult male germ cells for stem cell self-renewal. *Nat Genet*. 2004;36(6):647-652. doi:10.1038/ng1366
  84. Fillion GJP, Zhenilo S, Salozhin S, Yamada D, Prokhortchouk E, Defossez P. A Family of Human Zinc Finger Proteins That Bind Methylated DNA and Repress Transcription A Family of Human Zinc Finger Proteins That Bind Methylated DNA and Repress Transcription. *Mol Cell Biol*. 2006;26(1):169. doi:10.1128/MCB.26.1.169
  85. Weber A, Marquardt J, Elzi D, et al. Zbtb4 represses transcription of P21CIP1 and controls the cellular response to p53 activation. *EMBO J*. 2008;27(11):1563-1574. doi:10.1038/emboj.2008.85

86. Oyake T, Itoh K, Motohashi H, et al. Bach proteins belong to a novel family of BTB-basic leucine zipper transcription factors that interact with MafK and regulate transcription through the NF-E2 site. *Mol Cell Biol.* 1996;16(11):6083-6095. doi:10.1128/mcb.16.11.6083
87. Itoh-Nakadai A, Hikota R, Muto A, et al. The transcription repressors Bach2 and Bach1 promote B cell development by repressing the myeloid program. *Nat Immunol.* 2014;15(12):1171-1180. doi:10.1038/ni.3024
88. Igarashi K, Kurosaki T, Roychoudhuri R. BACH transcription factors in innate and adaptive immunity. *Nat Rev Immunol.* 2017;17(7):437-450. doi:10.1038/nri.2017.26
89. Ito N, Watanabe-Matsui M, Igarashi K, Murayama K. Crystal structure of the Bach1 BTB domain and its regulation of homodimerization. *Genes to Cells.* 2009;14(2):167-178. doi:10.1111/j.1365-2443.2008.01259.x
90. Rosbrook GO, Stead MA, Carr SB, Wright SC. The structure of the Bach2 POZ-domain dimer reveals an intersubunit disulfide bond. *Acta Crystallogr Sect D Biol Crystallogr.* 2012;68(1):26-34. doi:10.1107/S0907444911048335
91. Yurlova L, Derks M, Buchfellner A, et al. The fluorescent two-hybrid assay to screen for protein-protein interaction inhibitors in live cells: Targeting the interaction of p53 with Mdm2 and Mdm4. *J Biomol Screen.* 2014;19(4):516-525. doi:10.1177/1087057113518067
92. Suter B, Wanker EE. The investigation of binary PPIs with the classical yeast two-hybrid (Y2H) approach, Y2H variants, and other in vivo methods for PPI mapping. *Methods Mol Biol.* 2012;812:275-282. doi:10.1007/978-1-61779-455-1
93. Rothbauer U, Zolghadr K, Tillib S, et al. Targeting and tracing antigens in live cells with fluorescent nanobodies. *Nat Methods.* 2006;3(11):887-889. doi:10.1038/nmeth953
94. Schornack S, Fuchs R, Huitema E, Rothbauer U, Lipka V, Kamoun S. Protein mislocalization in plant cells using a GFP-binding chromobody. *Plant J.* 2009;60(4):744-754. doi:10.1111/j.1365-313X.2009.03982.x
95. Huynh KD, Bardwell VJ. The BCL-6 POZ domain and other POZ domains interact with the co-repressors N-CoR and SMRT. *Oncogene.* 1998;17(19):2473-2484. doi:10.1038/sj.onc.1202197
96. Zhou Y, Wu H, Zhao M, Chang C, Lu Q. The Bach Family of Transcription



- Factors: A Comprehensive Review. *Clin Rev Allergy Immunol*. 2016;50(3):345-356. doi:10.1007/s12016-016-8538-7
97. Stogios PJ, Chen LU, Prive GG. Crystal structure of the BTB domain from the LRF / ZBTB7 transcriptional regulator. *Protein Sci*. 2007;16(2):336-342. doi:10.1110/ps.062660907.)
98. Ahmad KF, Engel CK, Prive GG, Privé GG. Crystal structure of the BTB domain from PLZF. *Proc Natl Acad Sci U S A*. 1998;95(21):12123-12128. doi:10.1073/pnas.95.21.12123
99. Pollok BA, Heim R. Using GFP in FRET-based applications. *Trends Cell Biol*. 1999;9(2):57-60. doi:10.1016/S0962-8924(98)01434-2

## APPENDIX A

### Chemicals

Chemicals and Media Components	Supplier Company
2-Mercaptoethanol	Sigma, Germany
Acetic acid (glacial)	Merck Millipore, USA
Acrylamide/Bis-acrylamide (30%)	Sigma, Germany
Agarose	Sigma, Germany
Ammonium Persulfate	Sigma, Germany
Ampicilin Sodium Salt	Sigma, Germany
Boric Acid	Molekula, France
Chloramphenicol	Deva, Turkey
Coumaric Acid	Sigma, Germany
Coomassie Blue Brilliant Blue R	Sigma, Germany
Distilled Water	Merck Millipore, USA
DMEM	Thermo Fischer Scientific, USA
DMSO	Sigma, Germany
DNA Gel Loading Dye, 6X	NEB, USA
DTT	Fermentas, USA
EDTA	Sigma, Germany
Ethanol	Sigma, Germany
Ethidium Bromide	Sigma, Germany
Fetal Bovine Serum	Thermo Fischer Scientific, USA
Glycerol	Sigma, Germany
Glycine	Sigma, Germany
HBSS	Thermo Fischer Scientific, USA
HEPES	Sigma, Germany
HisPure Cobalt Superflow Agarose	Thermo Fischer Scientific, USA
Hydrochloric Acid	Sigma, Turkey
Hydrogen peroxide	Sigma, Turkey

Imidazole	Sigma, Germany
IPTG	Fermentas, USA
Isopropanol	Sigma, Germany
Kanamycin Sulfate	Thermo Fischer Scientific, USA
LB Agar	Sigma, Germany
LB Broth	Invitrogen, USA
L-Glutathione reduced	Sigma, Germany
Methanol	Sigma, Germany
PBS	Thermo Fischer Scientific, USA
Penicillin/Streptomycin	Thermo Fischer Scientific, USA
PIPES	Sigma, Germany
Potassium Acetate	Merck Millipore, USA
Protease Tablets (EDTA-free)	Roche, Germany
RNase A	Roche, Germany
SDS	Sigma, Germany
Sodium Azide	Amresco, USA
Sodium Chloride	Amresco, USA
Sodium Hydroxide	Sigma, Germany
TEMED	AppliChem, Germany
TCEP	Sigma, Germany
Terrific Broth	Sigma, Germany
Tris Base	Sigma, Germany
Tris Hydrochloride	Amresco, USA
Trypan Blue Solution	Thermo Fischer Scientific, USA
Tween20	Sigma, Turkey

## APPENDIX B

### Equipment

Equipment Supplier	Company
Autoclave	HiClave HV-110, Hirayama, Japan
Balance	Isolab, Germany
Centrifuge	5418R Eppendorf, Germany
	5702 Eppendorf, Germany
	5415R Eppendorf, Germany
	Allegra X-15R, Beckman Coulter, USA
	Sorvall Lynx 6000, Thermo Scientific, USA
CO2 Incubator	Binder, Germany
Column	HiLoad 16/60 Superdex p75 GE
	Healthcare Life Sciences, USA
	Superdex 200 Increase 5/150 GL
	Superdex 200 Increase 10/300 GL
Countless II Automated Cell Counter	Thermo Fischer Scientific, USA
Deepfreeze	-80°C, Forma 88000 Series, Thermo
	Fischer Scientific, USA
	-20°C, Bosch, Germany
Electrophoresis Apparatus	VWR, USA
	BIORAD, USA
Filters (0.22µm and 0.45µm)	Merk Millipore, USA
Freezing Container	Mr. Frosty, Thermo Fischer Scientific,
	USA
Gel Documentation	Gel Doc EZ, Biorad, USA
Heater	Thermomixer Comfort Eppendorf,
	Germany
Hemocytometer	Neubauer Improved, Isolab, Germany

Ice Machine	AF20, Scotsman Inc., USA
Incubator Shaker	Innova 44, New Brunswick Scientific USA
Laminar Flow	HeraSafe HS15, Heraeus, Germany HeraSafe HS12, Heraeus, Germany
Liquid Nitrogen	Taylor-Wharton, 300RS, USA
Magnetic Stirrer	SB162, Stuart, UK
Microliter Pipettes	Thermo Fischer Scientific, USA
Microscope	Primovert, Zeiss, Germany CK40, Olympus, Japan
Microwave Oven	Bosch, Germany
pH Meter	SevenCompact, Mettler Toledo, USA
Refrigerator	Bosch, Germany Arcelik, Turkey Panasonic, Japan Thermo Fischer Scientific, USA
RTCA system	ACEA Biosciences, USA
Sonicator	Qsonica Q500, USA
Spectrophotometer	NanoDrop 2000, Thermo Fischer Scientific, USA Ultrospec 2100 pro, Amersham Biosciences, UK
Surface Plasmon Resonance System	BIACORE T200, GE Healthcare Life Sciences, USA
Thermal Cycler	C1000 Touch, Biorad, USA PTC-200, MJ Reseach Inc., Canada
Vortex	VWR, USA
Water Bath	Innova 3100, New Brunswick Scientific, USA

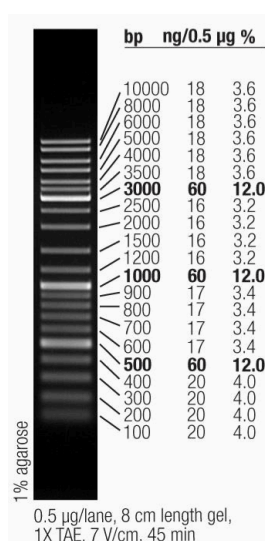
## APPENDIX C

### Molecular Biology Kits

GenElute Agarose Spin Columns	Sigma-Aldrich, USA
NucleoSpin Gel and PCR Clean-up	Macherey-Nagel, USA
Plasmid DNA purification (NucleoBond® Xtra Midi / Maxi)	Macherey-Nagel, USA
ZymoPure Plasmid Maxiprep Kit	Zymo Research, USA

## APPENDIX D

### DNA and Protein Molecular Weight Marker



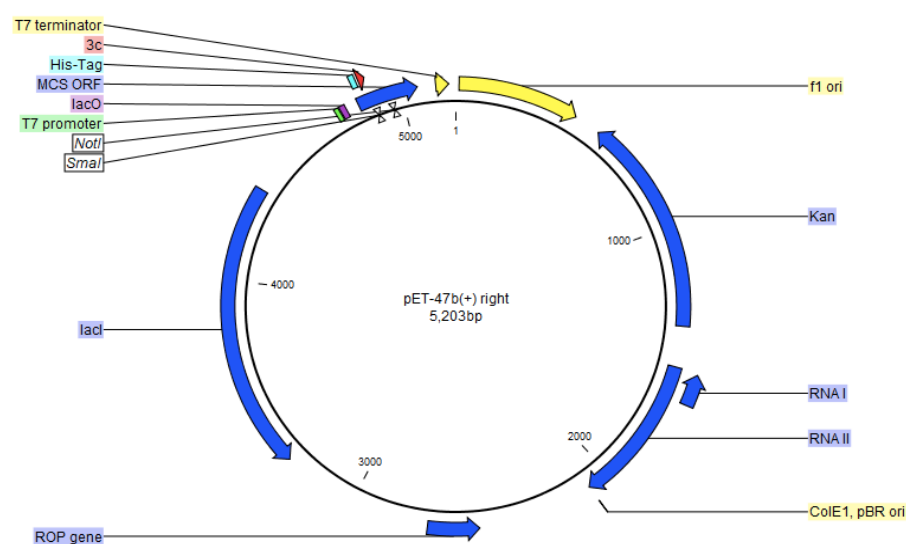
**Figure D1. GeneRuler DNA Ladder Mix (SM0331), Thermo Fischer Scientific, USA**



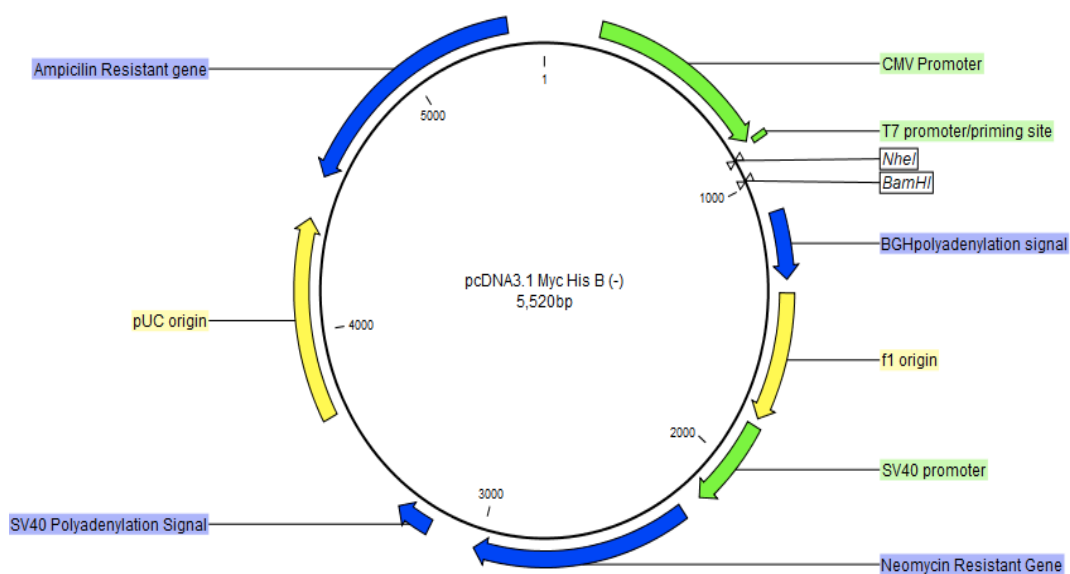
**Figure D2. Color Prestained Protein Standard, Broad Range (11-245 kDa) (P7712S), New England Biolabs**

## APPENDIX E

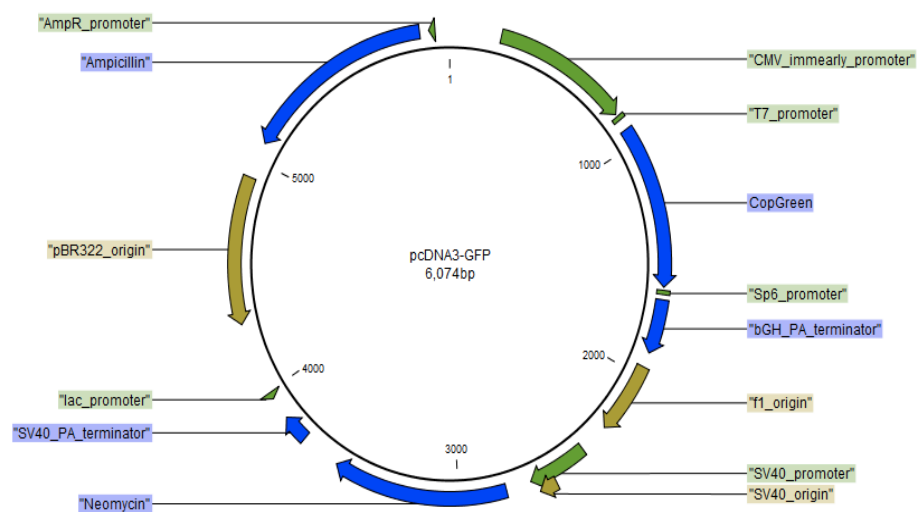
### Plasmid Maps



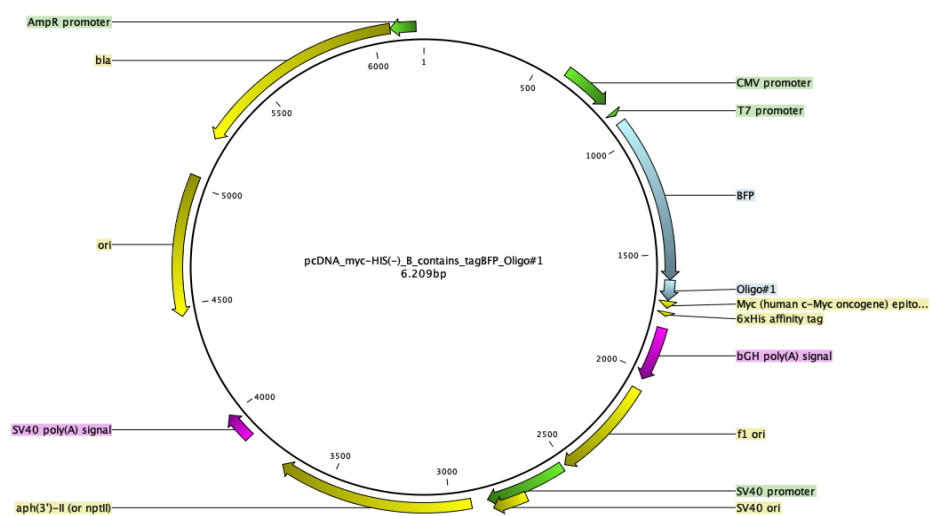
**Figure F1. The plasmid map of pET-47b(+)**



**Figure F2. The plasmid map of pcDNA3.1 Myc His B (-)**

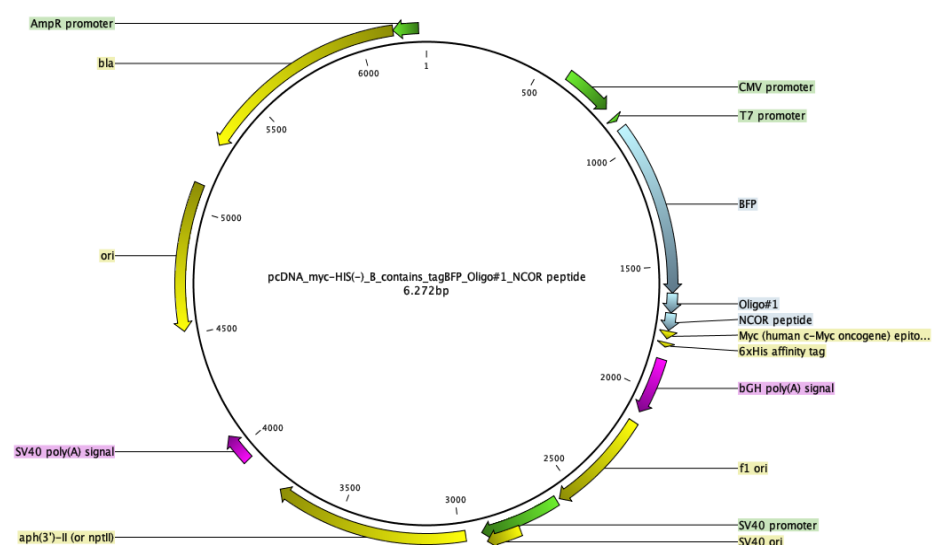


**Figure F3. The plasmid map of pcDNA3-GFP**

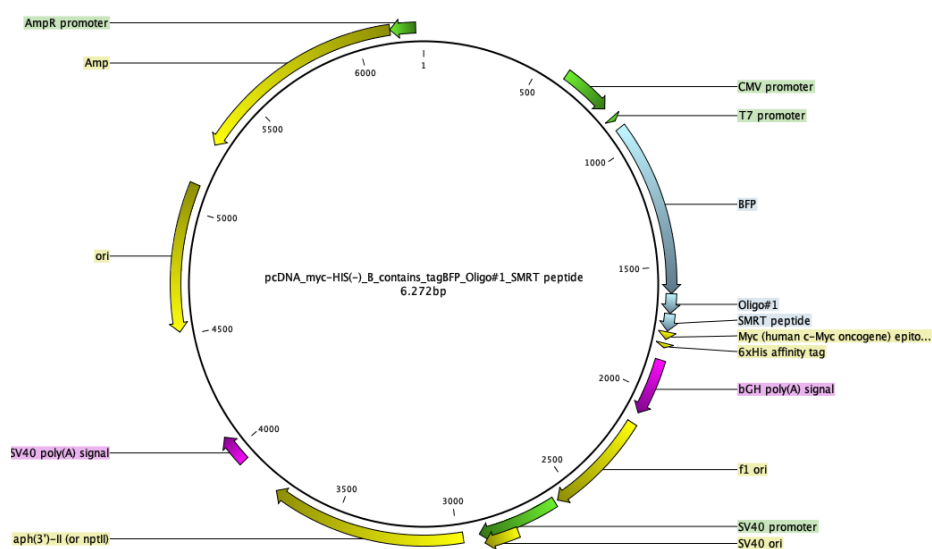


**Figure F4. The plasmid map of pcDNA3.1 Myc His B (-)-BFP-NLS**





**Figure F5. The plasmid map of pCDNA3.1/myc-His (-) B-BFP-oligo1-NCOR**



**Figure F6. The plasmid map of pCDNA3.1/myc-His (-) B-BFP-oligo1-SMRT**